

UNCLASSIFIED
AD

229466

FOR
MICRO-CARD
CONTROL ONLY

Reproduced by

Armed Services Technical Information Agency

ARLINGTON HALL STATION; ARLINGTON 12 VIRGINIA

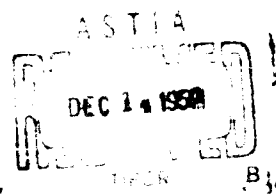
UNCLASSIFIED

NOTICE: When Government or other drawings, specifications or other data are used for any purpose other than in connection with a definitely related Government procurement operation, the U.S. Government thereby incurs no responsibility, nor any obligation whatsoever; and the fact that the Government may have formulated, furnished, or in any way supplied the said drawings, specifications or other data is not to be regarded by implication or otherwise as in any manner licensing the holder or any other person or corporation, or conveying any rights or permission to manufacture, use or sell any patented invention that may in any way be related thereto.

224466

HYDROGEN EMBRITTLEMENT IN STEELS, TITANIUM ALLOYS, AND SEVERAL FACE-CENTERED CUBIC ALLOYS

16



WADC TECHNICAL

REPORT

**HYDROGEN EMBRITTLEMENT IN STEELS,
TITANIUM ALLOYS, AND SEVERAL FACE-CENTERED
CUBIC ALLOYS**

P. A. Blanchard

R. J. Quigg

F. W. Schaller

E. A. Steigerwald

A. R. Troiano

Case Institute of Technology

APRIL 1959

Aeronautical Research Laboratory

Contract AF 33(616)-3431

Project 7021

Task 70645

WRIGHT AIR DEVELOPMENT CENTER
AIR RESEARCH AND DEVELOPMENT COMMAND
UNITED STATES AIR FORCE
WRIGHT-PATTERSON AIR FORCE BASE, OHIO

FOREWORD

This report deals with three separate, but related, aspects of the hydrogen embrittlement problem. The report is categorized into three distinct sections with each section representing a complete phase of the general problem under investigation. Section I involves the delayed failure in high strength steels. Section II is concerned with the hydrogen embrittlement and hydrogen-induced strain aging of titanium alloys, while Section III presents results on the hydrogen embrittlement of face-centered cubic metals.

This work represents the final report of the investigation performed at Case Institute of Technology, Cleveland, Ohio, under USAF Contract AF 33(616)-3431, during the period March 31, 1956 to March 31, 1959. The project was initiated under Project 7021, "Solid State Research and Properties of Matter," and Task 70245, "Effect of Environment on the Internal Structure of Solids."

The project was administered under the direction of Attwell M. Adair, Task Scientist, Metallurgy Research Branch, Aeronautical Research Laboratories, Directorate of Research, Wright Air Development Center.

Of the authors, P. A. Blanchard, R. J. Quigg, F. W. Schaller and E. A. Steigerwald are Graduate Assistants, and A. R. Troiano is Head, Department of Metallurgical Engineering.

PREVIOUS REPORTS AND PUBLICATIONS UNDER THIS CONTRACT

H. H. Johnson, J. G. Morlet and A. R. Troiano, "Hydrogen, Crack Initiation, and Delayed Failure in Steel," WADC TR 57-262, (May, 1957), also Trans. AIME, 212, 528-536, (August, 1958), also Nature, 179, 777, (April 13, 1957).

J. G. Morlet, H. H. Johnson, and A. R. Troiano, "A New Concept of Hydrogen Embrittlement in Steel," WADC TR 57-190, (March, 1957), also Jl. of Iron and Steel Inst., 189, 37, (May, 1958).

H. H. Johnson, E. J. Schneider, and A. R. Troiano, "The Recovery of Embrittled Cadmium Plated Steel," WADC TR 57-340, (June, 1957), also Iron Age, 182, No. 5, 47, (1958).

E. A. Steigerwald, F. W. Schaller, and A. R. Troiano, "Effect of Temperature on the Static Fatigue Characteristics of Hydrogen Embrittled 4340 Steel," WADC TR 58-175, (April, 1958).

P. Blanchard, and A. R. Troiano, "Delayed Failure and Notch Tensile Properties of a Vacuum Melted 4340 Steel," WADC TN 58-176, (June, 1958).

ABSTRACT

This report, which describes the influence of hydrogen on the mechanical properties of high strength steel, titanium and face-centered cubic metals, is divided into three sections.

SECTION I DELAYED FAILURE IN HIGH STRENGTH STEEL:

The initiation of localized cracking in a hydrogenated high strength steel specimen was found to be dependent on the development of a critical hydrogen concentration and relatively insensitive to the magnitude of the applied stress. The stress played an essential role in the delayed failure process by providing the means for grouping the hydrogen. Assuming that the rate of stress-induced diffusion was a direct function of the applied stress, the predicted relationship between incubation time and stress agreed reasonably well with experimental data.

SECTION II HYDROGEN EMBRITTLEMENT AND STRAIN AGING IN TITANIUM ALLOYS:

Low strain rate embrittlement in titanium alloys can be classified as a strain aging phenomenon. Prestraining and aging an alpha-beta titanium alloy resulted in a ductility minimum at some intermediate aging time. It appears that hydrogen migrates to a region of inhomogeneous strain, where a high stress state exists, and creates this embrittlement. The restoration of ductility at long aging times was attributed to recovery with subsequent redistribution of hydrogen.

Low strain rate hydrogen embrittlement was obtained for an alpha alloy and a beta alloy. Hydrogen in small quantities seemed to aid creep resistance in the alpha alloy. The beta alloy was resistant to nominal quantities of hydrogen (420 ppm), but did show embrittlement at higher levels.

SECTION III HYDROGEN EMBRITTLEMENT OF SEVERAL FACE-CENTERED CUBIC ALLOYS:

The hydrogen embrittlement of austenitic Ni-Cr-Fe alloys and OFHC copper has been investigated. Ni-Cr-Fe alloys were embrittled by hydrogen and their embrittlement was demonstrated to be of the same nature as that of steel.

A qualitative mechanism was presented which indicated that only the transition metals should be capable of conventional hydrogen embrittlement

This mechanism also accounted for the observed decrease of embrittlement in the austenitic Ni-Cr-Fe alloys with increasing (Fe + Cr) content.

TABLE OF CONTENTS

<u>Section I</u>			
I. INTRODUCTION	4		
II. MATERIALS AND PROCEDURE	7	II.	
1. Specimen Preparation	7		
2. Hydrogen Charging	7		
3. Testing Methods	8		
III. RESULTS AND DISCUSSION	9	III	
1. Incubation Time	9		
A. Relationship Between Stress and Hydrogen Content Necessary for Crack Initiation,	10		
B. The Role of Stress-Induced Diffusion	11		
2. Macroscopic Crack Growth	13		
IV. SUMMARY AND CONCLUSIONS	16		
V. BIBLIOGRAPHY	17		
 <u>Section II</u>			
I INTRODUCTION	34	IV.	
1. Hydrogen Embrittlement	34	V	
2. Strain Aging	36		
A. Strain Aging and the Yield Point in Steels	36	Section III	
B. Strain Aging in Titanium	37	I	
C. Strain Aging in Magnesium Alloys	38	II	

TABLE OF CONTENTS (CONT'D)

<u>Section II</u>		<u>Page</u>
3 Creep		38
4 Titanium Alloy Systems		39
II. MATERIAL AND PROCEDURES		40
1. Material		40
2. Specimen Preparation		41
3. Experimental Procedures		42
III. RESULTS AND DISCUSSION		43
1. Strain Aging and Hydrogen Embrittlement in an Alpha-Beta Titanium Alloy		43
A Effect of Hydrogen on the Ductility Obtained after Stress Rupture Testing of Unnotched Specimens		43
B Relation of Hydrogen Effects to Other Strain Aging Criteria		45
C Effect of Prestraining and Aging on Final Ductility of Hydrogenated Material		46
2. Effects of Hydrogen on an Alpha Titanium Alloy		50
3. Effects of Hydrogen on a Beta Titanium Alloy		53
IV. SUMMARY AND CONCLUSIONS		55
V. BIBLIOGRAPHY		57
 <u>Section III</u>		
I. INTRODUCTION		98
II. MATERIALS AND PROCEDURE		100

TABLE OF CONTENTS (CONT'D)

<u>Section III</u>		<u>Page</u>
1. Specimen Preparation	100	
2. Hydrogenation and Cadmium Plating	101	
3. Testing	102	
III. RESULTS AND DISCUSSION	103	
1. Similarity of the Hydrogen Embrittlement of Nickel and Nickel Base-Chromium-Iron Alloys with That of Steel	103	
A Strain Rate Dependence of the Embrittlement	103	
B Temperature Dependence of the Embrittlement	103	
C Recovery	103	
2. Notch Tensile and Delayed Failure Tests	104	
3. Variation of the Embrittlement of Ni-Cr-Fe Alloys with Composition	104	
4. The Hydrogen Embrittlement of OFHC Copper	105	
IV. GENERAL DISCUSSION	107	
V. SUMMARY AND CONCLUSIONS	110	
VI. BIBLIOGRAPHY	111	

SECTION I

DELAYED FAILURE IN HIGH STRENGTH STEEL

E. A. Steigerwald
F. W. Schaller
A. R. Troiano

ABSTRACT

The initiation of localized cracking in a hydrogenated high strength steel specimen was found to be dependent on the development of a critical hydrogen concentration and relatively insensitive to the magnitude of the applied stress. The stress played an essential role in the delayed failure process by providing the means for grouping the hydrogen. Assuming that the rate of stress-induced diffusion was a direct function of the applied stress, the predicted relationship between incubation time and stress agreed reasonably well with experimental data.

LIST OF FIGURES

Figure		Page
1	Schematic Representation of Static Fatigue Characteristics of a Hydrogenated High Strength Steel	19
2	Specimen Types Used in This Investigation	20
3	Effect of Prestressing Before Hydrogenation on the Incubation Time Specimen Type B, 230,000 PSI Strength Level, Baked 1 Hours at 300°F After Hydrogenation and Plating	21
4	Relationship Between Hydrogen Content and Current Density for 4340 Steel	22
5.	Effect of Hydrogen Content (Log Current Density) on the Ductility of 4340 Steel Tested at -321°F	23
6.	Relationship Between Pressure and Hydrogen Content Calculated by Method of De Kazinczy for Steel with 0.008% Voids	24
7.	Comparison of Calculated Relationship Between Applied Stress and Incubation Time and Experimental Data for Hydrogenated 4340 Steel, 230,000 PSI Strength Level	25
8	Relative Change in Crack Area as a Function of Crack Growth Time for Hydrogenated 4340 Steel, 230,000 PSI Strength Level	26
9	Relative Change in Crack Area as a Function of Crack Growth Time for Hydrogenated 4340 Steel, 230,000 PSI Strength Level	27

I INTRODUCTION

The ability of small quantities of hydrogen to drastically embrittle metals has long been recognized. Only recently, however, a new facet of hydrogen embrittlement which involves the ability of hydrogen to produce delayed failure, has been observed and studied (1-9)*.

Delayed failure, or as it is also termed - static fatigue, is defined as the property of a material to fail under the action of a sustained load, even though it is capable of supporting a higher load for a finite period of time. Steel parts which exhibit delayed failure have usually been subjected to a hydrogen environment sometime during their processing and static fatigue in high strength steels has been definitely attributed to hydrogen (1).

The major portion of the delayed failure studies have been conducted by testing electrolytically hydrogenated specimens at a constant tensile load and recording the time to failure. A typical static fatigue curve which charts the fracture time as a function of applied stress is shown in Fig. 1. It is characterized by three distinct regions: an upper critical stress which is the notched tensile strength, a lower critical limit below which no failure occurs and a range of delayed failure. The influence of strength level, notch acuity, hydrogen concentration, hydrogen distribution, prestressing and temperature on the delayed failure parameters has been extensively investigated (1, 4, 5, 7, 9).

Immediately after a short-time cathodic charging operation specimens have an extremely heterogeneous hydrogen concentration which is localized at the surface. Barnett and Troiano (3) used resistance measurements to determine the kinetics of crack growth in such specimens and concluded that the delayed failure was dependent on the growth of the crack which accompanies the macroscopic diffusion of hydrogen into the specimen. A quantitative analysis of the delayed failure mechanism, however, was difficult with a heterogeneous hydrogen distribution due to the continually changing hydrogen content as a result of redistribution and outgassing.

A more refined approach to the delayed failure problem from both a practical and theoretical viewpoint was employed by Johnson, Morlet and Troiano (7) who utilized a charging, plating and baking sequence to produce

* Numbers in parentheses pertain to references in the Bibliography.

a relatively low, but uniform hydrogen concentration. The general nature of the delayed failure behavior of uniformly hydrogenated material was similar to that obtained for specimens with a heterogeneous hydrogen content. The crack kinetics, however, were altered. With a uniform hydrogen content a definite incubation period preceded the initiation of a crack which ultimately led to failure. The incubation period was believed to be the time required for sufficient hydrogen to concentrate in a localized triaxial region and initiate a crack.

Tests conducted at low temperatures showed that the hydrogen-induced slow crack growth occurred discontinuously (9). This indicated that the delayed failure process involved a series of crack initiations with instantaneous, but limited propagation, rather than the continuous growth of a single crack. The low temperature results also showed that the activation energy for the incubation time agreed with that for the diffusion of hydrogen in alpha iron and that the relationship between stress and hydrogen necessary to initiate a crack was not significantly altered over the temperature range examined.

Since delayed failure is merely a series of crack initiations, the factors involved in determining the incubation time are particularly significant in explaining the delayed failure mechanism. The initiation of a hydrogen induced crack is dependent on two factors: (a) the stress-induced diffusion of hydrogen producing an appreciable hydrogen build up in a localized region and (b) the basic effect of hydrogen on the material causing localized failure, i. e. a crack.

The ability of hydrogen to lower the fracture stress, which represents the latter component of the initiation process, has been the primary subject of many theories dealing with hydrogen embrittlement. The majority of investigators have concluded that the hydrogen pressure in certain voids or imperfections which act as the fracture embryos tends to lower the stress at which these embryos become active. Petch and Stables (10) postulate that the surface adsorption of hydrogen lowers the surface energy necessary for the extension of a crack. De Kazinczy (11) presents a thermodynamic argument based on the fact that the hydrogen gas present in the voids releases energy through the expansion which accompanies crack growth. This energy then aids in the subsequent propagation of the crack. Zapffe (12), and Bastien and Azou (13) propose that the pressure of hydrogen in the voids or lattice imperfections produces a triaxial stress state which promotes fracture. A somewhat divergent viewpoint has been presented by Morlet, Johnson, and Troiano (14). As a result of presiraming and aging experiments on high strength steel, they concluded that the hydrogen concentration in the triaxial region in front of a void or large lattice imperfection, rather than the pressure within the void, is the determining factor

for embrittlement.

Since each of the theories used to explain hydrogen embrittlement is dependent on a critical combination of hydrogen and stress, they can in principle be applied to the presently proposed qualitative mechanism for delayed failure (7). There are several facets of the delayed failure problem, most notably the insensitivity of the incubation time to applied stress, which have not been completely explained. The purpose of this investigation was to examine the parameter of incubation time in an effort to extend the mechanism for the static fatigue process.

II MATERIALS AND PROCEDURE

I SPECIMEN PREPARATION

Aircraft quality SAE-AISI 4340 steel of the following chemical analysis was used for the investigation

Composition of 4340 Steel

C	Mn	Si	Ni	Cr	Mo
0.395%	0.82%	0.29%	1.76%	0.85%	0.25%

The material, designated as heat G, was furnished by the Republic Steel Co in 5/8" hot-rolled bars. Specimens were machined from stock heat treated to a 230,000 psi strength level according to the following sequence

- a) Normalize bar stock at 1650°F for one hour.
- b) Stress relieve at 1200°F for four hours and furnace cool,
- c) Rough machine specimen blanks (no notch) 0.030" oversize
- d) Austenitize blanks at 1550°F for 45 minutes in a salt bath and oil quench
- e) Temper one hour at 750°F
- f) Finish machine

Tensile specimens with geometries, as indicated in Figs. 2 were employed for the experiments. The specimen types were comparable to the normal unnotched and 60° V-notch specimens used in previous delayed failure studies (1-7).

2 HYDROGEN CHARGING

Two types of charging conditions were employed. For the delayed failure studies, specimens were degreased in carbon tetrachloride and then cathodically charged for five minutes in a 4% sulfuric acid solution at a current density of 0.02 amperes per square inch. Following charging the specimens were washed in water and cadmium plated in a sodium cyanide-cadmium oxide bath for fifteen minutes at twenty amperes per square foot (15). In order to homogenize the hydrogen distribution the specimens were

baked for three hours at 300°F in an air furnace. Previous work (7) has indicated that with baking times in excess of one-half hour a uniform hydrogen distribution is present.

Tensile tests were performed on specimens which had been charged for 24 hours in a solution of 4% sulfuric acid plus a poison. The poison was a solution of 2 grams of yellow phosphorus in 40 cc carbon disulfide and was added in the ratio of 10 cc to every 900 cc of electrolyte. The specimens were charged for 24 hours to obtain a uniform hydrogen content without baking. The current density which determines the hydrogen content under these conditions (16) was varied between 0.0005 and 0.20 amperes per square inch. Hydrogen analyses were performed by the Acid Open Hearth Committee at the University of Pittsburgh.

3. TESTING METHODS

Both the tensile and delayed failure tests were conducted with concentrically aligned fixtures which insured an eccentricity of less than 0.001" in uniaxial loading. The tensile tests were performed in liquid nitrogen at a constant crosshead speed of 0.05 inches per minute. The time between charging and testing in liquid nitrogen was in all cases less than five minutes. The static fatigue tests were conducted at room temperature on constant load, lever arm stress-rupture machines. The crack kinetics and incubation times were determined with the especially adapted Kelvin double bridge which has been previously described (3).

III RESULTS AND DISCUSSION

I INCUBATION TIME

A particularly perplexing problem in explaining static fatigue of high strength steels is the insensitivity of the incubation time to the magnitude of applied stress (7). Since the incubation period at a given stress is the time required for the hydrogen to build up to a sufficient concentration to initiate a crack, one would expect that at a high stress less hydrogen would be required hence a shorter incubation time would result. In addition the driving force for the diffusion is stress therefore as this driving force is increased the rate of diffusion should increase also leading to a shorter incubation period at higher stresses. In the static fatigue of glass the fracture time is strongly dependent on the applied stress (17), however no such dependency is present in the high strength steels (7).

A possible explanation for this behavior lies in the effect of plastic deformation (3, 7). At higher stresses more deformation should occur resulting in strain-induced trapping of hydrogen which could compensate for the stress, per se, and result in the observed insensitivity.

In an effort to determine the role of plastic deformation on the incubation time notched tensile specimens were loaded at 250,000 psi for two minutes prior to hydrogen charging. Following this prestressing the specimens were charged, plated and baked three hours at 300°F. A curve of the incubation time as a function of applied stress is presented in Figure 3. Prestressing had no influence on the general features of the incubation period which still exhibited only a very slight dependency on the applied stress. Since loading subsequent to the prestressing should not affect the size of the lattice void or imperfections which are believed to produce the strain-induced trapping of hydrogen, the factor of strain-induced trapping could not be the critical one accounting for the behavior of the incubation time.

In addition, if plastic flow were significant in determining the shape of the stress-incubation time relationship, the factors such as decreased temperature and increased strength level which inhibit flow should be reflected in the delayed failure behavior. Since neither of these factors alters the general features of the incubation time (1, 5, 9) it seems reasonable to conclude that in an analysis of the incubation time in sharp-notched specimens of high strength steels the role of strain-induced trapping of hydrogen can be neglected.

A Relationship Between Stress and Hydrogen Content Necessary for Crack Initiation

One basic component of the incubation time is the relationship between the hydrogen content and stress which is necessary to initiate a crack. A normal room temperature tensile test which measures some ductility or strength parameter as a function of hydrogen content does not yield the desired relation. At room temperature as a result of stress-induced diffusion during the test, the hydrogen content at the point of crack initiation is not known. In addition the stress at which the first crack initiates may not correspond with the stress at which failure of the specimen occurs. In determining the stress-hydrogen relationship which propagates a crack it is then necessary to test under conditions where the hydrogen content is measurable, that is, not altered during testing. The conditions of testing must also be such that the failure of the specimen is essentially coincident with the initiation of the first crack. Such conditions are attained at low temperatures. Previous work (9) has shown that at low temperatures the incubation time is prolonged in accordance with the reduced diffusion rate for hydrogen. Hence at liquid nitrogen temperature no diffusion during the test which might alter the local hydrogen concentration would be nil. At temperatures below -50°F the incubation time is so short that failure is also coincident with the fracture time (9), that is once the first crack initiates it instantaneously propagates through the specimen producing failure.

Tests were conducted in liquid nitrogen (-321°F) using type A specimens, which were charged for 24 hours in 10 percent 4% sulfuric acid. Percent reduction in area was used as the parameter to indicate degree of embrittlement and the hydrogen content was varied by regulating the charging current density. In accordance with previously published results (16) a linear relationship existed between the logarithm of the current density and the hydrogen content over a considerable range of current densities (Fig. 4). Above approximately 8 ppm of hydrogen, however, the hydrogen content became essentially independent of current density. This phenomenon has been discussed by de Kazinczy (17) who found that the point at which the hydrogen content became independent of charging current density corresponded to the current at which the specimen failed locally by blistering or cracking. In this investigation also the point at which the hydrogen content as a function of charging current density deviated from linearity was exactly where irreversible embrittlement started.

Figure 5 shows the effect of hydrogen content, indicated by the logarithm of current density, on the ductility of the high strength steel at -321°F. The results show that the relationship between hydrogen and stress necessary to initiate a crack is primarily dependent on the hydrogen content. Below approximately 5 ppm of hydrogen no embrittlement occurs, but

when this critical hydrogen content is attained catastrophic embrittlement takes place. The initiation of a hydrogen-induced crack above some threshold stress is therefore dependent on the development of a critical hydrogen content.

Since the basic nature of delayed failure is not markedly influenced by temperature, the initiation of a crack at room temperature would also be dependent on the development of a critical hydrogen content. Once above some threshold value the stress in the delayed failure process merely serves to produce sufficient hydrogen grouping to initiate a crack.

The theories of hydrogen embrittlement which are used to explain the basic action of hydrogen on the metal are dependent in some form on the calculated pressure developed by the hydrogen in a type of void or imperfection. The mechanisms proposed by Petch and Stables (10), de Kazinczy (11), Zapffe (12) and Bastien and Azou (13) are directly dependent on the pressure in an imperfection, while in the results presented by Morlet, Johnson, and Troiano (14) the pressure in the void influences the embrittlement by regulating the hydrogen content in the lattice adjacent to the void. Several methods, which yield essentially equivalent results may be used to determine the relationship between hydrogen content and hydrogen pressure (11, 19). Figure 6 represents the relationship between pressure and hydrogen content calculated by the method of de Kazinczy (11) for a steel with 0.006% voids. These results indicate that the calculated pressure rises extremely rapidly over a very narrow range of hydrogen contents. The similarity of the experimentally determined relationship between stress and hydrogen content (Fig. 5) and the calculated relationship between pressure and hydrogen (Fig. 6) is apparent. These results indicate, in agreement with the postulated mechanisms, that the pressure is the critical parameter influencing embrittlement.

Although the experimental results are qualitatively explainable on this basis no definite conclusion regarding the exact mechanism which is operative can be made since each is dependent in some form on the hydrogen pressure.

B The Role of Stress-Induced Diffusion

Since the embrittlement due to hydrogen is dependent almost entirely on the development of a critical hydrogen content rather than a critical relationship between hydrogen and stress, the relative insensitivity of the incubation time to applied stress is understandable on this basis alone. However, the role of stress-induced diffusion must still be clarified. In the analysis of the interaction between a carbon or nitrogen interstitial and the stress field of a dislocation Cottrell and Bilby (20) determined that in

in the initial stages of aging the relationship between interstitial concentration and time can be represented as

$$n = an_0 \left(\frac{ADt}{kT} \right)^{2/3} \quad (a)$$

where n = number of solute atoms which arrive in time t

n_0 = total number of atoms in solution per unit volume,

D = diffusion coefficient, k = Boltzmann constant

T = absolute temperature, a = constant, and

A = term dependent upon shear modulus, distortion due to interstitial, and the strength of the stress field about the dislocation.

The delayed failure in notched tensile specimens of high strength steel has been qualitatively explained on the basis of the stress-induced diffusion of hydrogen to the region where fracture is initiated (7). If the fracture embryo is considered as a blocked dislocation array of the type described by Stroh, Cottrell and others (21 - 24), the most effective fracture embryos will probably be located in the region of the elastic-plastic interface near the base of the notch, since at this point the macroscopic stresses will be triaxial and have their maximum values. The stress field about such a blocked array of dislocations will be comparable to the stress field about a dislocation (25). It then appears reasonable to assume that for the stress-induced diffusion of hydrogen the local hydrogen concentration as a function of time will be governed by a relationship similar to equation (a).

$$n_H = an_0 \left(\frac{pBD^2}{kT} \right)^m \quad (b)$$

In this case n_H is the number of hydrogen atoms at the point of maximum binding energy which arrive in time t , B is dependent on the distortion of the lattice due to hydrogen, on the elastic constants and the particular external notch geometry, and p is the applied stress. The exponent (m) would be different from $2/3$ as a result of the perturbation of the stress field of the dislocation by the applied stress and the external notch.

In order for embrittlement, i.e. local crack initiation, to occur n_H must equal the critical hydrogen content (n_c). Hence at a given tem-

perature and notch geometry equation (b) can be written as:

$$p_1 t_1 = \text{constant.} \quad (c)$$

where t_1 is the incubation time corresponding to an applied stress of p_1 . On this basis the incubation time as a function of applied stress can be calculated using one experimental point to evaluate the constant. Figure 7 represents a comparison of the relationship between stress and time as determined by equation (c) and by experiment. The slopes of the predicted curves agree reasonably well with the experimental behavior.

The delayed failure process is therefore essentially dependent only on the development of a critical hydrogen content. The stress in the failure range influences the process primarily through its ability to produce a critical amount of hydrogen grouping in the region where a fracture embryo exists.

2. MACROSCOPIC CRACK GROWTH

The mechanism of crack propagation in hydrogen-induced delayed failure involves the stress-induced diffusion of hydrogen to the region of a dislocation array. When a critical hydrogen concentration is attained, instantaneous, but limited crack growth takes place. The actual growth of the macroscopic crack occurs discontinuously with the total growth time being composed of a series of crack initiations (9).

Ideally the cross-sectional area of the specimen decreases concentrically by a small increment of area, ΔA , after each crack initiation. At room temperature in hydrogenated 230,000 psi strength level material each increment decrease of specimen area ΔA is very small and the resultant effect is that the macroscopic crack growth curve appears continuous. Since each initiation is dependent on the diffusion of hydrogen, the overall continuous crack growth curve should as a first approximation be governed by the rate of movement of hydrogen. The rate of interstitial movement can be expressed as

$$v_i = \frac{D}{kT} \cdot F \quad (d)$$

where v_i is the velocity of interstitial movement, D is the diffusion coefficient, F is the driving force which is the negative of the gradient of the

interaction energy (-grad U). k is Boltzmann's constant, and T is the absolute temperature ($^{\circ}\text{C}$). This interstitial movement, of course, is visualized as occurring concentric with the specimen axis and towards the point of maximum triaxiality.

$$v_i = \frac{D}{kT} F = \frac{-D}{kT} \text{ grad } U \quad (\text{e})$$

Since the velocity of interstitial movement (v_i) is assumed to be the controlling factor for macroscopic crack growth, the velocity of the concentric circular growth of the crack (v_c) should be proportional to the movement of the interstitial (v_i). Therefore

$$v_c = \frac{\Delta A}{\Delta t} = \frac{(\text{constant}) D}{kT} \text{ grad } U \quad (\text{f})$$

at room temperature where the crack appears to grow continuously. ΔA approaches zero as Δt approaches zero, hence in the limit

$$\frac{dA}{dt} = \frac{(\text{constant}) D}{kT} \text{ grad } U \quad (\text{g})$$

U is a function of stress and the stress concentration factor expressed as $U = (\text{constant}) \sigma K_f$. Since σ is the instantaneous stress, $\sigma = L/A$ where L is the applied load and A is the instantaneous area, then

$$U = [\text{constant}] \frac{L}{A} K_f$$

and the

$$\text{grad } U = [\text{constant}] \left[\frac{L}{A} \right] \text{ grad } K_f \quad (\text{h})$$

Once the crack has started, the maximum value of the stress concentration factor is attained and the gradient should remain essentially constant during the early stages of crack growth. Substituting equation (h) in equation (g)

$$\frac{dA}{dt} = \text{constant} \left[\frac{D}{kT} \right] \left[\frac{L}{A} \right]. \quad (\text{i})$$

Integrating this equation

$$\int_{A_0}^A AdA = \text{constant} \left(\frac{D}{kT} \right) (L) \int_{t_1}^t dt$$
$$\frac{A^2 - A_0^2}{2} = (\text{constant}) \left(\frac{D}{kT} \right) (L) (t - t_1)$$
$$\left(\frac{A}{A_0} \right)^2 = (\text{constant}) \left(\frac{D}{kT} \right) (L) \Delta t + 1 \quad (j)$$

where A_0 is the initial specimen area, and Δt is the difference between the total time and the incubation time. Using the calibration curve relating resistance changes with changes in specimen area (3) and room temperature crack growth curves (9) the parameter $\left(\frac{A}{A_0} \right)^2$ was plotted as a function of

Δt . The results presented in Figs. 8 and 9 indicate that the predicted linear relationship is obeyed during the early stages of crack growth. As shown in Fig. 8 for an applied stress of 175,000 psi considerable deviations from linearity occur during the later stages. In this region the assumptions concerning the constancy of the hydrogen content and the gradient of the stress concentration factor are least reliable.

On the basis of equation (j) the slope of the lines relating A^2/A_0^2 to Δt in Figs. 8 and 9 should be a direct function of the applied stress. In Fig. 8 the slopes decrease as the applied load decreases from 225,000 psi to 175,000 psi; however, as the applied stress is lowered further (Fig. 9) the consistent decrease in slope does not continue. Due to the scatter inherent in this type of brittle failure it is felt that the existing data are insufficient to determine whether or not this anomaly is real or merely due to chance variations.

IV SUMMARY AND CONCLUSIONS

The relationship between the applied stress and the time to initiate the first crack in a hydrogenated high strength steel specimen was analyzed. The analysis was based on a separation of the two factors which govern the incubation time, that is, the basic relation between stress and hydrogen necessary to initiate a crack and the preferential segregation of hydrogen due to stress.

Above a particular threshold stress the conditions necessary for localized cracking were essentially dependent only on the development of a critical hydrogen content. The basic relationship between hydrogen and stress is then virtually insensitive to the magnitude of the applied stress in the delayed failure range. An analogy was drawn between the stress-induced diffusion of carbon and nitrogen to the stress field surrounding a dislocation and the stress-induced diffusion of hydrogen to the stress field about a fracture embryo, located at the region of maximum triaxiality. On this basis the number of hydrogen atoms which arrived at the critical region where fracture is initiated was directly dependent on the stress. A relationship between the applied stress and the incubation time was derived and this relationship agreed reasonably well with the experimentally determined values

Employing appropriate assumptions, an analysis of the macroscopic crack growth curves in delayed failure was made. The predicted linear relationship between the square of the specimen area and the crack growth time was realized during the early stages of crack growth.

V. BIBLIOGRAPHY

1. R. P. Frohmberg, W. J. Barnett, and A. R. Troiano, "Delayed Failure and Hydrogen Embrittlement in Steel," *Trans ASM*, 47, 892-925, (1955).
2. E. R. Slaughter, E. E. Fletcher, A. R. Elsea, and G. K. Manning, "An Investigation of the Effects of Hydrogen on the Brittle Failure of High Strength Steels," *WADC TR 56-83* (April 1956)
3. W. J. Barnett and A. R. Troiano, "Crack Propagation in the Hydrogen-Induced Brittle Fracture of Steel," *Trans AIME*, 209, 486-494, (1957).
4. R. D. Johnson, H. H. Johnson, W. J. Barnett and A. R. Troiano, "Hydrogen Embrittlement and Static Fatigue in High Strength Steel," *WADC Interim Report*, (August 1955)
5. H. H. Johnson, R. D. Johnson, R. P. Frohmberg, and A. R. Troiano, "Static Fatigue in Twelve Heats of 4340 Steel Embrittled with Hydrogen," *WADC TN 55-30c*, (August 1955)
6. R. D. Johnson, H. H. Johnson, J. G. Morlet and A. R. Troiano, "Effect of Physical Variables on Delayed Failure in Steel," *WADC TR 56-220*, (June, 1956).
7. H. H. Johnson, J. G. Morlet, and A. R. Troiano, "Hydrogen, Crack Initiation, and Delayed Failure in Steel," *Trans AIME*, 212, 528-536, (August 1958). also *NATURE*, 179 777, (April 13, 1957).
8. R. D. Daniels, R. J. Quigg, and A. R. Troiano, "Delayed Failure and Hydrogen Embrittlement in Titanium," *Trans ASM*, 51, (1959).
9. E. A. Steigerwald, F. W. Schaller and A. R. Troiano, "Effect of Temperature on the Static Fatigue Characteristics of Hydrogen Embrittled 4340 Steel," *WADC TR 58-178*, (April, 1958).
10. N. J. Petch and P. Stavles, "Delayed Fracture of Metals Under Static Load," *Nature* 169, 842-843 (May 17, 1952) also N. J. Petch, "Lowering of the Fracture Stress Due to Surface Adsorption," *Phil. Mag.*, 1, 331-335, (1956).
11. F. de Kazinczy, "A Theory of Hydrogen Embrittlement," *Jl. of Iron and Steel Inst.*, 177, 85-92 (1954)

12. C. Zapife, discussion of "Metal Arc Welding of Steel," by S. A. Herres, Trans. ASM, 39, 191, (1947).
13. P. Bastien and P. Azou, "Effect of Hydrogen on the Deformation and Fracture of Iron and Steel in Simple Tension," Proc. of the First World Met. Cong. ASM, 535-552, (1951)
14. J. G. Morlet, H. H. Johnson, and A. R. Troiano, "A New Concept of Hydrogen Embrittlement in Steel," Jl. of Iron and Steel Inst., 189, 37, (May, 1958).
15. H. H. Johnson, E. J. Schneider and A. R. Troiano, "The Recovery of Embrittled Cadmium Plated Steel," Iron Age, 182, No. 5, 47-50, (1958)
16. A. E. Schuetz and W. D. Robertson, "Hydrogen Absorption, Embrittlement and Fracture of Steel," Corrosion, 13, 437-458, (1957).
17. T. C. Baker and F. W. Preston, "Fatigue of Glass Under Static Loads," Jl. App. Phys., 17, 170, (1946).
18. F. de Kazinczy, "Hydrogen Occlusion and Equilibrium Hydrogen Pressure in Steel During Electrolytic Charging," Jernkontorets Annaler, 139, 466-480, (1955).
19. C. Sykes, H. H. Burton, and C. C. Gegg, "Hydrogen in Steel Manufacture," Jl. of Iron and Steel Institute, 156, 155-180, (June, 1947).
20. A. H. Cottrell and B. A. Bilby, "Dislocation Theory of Yielding and Strain Aging of Iron," Proc. Phys. Soc., A62, 49, (1949).
21. A. N. Stroh, "A Theory of the Fracture of Metals," Advances in Physics, 6, 418, (1957)
22. A. H. Cottrell, "Theory of Brittle Fracture in Steel and Similar Metals," Trans. Met. Soc. AIME, 192, (April 1958)
23. C. Zener, "The Micro-Mechanism of Fracture," Trans. ASM, 40B, 3, (1948).
24. N. F. Mott, "Fracture in Metals," Jl. Iron and Steel Inst., 183, 233, (1956).
25. A. N. Stroh, "The Formation of Cracks as a Result of Plastic Flow," Proc. Roy. Soc. [A], 223, 404, (1954).

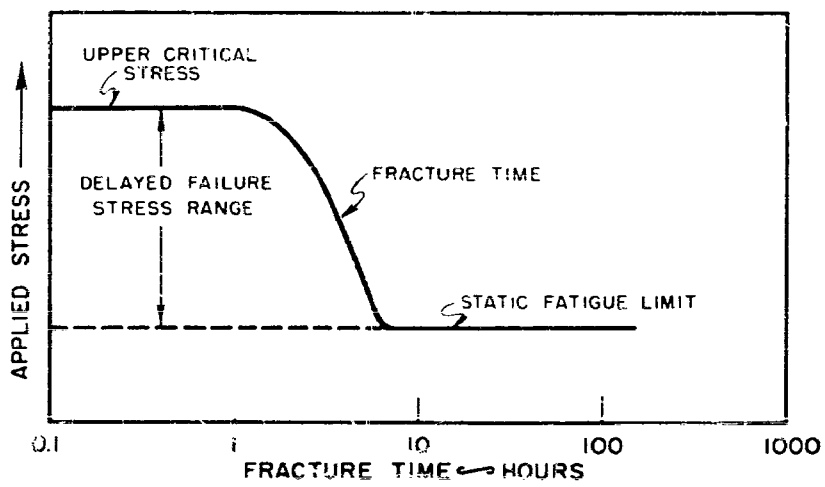
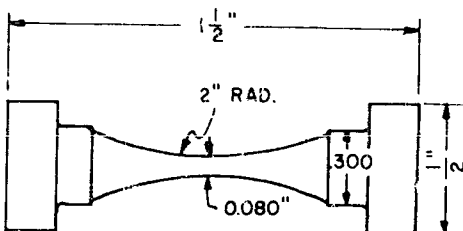
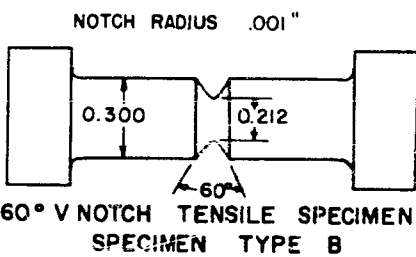


FIG. 11. SCHEMATIC REPRESENTATION OF STATIC FATIGUE CHARACTERISTICS OF A HYDROGENATED HIGH STRENGTH STEEL.



UNNOTCHED TENSILE SPECIMEN
SPECIMEN TYPE A



60° V NOTCH TENSILE SPECIMEN
SPECIMEN TYPE B

FIG. 2 : SPECIMEN TYPES USED IN
THIS INVESTIGATION.

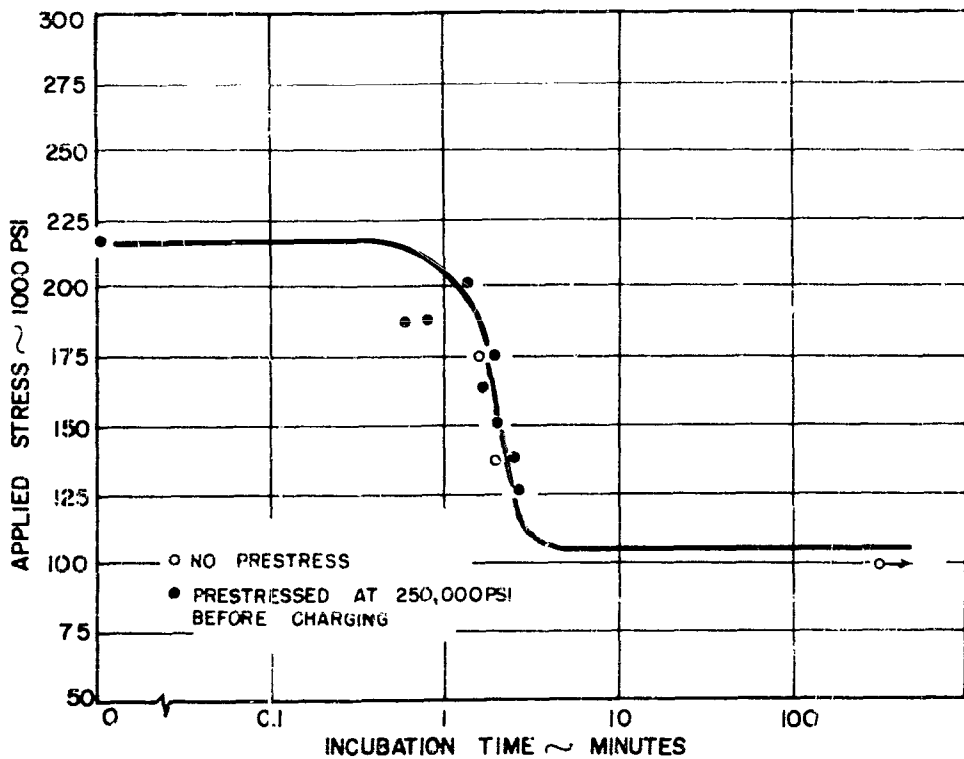


FIG. 3 EFFECT OF PRESTRESSING BEFORE HYDROGENATION ON THE INCUBATION TIME. SPECIMEN TYPE B 230,000 PSI STRENGTH LEVEL, BAKED 3 HOURS AT 300°F AFTER HYDROGENATION AND PLATING.

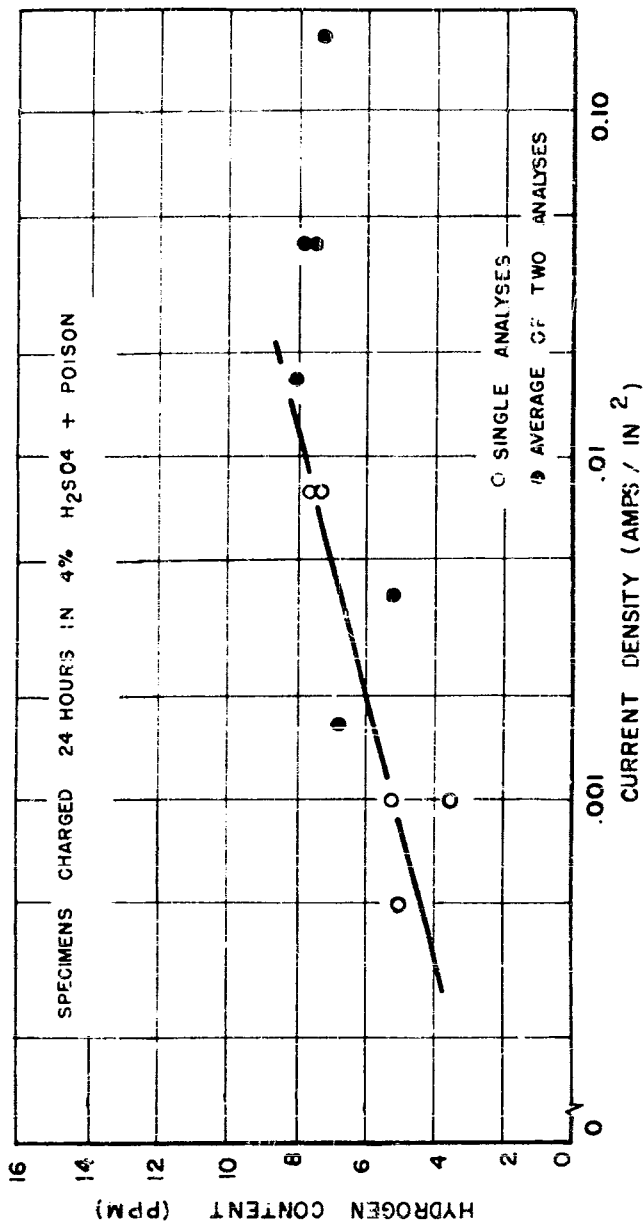


FIG. 4 .RELATIONSHIP BETWEEN HYDROGEN CONTENT AND CURRENT DENSITY FOR 4340 STEEL.

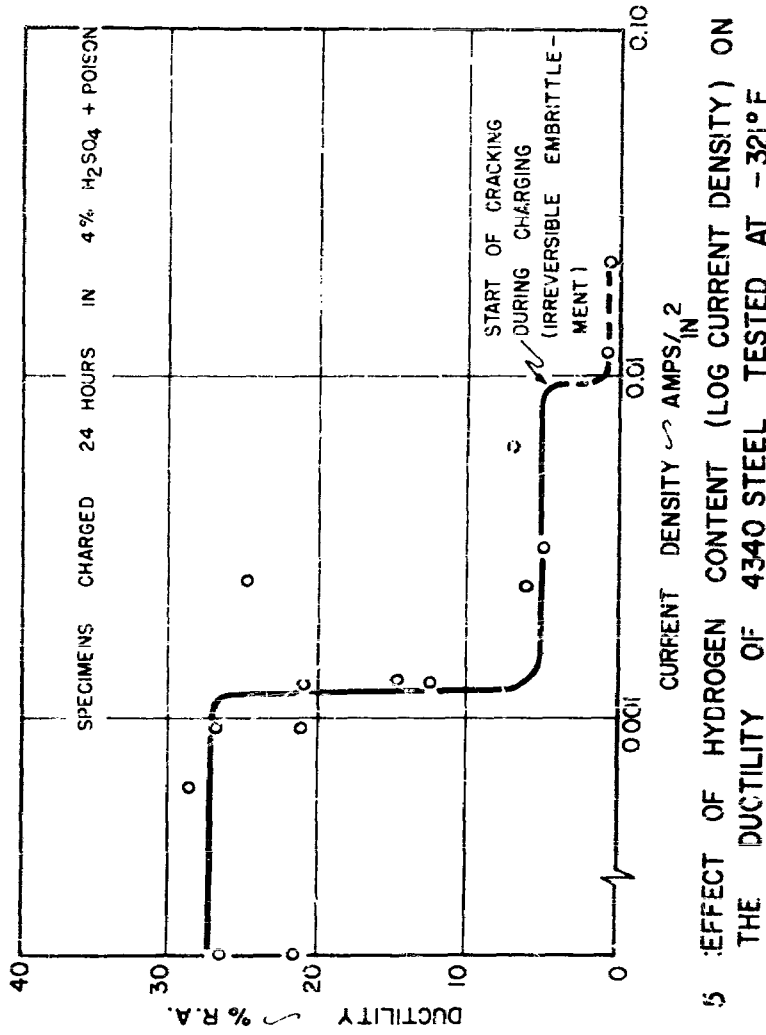


FIG. 5 EFFECT OF HYDROGEN CONTENT (LOG CURRENT DENSITY) ON THE DUCTILITY OF 4340 STEEL TESTED AT -32°F.

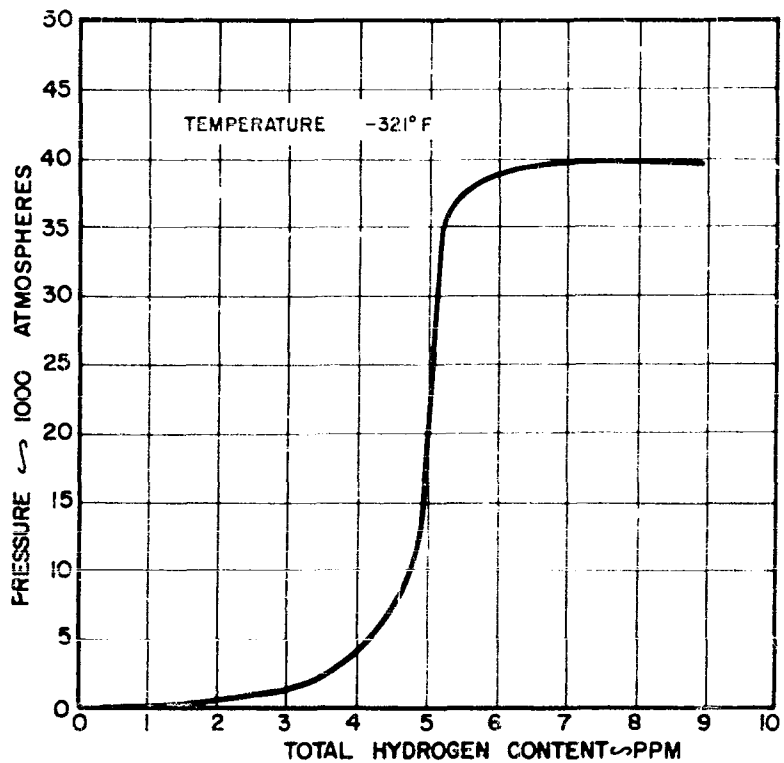


FIG.6 :RELATIONSHIP BETWEEN PRESSURE AND HYDROGEN CONTENT CALCULATED BY METHOD OF DE KAZINCY(11) FOR STEEL WITH 0.008% VOIDS.

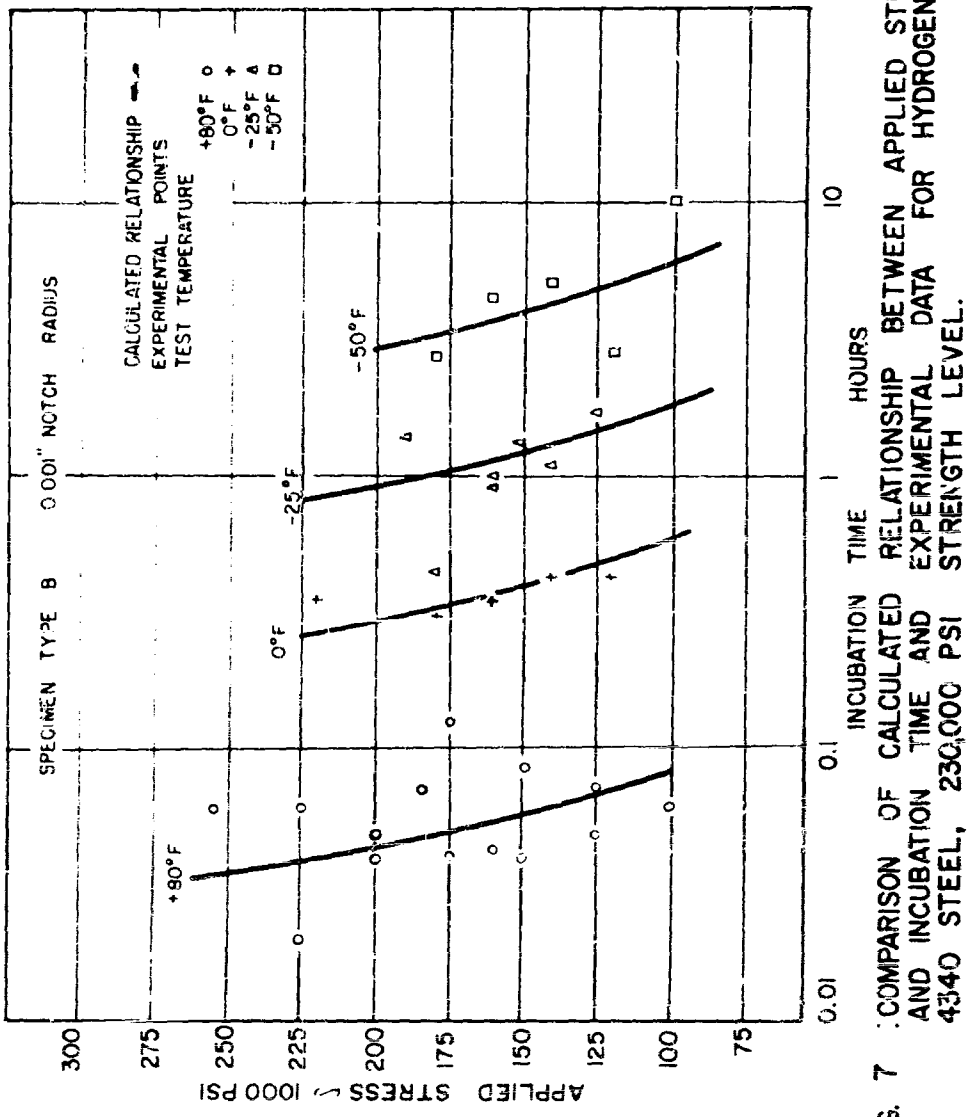


FIG. 7 COMPARISON OF CALCULATED RELATIONSHIP BETWEEN APPLIED STRESS AND INCUBATION TIME AND EXPERIMENTAL DATA FOR HYDROGENATED 4340 STEEL, 230,000 PSI STRENGTH LEVEL.

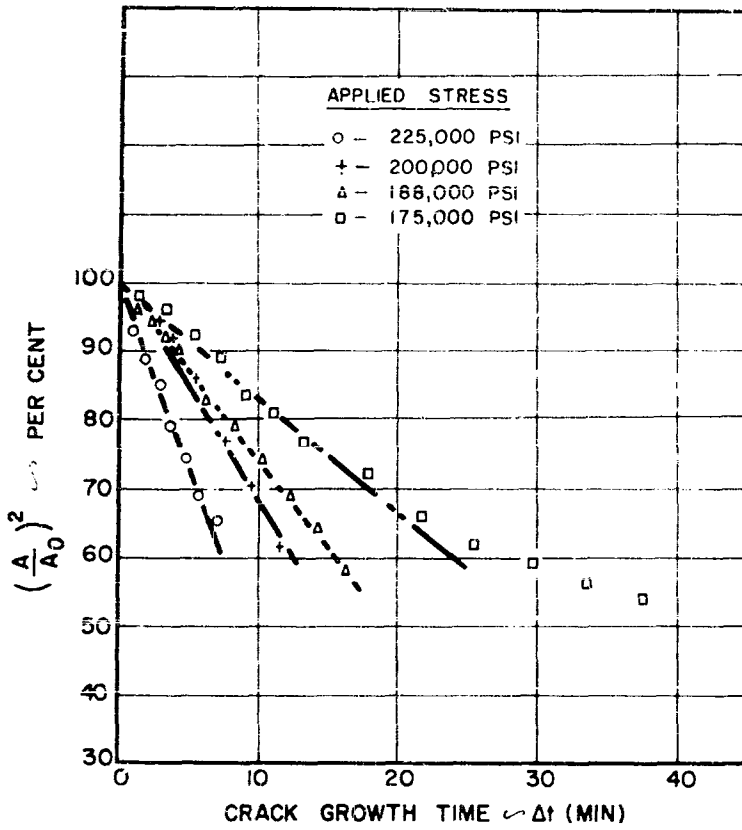


FIG. 8 : RELATIVE CHANGE IN CRACK AREA AS A FUNCTION OF CRACK GROWTH TIME FOR HYDROGENATED 4340 STEEL, 230,000 PSI STRENGTH LEVEL.

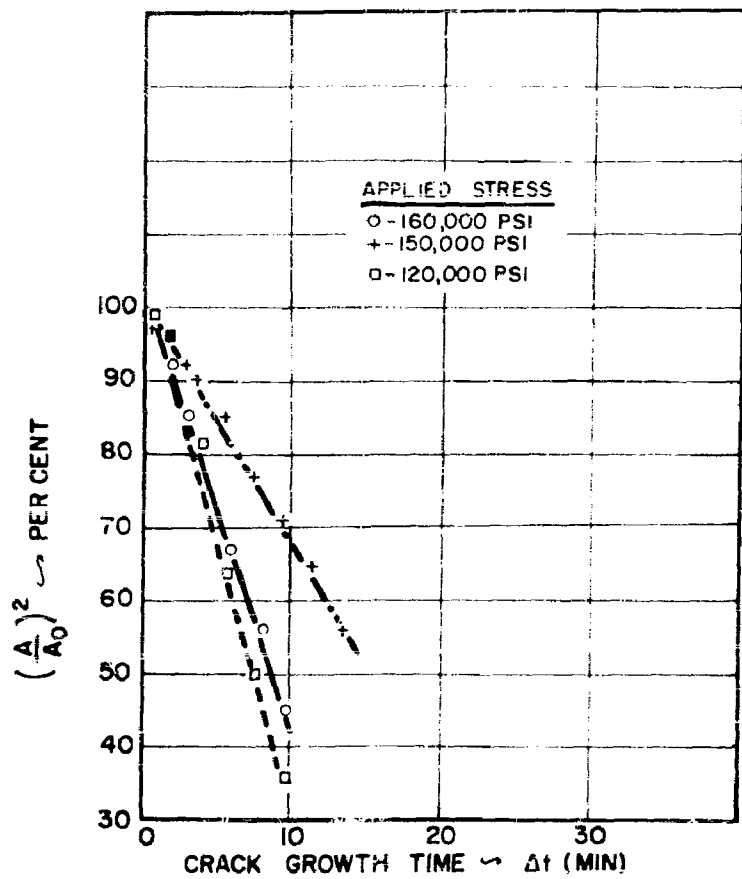


FIG. 9 RELATIVE CHANGE IN CRACK AREA AS A FUNCTION OF CRACK GROWTH TIME FOR HYDROGENATED 4340 STEEL, 230,000 PSI STRENGTH LEVEL.

SECTION II

HYDROGEN EMBRITTLEMENT AND STRAIN AGING
IN TITANIUM ALLOYS

R. J. Quigg
A. R. Troiano

ABSTRACT

Low strain rate embrittlement in titanium alloys can be classified as a strain aging phenomenon. Prestraining and aging an alpha-beta titanium alloy resulted in a ductility minimum at some intermediate aging time. It appears that hydrogen migrates to a region of inhomogeneous strain, where a high stress state exists, and creates this embrittlement. The restoration of ductility at long aging times was attributed to the low temperature recovery with subsequent redistribution of hydrogen.

Low strain rate hydrogen embrittlement was obtained for an alpha alloy and a beta alloy. Hydrogen in small quantities seemed to aid creep resistance in the alpha alloy. The beta alloy was resistant to nominal quantities of hydrogen (420 ppm), but did show embrittlement at higher levels.

LIST OF TABLES

	Page
I. Composition of Titanium Alloys	40
II. Effect of Prior Heat and Stress on the Room Temperature Ductility of Ti-140A	47

LIST OF FIGURES

Figure	Page
1. Specimen Types Used in This Investigation	61
2. Applied Stress for Delayed Failure and Reduction in Area at Failure for C-130AM Alloy, 200 PPM Hydrogen, 170,000 PSI Strength Level, Unnotched Specimens	62
3. Applied Stress for Delayed Failure and Reduction in Area at Failure for C-130AM Alloy, 260 PPM Hydrogen, 170,000 PSI Strength Level, Unnotched Specimens	63
4. Applied Stress for Delayed Failure and Reduction in Area at Failure for C-130AM Alloy, 330 PPM Hydrogen, 170,000 PSI Strength Level, Unnotched Specimens	64
5. Applied Stress for Delayed Failure and Reduction in Area at Failure for C-130AM Alloy, 80 PPM Hydrogen, 170,000 PSI Strength Level, Unnotched Specimens	65
6. Applied Stress for Delayed Failure and Reduction in Area at Failure for C-130AM Alloy, 20 PPM Hydrogen, 170,000 PSI Strength Level, Unnotched Specimens	66
7. Applied Stress for Delayed Failure and Reduction in Area at Failure for C-130AM Alloy, 420 PPM Hydrogen, 170,000 PSI Strength Level, Unnotched Specimens	67
8. Typical Stress-Strain Curve for C-130AM Alloy, Quenched and Aged, 170,000 PSI Strength Level	68
9. Typical Stress-Strain Curve for C-130AM Alloy, Annealed Condition, 140,000 PSI Strength Level	69
10. Applied Stress for Delayed Failure and Reduction in Area at Failure for C-130AM Alloy, 15 PPM Hydrogen, Annealed Condition, Unnotched Specimens	70
11. Applied Stress for Delayed Failure and Reduction in Area at Failure for C-130AM Alloy, 80 PPM Hydrogen, Annealed Condition, Unnotched Specimens	71
12. Applied Stress for Delayed Failure and Reduction in Area at	

LIST OF FIGURES (CONT.)

Figure		Page
	Failure for C-130AM Alloy, 430 PPM Hydrogen Annealed Condition Unnotched Specimens	72
13	Effect of Test Temperature on Strength and Ductility of C-130AM Alloy, 250 PPM Hydrogen, 170,000 PSI Strength Level Unnotched Specimens, .05 in./in/min Strain Rate	73
14	Effect of Aging Time at Room Temperature on Final Strength and Ductility of C-130AM Alloy, Prestrained 6 percent, 250 PPM Hydrogen 170,000 PSI Strength Level Unnotched Specimens	74
15	Effect of Aging Time at Room Temperature on Final Strength and Ductility of C-130AM Alloy Prestrained 6 percent, 80 PPM Hydrogen 170,000 PSI Strength Level Unnotched Specimens	75
16	Effect of Aging Time at Room Temperature on Final Ductility of C-130AM Alloy Containing 20 or 420 PPM Hydrogen, Prestrain 4 - 6 percent 170,000 PSI Strength Level, Unnotched Specimens	76
17.	Effect of Aging at 32° F and 75° F on Final Ductility of C-130 AM Alloy Prestrained 6 percent 300 PPM Hydrogen 170,000 PSI Strength Level	77
18.	Effect of Aging Time at 125° F and 175° F on Final Ductility of C-130AM Alloy Prestrained 6 percent 300 PPM Hydrogen, 170,000 PSI Strength Level	78
19.	Effect of Aging Time at 500° F on Final Strength and Ductility of C-130AM Alloy, Prestrained 6 percent, 80 PPM Hydrogen, 170,000 PSI Strength Level, Unnotched Specimens	79
20.	Effect of Aging Time at Room Temperature on Final Strength and Ductility of C-130AM Alloy, Prestrained 6 percent, Aged 120 hrs at Room Temperature then Prestrained Again 4 percent, 250 PPM Hydrogen, 170,000 PSI Strength Level, Unnotched Specimens	80
21.	Electrical Resistance Versus Time for Sharp Notched Speci-	

LIST OF FIGURES (CONT.)

Figure		Page
	mens Under Static Load After Daniels, Quigg, and Trotano (7)	81
22.	Notched Stress Rupture Curves for A-110AT Alloy at Various Hydrogen Levels	82
23.	Evidence of Crack Growth in the A-110AT Alloy	83
24.	Applied Stress for Delayed Failure and Reduction in Area at Failure for 5Al-2.5Sn Alloy, 100 PPM Hydrogen, Unnotched Specimens	84
25.	Applied Stress for Delayed Failure and Reduction in Area at Failure for 5Al-2.5Sn Alloy, 285 PPM Hydrogen, 140,000 PSI Strength Level, Unnotched Specimens	85
26.	Applied Stress for Delayed Failure and Reduction in Area at Failure for 5Al-2.5Sn Alloy, 690 PPM Hydrogen, Unnotched Specimens	86
27.	Effect of Test Temperature on Strength and Ductility of A-110AT Alloy, 45 PPM Hydrogen, Unnotched Specimens, .05 in/in/min Strain Rate	87
28.	Typical Stress-Strain Curve for A-110AT Alloy, 140,000 PSI Strength Level	88
29.	Delayed Failure Curves for B-120VCA Alloy, 150 - 720 PPM Hydrogen, Sharply Notched Specimens	89
30.	Delayed Failure Curves for B-120VCA Alloy 720 and 1150 PPM Hydrogen, Sharply Notched Specimens	90
31.	Applied Stress for Delayed Failure and Reduction in Area at Failure for B-120VCA Alloy, 150 and 420 PPM Hydrogen, Unnotched Specimens	91
32.	Applied Stress and Reduction in Area at Failure for B-120VCA Alloy, 720 and 1150 PPM Hydrogen, Unnotched Specimens	92
33.	Delayed Failure Curves for B-120VCA Alloy, 150 - 1250 PPM Hydrogen, Mild Notched Specimens	93

1 INTRODUCTION

Hydrogen has been associated with several modes of embrittlement. One common form is low strain rate embrittlement or "delayed failure" where failures can occur under static loading at lower stresses than normal creep failures would be expected. Another form is an embrittlement most pronounced at impact speeds. This type is generally obtained when a hydride is present in the material.

The object of this investigation is to show the many similarities between low strain rate hydrogen embrittlement in titanium alloys and conventional strain aging as might be attributable to nitrogen or carbon in steels. A mechanism for hydrogen embrittlement of titanium alloys might then be evolved.

Another objective in this investigation is to evaluate the effects of hydrogen on an alpha and on a beta alloy. Since many theories of low strain rate hydrogen embrittlement require an alpha-beta interface, the incidence of hydrogen-induced delayed failure in the alpha or the beta alloys would tend to make this an untenable supposition. Evaluation of the single phase alloys should also aid in gaining an understanding of the overall problem of hydrogen in titanium.

Since this report deals with several diverse but fundamentally related subjects each topic will be introduced separately and then correlated in the discussion. The topics are as follows:

1. Hydrogen Embrittlement
2. Strain Aging
3. Creep
4. Titanium Alloy Systems

1. HYDROGEN EMBRITTLEMENT

Hydrogen has been shown to have an embrittling effect in titanium, steel, nickel, vanadium, zirconium and molybnum. Of these, the first two have received the most attention.

Unalloyed titanium has been reported to be most sensitive to hydrogen

embrittlement at impact speeds (1)*. Since the solubility is quite low (approximately 30 ppm), titanium hydride (TiH) can be readily formed. This hydride is said to have either a face centered cubic or a face centered tetragonal structure (1).

Alpha stabilizing additions, such as aluminum, seem to greatly increase the solubility of hydrogen in titanium and, consequently, lower the sensitivity of the alloy to hydride-induced impact embrittlement (2). Alpha alloys, however, appear to be somewhat sensitive to low strain rate embrittlement (3) (4) (5).

By far the most extensively investigated phase of hydrogen embrittlement in titanium is the alpha-beta alloys. These alloys are sensitive to hydrogen at low strain rates, thus, hydrogen is able to induce failures over a wide range of stresses. One of the alloys extensively studied for this hydrogen-induced delayed failure was the 4 Al - 4 Mn alloy (C-130 AM) (6) (7) (8).

Hydrogen-induced delayed failure has been shown to be a process of crack initiation and crack growth (6). It is dependent upon microstructure, the greater the amount of the alpha phase, the wider the range of failures and upon temperature, the effects of hydrogen disappearing at both high and low temperatures (7) (8) (9). Hydrogen-induced delayed failure also appears to be dependent on strength level although some controversy exists on this point (10) (11). It is also dependent on the type of alloying addition employed (12).

Beta titanium alloys have had the least amount of study of any of the allotropic modifications. The solubility of hydrogen in beta is quite high and from the meager data available, these alloys seem to be resistant to the effects of hydrogen (3) (4).

The effect of hydrogen in steel is in many ways similar to that in alpha-beta titanium alloys (13) (14). In both cases the influence of hydrogen is most pronounced at lower strain rates and in both cases the embrittlement process is one of crack initiation and crack growth.

There are several major differences between the steels and alpha-beta titanium alloys. The amount of hydrogen required to embrittle titanium alloys is an order of magnitude greater than in steel. Steels will outgas at room temperature, titanium alloys will not. Titanium forms a hydride, steel does not. Also, titanium alloys creep a significant amount

* Numbers in parentheses refer to references listed in the Bibliography

at room temperature while little or no creep is found in steels at this temperature.

2. STRAIN AGING

Strain aging may be defined as "the changes which are obtained when a cold worked material is aged at some temperature below the recrystallization temperature." These changes are generally manifested by an increase in hardness, yield strength and tensile strength, a lowering of ductility or impact resistance and the reappearance of a yield point (15) (16) (17)

A Strain Aging and the Yield Point in Steels

Strain aging is most potent in low carbon steels although very few steels are completely non-aging. The yield point is also generally a low carbon phenomenon, but Fritzsche has reported a yield point with up to 70% C in a spheroidized structure (18).

Aging after cold work can take place at room temperature or up to 400°F. The higher the temperature the shorter the aging time required to obtain maximum strain aging effects. A common experimental aging time would be three hours at 200°F. Overaging is quite sluggish, at least as compared to quench aging (19). At higher temperatures (300° - 700°F) aging can become so rapid that it would seem to take place during the deformation process itself. This phenomenon is called "blue brittleness." The temperature of embrittlement is lower in a tensile test than in the higher speed impact test. "Blue brittleness" is often termed spontaneous strain aging.

Apparently the amount of strain aging obtained is relatively independent of the degree of cold work (as long as it is greater than 2%). Generally, from 6 to 15% cold work is quite common (20).

A yield point is generally found in strain aging steels. Cold work will cause the disappearance of this yield point, but additional aging results in its restoration at a higher load. The time and temperature combinations necessary for the return of the yield point are quite similar to those required for maximum strain aging. Pilling, however, has stated that yield strength and tensile strength may have increased materially before the yield point reappears (21).

Both strain aging and the yield point have been conclusively attributed to nitrogen and/or carbon. Low and Gensamer (20) and Fast (22) showed

that when carbon and nitrogen were eliminated from a steel (either by using very high purity iron or a wet hydrogen treatment), then no yield point or strain aging was obtained. When this material was carburized or nitrided, strain aging and the yield point returned. Nitrogen was found to be the principal cause of both phenomena at room temperature, while carbon was the major cause at elevated temperatures (300°F or above).

Hydrogen can suppress the yield point obtained at room temperature in mild steel (23). Also, hydrogen has been shown to create a yield point at very low temperatures (-150°C) (24).

Some alloying additions to steel, such as aluminum, silicon, titanium, boron, vanadium, or chromium, tend to minimize strain aging (16) (25). This can be primarily attributed to the formation of stable nitrides and carbides with these additions. Slow cooling will aid the formation of these compounds and, hence, enhance the resistance to strain aging.

Cottrell has presented a workable mechanism for the yield point in iron (26, 27). Cottrell predicts that the interstitial solute atoms, carbon and nitrogen, tend to form a "cloud" or "atmosphere" which prevents dislocation movement. When sufficient stress is applied, the dislocations will break away from this cloud and move without increase in load. Cold work or prestrain causes the dislocations to break free, but if a sufficient time interval elapses (aging time), the interstitial solute atoms will form another "cloud" and a yield point is again obtained.

B Strain Aging in Titanium

Strain aging and its associated effects on mechanical properties have been detected in unalloyed commercial purity titanium (28) (29). Rosi and Perkins have shown the incidence of yield points ($117\text{-}282^{\circ}\text{C}$), ductility minima ($232\text{-}452^{\circ}\text{C}$), and serrated stress-strain curves ($452\text{-}652^{\circ}\text{C}$). The yield points obtained could be removed by cold work and then returned by aging in a manner much similar to that employed for mild steel.

Makrides showed evidence of strain aging in an all alpha titanium alloy (5 Al - 2.5 Sn) (30). The temperature ranges of ductility minima obtained were quite dependent on the strain rate, varying from $200\text{-}400^{\circ}\text{C}$ at average testing speeds (.05 in/in/min) to $600\text{-}700^{\circ}\text{C}$ at impact speeds (19,000 in/in/min). This variation with strain rate was so great that stress rupture data at intermediate temperatures revealed a ductility minimum at an intermediate time (or strain rate) normal ductility being obtained at either very short or very long times. Makrides attempted, with little success, to isolate this strain aging effect, evaluating carbon, nitrogen, and oxygen.

Low strain rate hydrogen embrittlement of alpha-beta titanium alloys has been called a strain aging phenomenon by Burte (31). In this mechanism hydrogen is said to segregate to grain boundary regions after plastic deformation. No reference was made to other more classic forms of strain aging in this paper.

C. Strain Aging in Magnesium Alloys

Toaz and Rippling found ductility minima attributable to strain aging in a series of magnesium-lithium alloys (32). They investigated pure magnesium, Mg - 4 Li (C. P. H.), Mg - 6 Li (mixed C. P. H. and B. C. C.), and Mg - 11 Li (B. C. C.). Only the alloys containing lithium exhibited a ductility minimum. These minima were both strain rate and temperature sensitive. The alloys containing 6 and 11% lithium also had serrated stress-strain curves.

3. CREEP

The fact that titanium alloys creep considerably at low temperatures must be considered in evaluating the hydrogen sensitivity of these alloys (7). Also strain aging may have an effect on creep properties (33) (27).

Creep may be defined as "time dependent plastic deformation" (7). There are two basic modes of creep deformation, crystallographic slip (dislocation glide) and grain boundary flow. Generally slip is operative at low temperatures and grain boundary flow at high temperatures. The transition temperature between the two where the grain boundaries and the grains are considered to be of equal strength has been termed equi-cohesive temperature (ECT) (34).

Creep is a thermally activated process. It is in effect a combination of applied stress and thermal fluctuations (35). The activation energy for creep in titanium at 210°F has been calculated to be approximately 3500 calories per mole (36).

Generally, in a creep process there is (1) formation (2) movement and (3) rearrangement or annihilation of dislocations (35). Dislocation movement causes dislocation interaction with impurities (solute atoms clouds, or precipitates), grain boundaries, and other dislocations. One of the results of this is work hardening. Tending to offset this work hardening is recovery.

4. TITANIUM ALLOY SYSTEMS

Pure titanium undergoes an allotropic modification at 880°C; the high temperature phase (beta) is body-centered cubic and the low temperature phase (alpha) is hexagonal close-packed. The transformation temperature can be raised with alpha stabilizing additions, such as Al, Sn, O, or N, or lowered with such beta stabilizing additions as Mo, Mn, V, Fe, or Cr. If sufficient beta stabilizers are alloyed with titanium, it is possible to obtain a two-phase alpha-beta structure or even a completely beta structure at room temperature.

Unlike the other interstitial elements, hydrogen stabilizes the beta phase. The beta transformation temperature is lowered approximately 10°F per 100 ppm (by weight) hydrogen.

The results of this report are divided into three separate divisions with a discussion for each part. These divisions are as follows.

- 1 Strain Aging and Hydrogen Embrittlement in an Alpha-Beta Titanium Alloy
- 2 Effects of Hydrogen on an Alpha Titanium Alloy
3. Effects of Hydrogen on a Beta Titanium Alloy

All three divisions are summarized at the close of the report.

II. MATERIAL AND PROCEDURES

I. MATERIAL

A. Alpha-Beta Alloy

The alpha-beta titanium alloy employed was a 4 Al-4 Mn alloy (C130AM). This material was obtained from Rem-Cru Titanium Inc as 5/8 inch round bar stock. It had been hot rolled in the alpha-beta region and the "as received" tensile strength was about 140,000 psi. All of the material was from a single heat. The chemical analyses are summarized in Table I.

B. Alpha Alloy

The alpha titanium alloy used was a 5 Al-2.5 Sn alloy (A110AT). It was obtained from Crucible Steel as 5/8 inch bar stock. Its "as received" tensile strength was also approximately 140,000 psi. The chemical analyses of the heat employed are listed in Table I.

C. Beta Alloy

The work performed on beta material was done on a 13 V - 11 Cr - 3 Al alloy (B120 VCA). This material was secured from Crucible Steel as 1/2" bar stock. Its "as received" tensile strength was approximately 155,000 psi. The chemical analyses of the heat used are shown in Table I.

TABLE I
COMPOSITION OF TITANIUM ALLOYS

Trade Design	Nominal Composition	H (ppm)	Al	Mn	Sn (Weight Percent)	Cr	V	C	N
C130AM	4 Al-4 Mn	80	3.9	3.8	-	-	-	.01	.01
A110AT	5 Al-2.5 Sn	46	5.0	-	2.7	-	-	-	.04
B120VCA	13V-11Cr-3Al	150	4.1	-	-	11.1	12.8	.02	.03

2 SPECIMEN PREPARATION

A. Hydrogenation Technique

Hydrogen was introduced into the material used in this investigation by a thermal charging technique. The hydrogen charging was performed prior to heat treatment of the alloys. Rough machined tensile specimens were heated to either 1200°F or 1250°F in a hydrogen atmosphere for varying periods of time, depending on the hydrogen level desired, and then furnace cooled. Hydrogen contents were checked by analysis (vacuum extraction).

When very low hydrogen contents were desired, vacuum annealing was employed. In this process the specimens were heated to 1400°F under vacuum. Hydrogen contents as low as 10 ppm could be obtained in this manner.

B. Post-Hydrogenation Heat Treatments

In most cases the alpha beta alloy (4 Al - 4 Mn) was used in a high strength quenched and aged condition. The solution treatment was conducted in air without measurable loss of hydrogen. The specimens were quenched in water and then aged in a salt bath at some intermediate temperature. A typical heat treating cycle for material containing 250 ppm hydrogen would be one hour at 1575°F, water quench, and then age one hour at 1040°F. This results in a strength level of approximately 170,000 psi.

The annealing cycle used on this alpha-beta alloy was one hour at 1500°F and furnace cool at a rate of 5°F per minute to 1100°F. This resulted in a strength level of 140,000 psi.

The beta alloy (13 V - 11 Cr - 3 Al) had to be re-solution treated to dissolve the TiCr₂ which formed during slow cooling after hydrogenation. The treatment used was one hour at 1500°F and water quench. Normal ductility is then restored. Strengthening could be obtained in this material by merely heating to 800° or 900°F to precipitate the chromium eutectoid.

C Specimen Types and Geometries

Specimen sizes and notch geometries employed in tensile and stress-rupture tests are indicated in Fig. 1. Note that the "unnotched" specimens actually have a two inch notch radius. All material was rough machined before hydrogenation and heat treatment with .030 inches of stock left for finishing. After finish machining the unnotched specimens were polished longitudinally to remove machining marks. This was done to eliminate localized stress-risers resulting from transverse scratches.

D Metallography

Specimens were prepared for metallographic examination by mechanical polishing and then etching with a reagent consisting of 1 part HF, 1 part HNO_3 , and 6 parts glycerine.

3. EXPERIMENTAL PROCEDURES

A. Stress Rupture and Tensile Testing

Stress rupture and tensile tests were performed with concentric alignment fixtures which insured a minimum of eccentricity. Tensile tests were carried out at a constant head travel speed of 0.05 inches per minute. A standard, lever arm type stress rupture machine was employed for creep and delayed failure tests.

B Testing and Aging at Other than Ambient Temperature

Tensile tests were performed at low temperatures using either liquid nitrogen or dry ice (CO_2) in pentane as a refrigerant. Testing at elevated temperatures was carried out in air in resistance heated furnaces with the temperature controlled to $\pm 5^{\circ}F$.

Aging at $32^{\circ}F$ was performed in an ice water bath. Aging at moderate elevated temperatures (125° - $175^{\circ}F$) was accomplished in a heated oil bath while aging at the higher temperature ($500^{\circ}F$) was done in a circulating air furnace.

C Study of Crack Growth and Creep

Crack propagation and creep deformation during delayed failure tests were studied by the electrical resistance technique developed by Barnett and Troiano (37). This method utilized a Kelvin double-bridge circuit to measure changes in electrical resistance across the notch cross-section resulting from plastic flow or crack propagation. The sensitivity of the instrument is of the order of 3×10^{-8} ohms. The initial electrical resistance across a sharp notch is about 2×10^{-4} ohms.

III RESULTS AND DISCUSSION

1. STRAIN AGING AND HYDROGEN EMBRITTLEMENT IN AN ALPHA-BETA TITANIUM ALLOY

Hydrogen embrittlement can be likened to other more classic strain aging systems. The following sections describe some of these similarities for an alpha-beta titanium alloy, 4 Al-4 Mn (C130AM).

A Effect of Hydrogen on the Ductility Obtained after Stress Rupture Testing of Unnotched Specimens

It has been illustrated that an alpha-beta titanium alloy may be quite ductile when tested in a normal tensile test yet be embrittled at very low strain rates (6). This embrittlement at low strain rates is obtained at an intermediate hydrogen level. Hydrogen contents greater than this intermediate range will create an embrittlement at all testing speeds; hydrogen contents below this level will cause no embrittlement. With the C130AM alloy treated to 170,000 psi by quenching and aging, the tensile ductility obtained at normal testing speeds is lowered by hydrogen contents in excess of 430 ppm (7). Thus, approximately 250 ppm hydrogen would probably be an intermediate level where low strain rate embrittlement might take place, but normal ductility could be obtained in a simple tensile test.

A wide variety of low strain rates can be simulated with the stress rupture test. By measuring ductility in this test, one can obtain an approximation of the influence of strain rate on ductility at a given hydrogen level. Data for the C130AM alloy, strengthened to 170,000 psi, and containing 200 ppm hydrogen are shown in Fig. 2. Note that ductility remains essentially constant for failure times less than two hours but then drops off rapidly, reaching a minimum near nine hours. With failure times greater than twenty hours, however, ductility is gradually restored until at very long times normal ductility is again obtained. A similar behavior is encountered for material containing 260 and 330 ppm hydrogen as is shown in Figs. 3 and 4.

This ductility minimum is caused by hydrogen as evidenced by examining this alloy at lower hydrogen levels. Data for material containing 80 ppm (the as-received hydrogen content) are illustrated in Fig. 5. It is obvious from this figure that no ductility minimum is obtained. Material vacuum annealed to 20 ppm showed no evidence of a minimum in fact ductility increased at lower strain rates, Fig. 6.

At very high hydrogen levels ductility was lowered somewhat at low

strain rates but no recovery was obtained at long times. Data for material containing 420 ppm hydrogen are shown in Fig. 7. Note that at this hydrogen level some lowering in normal tensile ductility was encountered.

A ductility decrease at low strain rates is not unexpected on the basis of previous studies (1, 6, 7, 31). This type of ductility loss would be most prevalent at intermediate hydrogen contents where randomly distributed hydrogen causes no embrittlement. If some driving force for the agglomeration of hydrogen exists, then diffusion of hydrogen to a specific region could enable sufficient hydrogen to accumulate so that brittleness would result. This agglomeration to a region of high stress has been pictured for a notched specimen where triaxial stresses exist (7). For an unnotched specimen such as was used in obtaining Figs. 2-6, inhomogeneous plastic deformation apparently can create regions to which hydrogen can diffuse, accumulate, and then cause embrittlement. Thus, the time delay for embrittlement is needed for (a) sufficient plastic deformation to take place and (b) diffusion and accumulation of hydrogen. The actual manner in which hydrogen embrittles will be discussed later in the report.

The return of ductility at long times (or very low strain rates) could be more easily rationalized if the ductility minimum were looked upon as a strain aging phenomenon. Generally, strain aging is quite strain rate and temperature dependent. For example, a ductility minimum could be obtained as much as 400°F lower at very slow strain rates than at very fast strain rates (30). Hence, it is indeed possible that at a temperature between the two ductility would be normal at both high and very low strain rates, but some embrittlement would be obtained at an intermediate strain rate. Temperatures where this was the case were successfully located for strain aging attributable to nitrogen and carbon in titanium alloys at 1000°F by Makrides and Gurev and Baldwin (30) (38).

Cottrell has developed an empirical equation to predict the temperature where strain aging might occur based on data obtained on steels (27). This equation is as follows:

$$\left(\frac{D}{\epsilon^0} \right)^{1/2} = 10^{-5} \text{ cm}$$

where D = diffusivity in cm^2/sec

ϵ^0 = strain rate in $1/\text{sec}$.

Apparently an equation of this nature can also apply to titanium. Using Gurev and Baldwin's data of carbon-induced strain aging in alpha titanium

at 1000°F , a number on the order of 10^{-3} cm is obtained. A similar number is obtained for the hydrogen-induced strain aging of Figs. 2-4. The similarity between the number obtained for a known strain aging interstitial (carbon) and that obtained for hydrogen lends further support to the postulate that hydrogen can induce a strain aging effect. Apparently the exact magnitude of the equation depends on the material being evaluated.

If the hydrogen-induced ductility minima of Figs. 2-4 were thought of as being part of a strain aging phenomenon, then ductility recovery at very low strain rates would be expected. The migration of hydrogen to regions of inhomogeneous strain could also be incorporated in this strain aging mechanism.

B Relation of Hydrogen Effects to Other Strain Aging Criteria

In the previous section explanations of hydrogen-induced low strain rate embrittlement and the lack of this embrittlement at long failure times have suggested a strain aging type mechanism. In order to complete the picture it is essential that other criteria of strain aging such as yield points, serrations, and temperature dependent ductility minima be evaluated.

The stress-strain curve for the C130AM alloy in the quenched and aged condition (170,000 psi strength level) and containing 250 ppm hydrogen is illustrated in Fig. 8. Note the lack of a yield point. This curve is representative of all stress-strain curves obtained on this alloy in this condition at all hydrogen levels from 20 to 330 ppm and at all temperatures from -110°F to 500°F . It is obvious that no apparent hydrogen-induced yield point is connected with the ductility minima of Figs. 2-4.

The incidence of a yield point in alpha-beta titanium alloys is not uncommon. With the C139 AM alloy in the low strength annealed condition a yield point is obtained from room temperature up to 650°F . A typical example is shown in Fig. 9. At 650°F a series of yield points are obtained much like "serrations" in mild steels. Hydrogen contents up to 430 ppm seemed to have no effect on this yield point at room temperature and above. The yield point could be suppressed by cold work but returns with aging.

Unnotched stress rupture data for the C130 AM in the annealed condition revealed no tendency for a ductility minimum with either 15, 80 or 430 ppm hydrogen as is shown in Fig. 10, 11 and 12. Thus, it can be concluded that no connection exists between the ductility minima of Figs. 2-4 and the yield point of Fig. 9.

If the ductility minimum is truly a strain aging phenomenon, then a minimum should be obtained when ductility is plotted against temperature

This ductility minimum has been obtained by Daniels et al. on C130AM in the quenched and aged condition containing 800 ppm hydrogen (7). Ductility minima on Ti140A (2 Cr - 2 Mo - 2 Fe) have been obtained by Williams, et al. (4) and by Rippling (9). At normal testing speeds the minimum is generally found at room temperature or slightly below. In general, most authors are in agreement that the disappearance of hydrogen embrittlement at low temperatures can be attributed to the lowered diffusivity of hydrogen, while the disappearance at high temperatures is due to the increased solubility of hydrogen.

Since at normal testing speeds the C130AM alloy containing 200-330 ppm hydrogen was sufficiently ductile at room temperature, it was felt that possibly a minimum in ductility could be discovered at a slightly higher temperature because of greater diffusivity. The data of Fig. 13 show that no minimum was obtained. This is not unexpected since the solubility of hydrogen increases quite rapidly with rising temperature in this range.

C Effect of Prestraining and Aging on Final Ductility of Hydrogenated Material

If hydrogen is migrating to the regions of inhomogeneous plastic deformation as was postulated in part I of this section, there would be no need for a constant applied load as is obtained in a stress rupture test, but rather a plastic prestrain followed by removal of the load could serve also to provide a driving force for agglomeration of hydrogen. If sufficient hydrogen were able to accumulate, then some ductility effects could be detected.

The influence of aging at room temperature on the ductility of prestrained tensile specimens containing 250 ppm hydrogen can be seen from Fig. 14. It is apparent from this figure that final ductility is dependent upon the aging time. The shape of this curve is roughly comparable to the ductility vs. failure time curves of Figs. 2-4. Like the stress rupture curves, a loss of ductility was obtained after aging for 6 hours and this embrittlement was recoverable after long time aging.

This ductility minimum is not obtained at lower hydrogen levels using this prestrain method. These data are shown for 80 ppm hydrogen in Fig. 15 and for 20 ppm in Fig. 16A. At higher hydrogen levels, such as 420 ppm, where some embrittlement is encountered in a normal tensile test, evidence of a ductility minimum is also obtained, Fig. 16B.

It is evident that hydrogen creates a time dependent embrittlement after aging for some time greater than one hour at room temperature pro-

video that such accumulation of strain is present to provide a driving force for creating a high rate of diffusion. This plastic strain is probably inhomogeneous and continually applied stress is required. The stress causes little or no strengthening of the material.

Apparently plastic strain applied at an elevated temperature can also serve to aid in the accumulation of hydrogen. For example observe the following data of Burte, Erbin, et al. on Ti140A (39).

TABLE II

EFFECT OF PRIOR HEAT AND STRESS ON THE ROOM TEMPERATURE DUCTILITY OF Ti140A

Stress	Previous Treatment		R. A.	
	Temp.	Time	20 ppm	250 ppm
As Annealed				
95,000	70°F	500 hr.	56	49
80,000	200	100	55	43
80,000	200	500	55	27
50,000	600	100	51	30
50,000	600	500	54	37

It is possible that hydrogen diffused to the regions of plastic deformation at room temperature while the specimens were awaiting testing. If this is the case, then the stress rupture test served only to strain the material plastically. It is unlikely that 250 ppm of hydrogen could create any embrittlement at 600°F.

The variation of the ductility minimum with temperature is illustrated in Figs. 17 and 18. Note that the minimum is shifted to shorter times with decreasing temperatures below 125°F. This would indicate a diffusion dependent phenomenon. A rough approximation of the activation energy of this process (10,000 cal/mole) can be obtained from these three points. The activation energy for diffusion in C130AM has been reported as 9000 cal/mole (1); in alpha titanium, it is 12,380 cal/mole and in beta titanium 5640 cal/mole (40).

At 175° F the ductility minimum is shifted to a longer time. This may be attributed to the increase in the solubility of hydrogen at higher temperatures. A greater quantity of hydrogen must accumulate in order to achieve the proper conditions for embrittlement. Daniels, et al obtained longer failure times in notched specimens at elevated temperatures (7). They attributed this to the increased solubility and decreased driving force obtained at elevated temperatures.

The data obtained appear to support the concept that hydrogen migrates to the region of inhomogeneous plastic deformation (where a stress field exists). With a two phase structure it is unlikely that the alpha and beta grains will be deformed homogeneously. Also, low temperature creep will probably take place by trans-crystalline slip (dislocation glide) with the grain boundaries acting as barriers. Thus, the inhomogeneous plastic deformation could create a region to which hydrogen can diffuse near the grain boundaries and the brittle fracture will emanate from this area as postulated by Burke (31). When a notched specimen is used, however, the region of inhomogeneous plastic deformation will be near the base of the notch (41) and crack initiation and propagation will begin in this vicinity comparatively independent of the grain boundary region, as has been illustrated by Daniels (7).

The restoration of ductility after long aging times may be explained by two mechanisms, (1) recovery of plastic strain and redistribution of hydrogen or (2) overaging. Low temperature recovery (often called "metarecovery") has been found in nickel, aluminum base alloys, zinc, and cadmium (42, 43). This low temperature recovery is generally attributed to vacancy migration since the temperatures at which "metarecovery" is obtained are too low for any appreciable self-diffusion which is necessary for "climb" (annihilation of edge dislocations) to take place. "Metarecovery" can occur at quite low temperatures particularly in hexagonal metals. It appears that low temperature recovery is a distinct possibility in titanium alloys. If the migration of hydrogen is to the region of inhomogeneous strain where a stress field exists, then a small amount of recovery and accompanying stress relief could cause the hydrogen to redistribute itself and eventually restore ductility.

A mechanism involving overaging would be dependent upon the precipitation of a hydride. Growth of this hydride would then result in a stable precipitate and eventual restoration of ductility.

The return of ductility with additional aging following a strain aging type embrittlement is not unique to hydrogen in titanium. Garafalo and Smith obtained what appeared to be overaging in strain-aged mild steels (19). It appears also that the strain aging attributable to carbon, nitrogen

or oxygen in alpha-beta titanium exhibits some evidence of ductility restoration. These data are shown in Fig. 19.

The embrittlement caused by hydrogen and the eventual restoration of ductility can be explained by several mechanisms. Of these, the following appear plausible.

1 Hydrogen accumulates and embrittles while present in solution. Recovery of plastic strain diminishes the driving force and causes the hydrogen to resume an equilibrium distribution.

2 Hydrogen accumulates and precipitates as a fine hydride which decomposes upon recovery of plastic strain causing restoration of ductility.

3 Hydrogen accumulates and precipitates as a fine hydride which causes embrittlement. Additional aging causes this hydride to grow and overaging is accomplished.

4 Hydrogen causes embrittlement while in solution. Hydride precipitation results in restoration of ductility.

If hydrogen were merely redistributed or randomized by a recovery process at long aging times, then it would seem plausible that the entire process could be reversible, i.e. re-prestraining and aging would again create a time dependent ductility minimum. If, however, a stable hydride were the end result of this aging process, then it would be unlikely that recycling would again produce a ductility minimum.

Data for the C130AM alloy prestrained 6%, aged for 120 hours at room temperature, then restrained an additional 4%, and aged for varying lengths of time are illustrated in Fig. 20. From this figure it is quite evident that a ductility minimum is again obtained after the second prestrain and subsequent aging. These data seem to indicate that overaging or growth of a stable hydride did not cause the restoration of ductility in Figs. 2-4 and Figs. 14-17 and 18, but rather that the resumption of ductility at longer times was attributable to recovery and subsequent redistribution of accumulated hydrogen. Since the randomization of segregated hydrogen would be much more difficult if a fine hydride were precipitated, the authors feel that it is more likely that hydrogen causes embrittlement while still in solution. The many similarities between hydrogen embrittlement in steel and in alpha-beta titanium tend to support this concept.

In summary, the following hypothesis can be advanced for low strain

rate hydrogen embrittlement of alpha-beta titanium.

Inhomogeneous plastic strain creates a region to which hydrogen can diffuse. This may be at the grain boundary area between alpha and beta grains where slip lines interact with grain boundaries or near the base of a sharp notch. If sufficient time elapses, recovery may take place enabling hydrogen to redistribute, and the embrittlement is minimized. Since the process is reversible with additional plastic strain, hydride precipitation does not appear to be an essential part of this model.

Hydrogen embrittlement in alpha-beta titanium can be likened to the more classic strain aging process caused by nitrogen and carbon in mild steel. No connection between hydrogen and the yield point was obtained in this investigation.

2. EFFECTS OF HYDROGEN ON AN ALPHA TITANIUM ALLOY

The object of this phase of the investigation was to evaluate the effects of hydrogen on a typical alpha titanium alloy, Al10AT (5 Al-2.5 Sn). Since the addition of aluminum increases the solubility of hydrogen in titanium, particular emphasis was placed on low strain rate embrittlement. The possibility of low strain rate embrittlement in this alloy has been reported previously (5).

Because delayed failure can either be caused by a normal creep process or by hydrogen embrittlement, it is often necessary to separate these two. With unnotched specimens the ductility obtained after a hydrogen-induced delayed failure is often less than after a creep failure. Since it is difficult to obtain exact ductility measurements with notched specimens it is often necessary to use different techniques to separate hydrogen embrittlement from creep. Daniels, Quigg, and Troiano were able to separate these delayed failure processes by using three criteria which were as follows (7) (8):

1. Electrical resistance measurements.
2. Sectioning of unbroken specimens for hydrogen-induced cracks.
3. Elevated temperature testing.

Low temperature creep is characterized by continuous flow (usually transcrystalline), generally occurring in three stages, with no measurable crack formation at least until the third stage of creep. A graphical illus-

tration of the electrical resistance changes associated with a typical creep failure is shown in Fig. 21A. When the delayed failure is caused by hydrogen, a delay period or "incubation period" is required for the formation of a crack. This crack then propagates until it is large enough for failure to occur. Electrical resistance changes for a typical hydrogen-induced crack initiation and propagation process are shown in Fig. 21B. Note from this curve that little measurable plastic deformation has taken place prior to the initiation of the crack.

Sometimes the shape of the electrical resistance curve does not clearly describe the mode of failure. In these cases, Daniels et al., recommended the stopping of the test sometime prior to failure in order to examine the specimen for cracks. If a crack were located, this would tend to indicate hydrogen-induced delayed failure rather than creep (7) (8).

As a final resort, Daniels used elevated temperature testing to separate creep and hydrogen-induced delayed failure. The thought in this case was that creep-type failures would tend to be emphasized at moderate elevated temperatures while hydrogen-induced delayed failures would be minimized at these temperatures.

In the present investigation of alpha alloys electrical resistance studies and, in some cases, sectioning of unbroken specimens were employed to separate creep failure from hydrogen embrittlement. No elevated temperature testing was conducted.

The effects of hydrogen on the notched stress rupture properties of the Al110AT alloy are illustrated in Fig. 22. Note from these curves that hydrogen in quantities up to 175 ppm decreases the range of stresses in which delayed failure can take place without greatly altering the notched tensile strength. Additional hydrogen up to 285 ppm increases the range of failures only slightly over the 175 ppm level, but again the range of stresses is not nearly as great as at the 45 ppm level. The addition of 680 ppm hydrogen lowers the notched tensile strength, but, in addition, a range of delayed failure is obtained.

Electrical resistance measurements showed quite clearly that the delayed failure obtained at the 45 ppm and 175 ppm levels were of the "creep type", i.e. the changes during the test followed a pattern similar to Fig. 21A. Electrical resistance changes at the 680 ppm level indicated that these failures were a case of hydrogen-induced delayed failure, i.e. a process of crack initiation and growth similar to that shown in Fig. 21B was outlined. Examination of the fracture surface of a specimen containing 680 ppm hydrogen revealed a pattern of concentric crack formation sustaining the hypothesis that hydrogen-induced crack initiation and growth

had caused the delayed failure. The surface of a fractured specimen containing 680 ppm is shown in Fig. 23A.

At the 285 ppm level the demarcation between creep and hydrogen-induced delayed failure was not as sharp. Electrical resistance measurements indicated a large amount of creep plus the possibility of some influence of hydrogen. Sectioning a specimen prior to failure showed the incidence of a crack, supporting the concept that hydrogen-induced delayed failure was also a factor in these failures. This crack is shown in Fig. 23B.

Since the delayed failure found at 45 ppm and 175 ppm hydrogen levels are attributable to creep, it appears that small quantities of hydrogen can greatly improve the creep resistance of this alloy without causing any embrittlement or hydrogen-induced delayed failures. This enhancement of creep resistance by hydrogen can be rationalized by consideration of the thoughts of Cottrell (27). Cottrell states for the case of transcrystalline creep that when dislocation glide first commences, the speed of the dislocation movement will either rapidly increase or quickly decelerate with subsequent interaction with other dislocations and grain boundaries. In alpha titanium it appears that hydrogen (probably in cloud form) served to hamper dislocation movement in transcrystalline creep (not necessarily to block dislocation movement), enabling dislocation and grain boundary interaction (with resultant work hardening) to take place. Thus it appears that small quantities of hydrogen can greatly aid in the minimization of low temperature creep by serving merely to decelerate moving dislocations. Hydrogen is probably the only interstitial mobile enough to create this effect at room temperature.

The data obtained at the 680 ppm hydrogen level illustrate the susceptibility of alpha alloys to hydrogen-induced delayed failure. Since the diffusion of hydrogen is quite slow in alpha titanium, long times are required for hydrogen to accumulate and cause delayed failure. The range of stresses over which hydrogen-induced delayed failure can take place is not nearly as great as in the alpha-beta alloy (7).

Unnotched stress rupture data also illustrate the incidence of low strain rate hydrogen embrittlement. Tests conducted on Al10AT containing 160 ppm hydrogen showed no embrittlement, Fig. 24 while data obtained at the 285 ppm level exhibited some embrittlement at very low strain rates, Fig. 25. At the 690 ppm hydrogen level this alpha alloy was ductile in a normal tensile test but exhibited embrittlement in all the low strain rate stress rupture tests (Fig. 26).

Apparently here, as in the alpha-beta alloy, hydrogen diffuses to

the region of inhomogeneous plastic deformation. It is probable that the driving force for accumulation of hydrogen is not as great as in the two-phase structure. Also, the diffusion of hydrogen is much slower in the alpha structure. For these reasons, the incidence of low strain rate embrittlement is not as pronounced in the alpha alloy as in the alpha-beta alloy.

Another ductility minimum at higher temperatures probably attributable to C, N, or O was located for this alpha alloy in the 600° - 1000°F range. These data are shown in Fig. 27. This is the same minimum reported by Makrides (30).

No yield point was obtained in this alloy at any temperature between -110°F and 1000°F. A typical stress-strain curve is shown in Fig. 28.

3 EFFECTS OF HYDROGEN ON A BETA TITANIUM ALLOY

With the addition of sufficient beta-stabilizing elements, an all beta structure (body-centered cubic) can be stabilized at ambient temperatures. The only commercially important beta titanium alloy is the B120VCA (13V-11Cr-3Al) alloy which was studied in this section.

Hydrogen has been reported to have a greater solubility in beta titanium (1) (4), hence, a greater resistance to the effects of nominal quantities of hydrogen might be expected for the beta alloys. At high hydrogen levels, however, both hydrogen embrittlement and hydrogen-induced delayed failure may be encountered. The object of the following investigation is to examine this beta alloy for these phenomena.

The effects of hydrogen on the notched stress rupture properties of "soft" (solution treated) B120VCA are illustrated in Figs. 29 and 30. From Fig. 29 it is apparent that hydrogen contents as high as 420 ppm did not alter the delayed failure curves. These failures are all attributable to creep (confirmed by electrical resistance). A hydrogen level as high as 1150 ppm, greatly lowered the notched tensile strength but no region of delayed failure was obtained (Fig. 30). At an intermediate level, such as 720 ppm, some embrittlement was detected in the notch tensile strength, but, in addition, a region of delayed failure was obtained. These failures at 720 ppm seemed to be hydrogen-induced delayed failures following a pattern previously described in Fig. 21B.

With unnotched specimens, the effects of 420 ppm were again virtually negligible, Fig. 31. A hydrogen content of 720 ppm had only a slight embrittling effect on the final ductility of unnotched stress rupture

specimens, Fig. 32. With 1150 ppm, however, even though tensile ductility was nearly normal (50% R. A.), the low strain rate stress rupture failures were quite brittle (Fig. 32).

Since the solubility of hydrogen in beta titanium is quite high, large amounts of hydrogen would be required for embrittlement. In the case of B120VCA, greater than 420 ppm hydrogen is required before any embrittlement can be detected.

The diffusion of hydrogen in beta titanium is quite rapid, at least as compared to alpha and alpha-beta alloys (44). When a driving force, such as a sharp notch, is present, then hydrogen accumulation will be quite fast, so rapid that delayed failure can occur in a time short enough to show embrittlement in a notched tensile test. This seems to be the case for notched specimens containing 1150 ppm. With unnotched specimens, a sufficient driving force for the accumulation of hydrogen exists only after substantial plastic deformation has taken place. Thus, only the unnotched specimens tested at low strain rates were significantly embrittled at 1150 ppm hydrogen.

A wide region of delayed failure was encountered with notched specimens at the 720 ppm level. Because the notch created a region where hydrogen could accumulate, embrittlement was not only obtained in the notch tensile test, but also in stress rupture tests at lower applied loads.

In an effort to show hydrogen-induced delayed failure at a higher hydrogen level (1250 ppm), stress rupture tests were conducted using mildly notched specimens. It was hoped that the mild notch would provide a lower driving force for the accumulation of hydrogen than the sharply notched specimen and, hence, would lead to a more time dependent embrittlement. The data obtained on B120VCA containing 1250 ppm hydrogen and 150 ppm are shown in Fig. 33. The range of delayed failure with 1250 ppm was narrow, but one point showing hydrogen-induced delayed failure was obtained. The failures at the 150 ppm level were all attributable to creep.

Thus, from these data it can be concluded that low strain rate hydrogen embrittlement (or hydrogen-induced delayed failure) can occur in straight beta alloys. Despite the high diffusion rates in beta alloys, this low strain rate embrittlement is not as pronounced as in alpha-beta alloys, probably because of the increased solubility or tolerance for hydrogen in the beta structure.

IV SUMMARY AND CONCLUSIONS

A ductility minimum was obtained in unnotched stress rupture tests conducted on a heat treated alpha-beta titanium alloy. This minimum was obtained only at intermediate hydrogen levels (200 - 420 ppm); at lower hydrogen contents no embrittlement was encountered, and at higher hydrogen contents embrittlement was obtained in all stress rupture tests. This ductility minimum was presumed to be part of a strain aging mechanism.

Prestraining and then aging this alpha-beta alloy containing this same intermediate quantity of hydrogen created a lowering of ductility after a given aging time (generally 2 - 6 hours). The ductility was restored after longer periods of aging (approximately 100 hours). This ductility minimum after prestraining was not obtained at lower hydrogen levels (20 - 80 ppm). These data seemed to confirm the fact that slow strain rate hydrogen embrittlement in alpha-beta titanium alloys is actually a strain aging phenomenon.

A hypothesis was advanced for low strain rate hydrogen embrittlement in titanium. In this model it is said that hydrogen migrates to a region created by inhomogeneous plastic strain (where a stress field exists). This region may be either at the intersection of slip lines and grain boundaries, or near the base of a sharp notch. Recovery of plastic strain will result in the redistribution of hydrogen with subsequent minimization of the embrittlement. Hydride precipitation is not an essential part of this mechanism.

Slow strain rate hydrogen embrittlement can also be obtained in an alpha alloy. The range of stresses over which hydrogen-induced delayed failures can occur was not large because of the relatively slow diffusion rate of hydrogen in alpha alloys.

Small quantities of hydrogen can also create an improvement in the creep resistance of an alpha alloy. This can be attributed to the interaction between moving dislocations and hydrogen clouds, causing a deceleration of the dislocation movement.

Slow strain rate hydrogen embrittlement was obtained in a beta alloy. Because the high solubility of hydrogen in beta titanium, no hydrogen effects were encountered with 420 ppm hydrogen or less. Notched specimens were subject to low strain rate embrittlement at a lower level than unnotched specimens (720 ppm vs. 1150 ppm hydrogen). Because of the high diffusivity of hydrogen in beta titanium, in some instances "delayed" failures apparently took place in times short enough to cause embrittlement in a notched tensile test.

The incidence of low strain rate embrittlement in an alpha and a beta alloy rules out the necessity of an alpha-beta interface for hydrogen-induced delayed failures. In both cases apparently some strain was necessary before delayed failure could occur.

For low strain rate hydrogen embrittlement to occur in titanium alloys it appears the following are necessary:

- a. a sufficient quantity of hydrogen
- b. a sufficient diffusivity of hydrogen
- c. a driving force for the accumulation of hydrogen (as postulated previously - inhomogeneous strain can create this force)

V BIBLIOGRAPHY

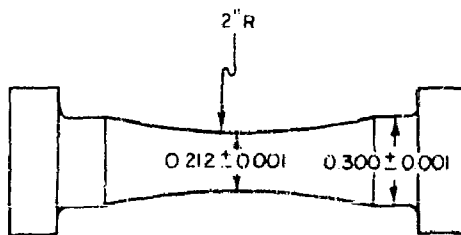
1. D. N. Williams, "Hydrogen in Titanium and Titanium Alloys," Titanium Metallurgical Laboratory Report No. 100, (May, 1958)
2. G. A. Lenning, J. W. Spretnak, and R. I. Jaffee, "Effects of Hydrogen on Alpha Titanium Alloys," Journal of Metals - Transactions Section, 8, 1235-1241, (October, 1956).
3. R. J. Quigg, "Delayed Cracking of Titanium Base Alloys," Rem-Cru Internal Report CR-34, (August, 1950)
4. D. N. Williams, F. R. Schwartzberg, and R. I. Jaffee, "Hydrogen Contamination in Titanium and Titanium Alloys - Part V. Hydrogen Embrittlement," WADC Report No. 54-616, Part V, (March, 1958)
5. R. J. Quigg, "Delayed Cracking of Al110AT," Rem-Cru Internal Report DDS 772, (October, 1955)
6. R. D. Daniels, E. L. Harmon, Jr., and A. R. Troiano, "The Influence of Hydrogen on Delayed Failure in Titanium Alloys," WADC Report No. 57-30, (February, 1957)
7. R. D. Daniels, R. J. Quigg, and A. R. Troiano, "Delayed Failure and Hydrogen Embrittlement in Titanium," WADC Report No. 58-39, (February, 1958).
8. R. D. Daniels, R. J. Quigg, and A. R. Troiano, "Hydrogen Embrittlement and Delayed Failure in Titanium Alloys," Trans ASM, 51, (1959).
9. E. J. Rippling, "Hydrogen Embrittlement of a Commercial Alpha-Beta Titanium Alloy," Trans. AIME, 206, 502-503 (1956).
10. D. N. Williams, F. R. Schwartzberg, and R. I. Jaffee, "The Effects of Microstructure and Heat Treatment on the Hydrogen Embrittlement of Alpha-Beta Titanium Alloys," Trans ASM, 51, (1959).
11. R. J. Quigg, Discussion to Reference 10, Trans ASM, 51, (1959).
12. R. I. Jaffee and D. N. Williams, "The Effect of Composition on the Hydrogen Embrittlement of Alpha-Beta Titanium Alloys," Trans ASM, 51, (1959).

13. R. P. Frohmberg, W. J. Barnett, and A. R. Troiano, "Delayed Failure and Hydrogen Embrittlement in Steel," Trans ASM, 47, 892-925, (1955).
14. H. H. Johnson, J. Morlet, and A. R. Troiano, "Hydrogen, Crack Initiation and Delayed Failure in Steel," WADC Technical Report No. 57-262, (May, 1957).
15. G. Sachs, "Strain Aging Criteria," Iron Age, 161, 78-83, (May 13, 1948)
16. E. R. Morgan, "Quench Aging, Strain Aging, Yield and Flow Phenomena in Low Carbon Steel," The Annealing of Low Carbon Steel, Lee Wilson Co., 19-28, (1958).
17. E. S. Davenport and E. C. Bain, "The Aging of Steel," Trans ASM, 23, 1047-1106, (1935).
18. J. Fritzsche, "The Resistance to Flow in Bending Steel Girders and Columns," Der Stahlbau, 11, 1954, (1938).
19. F. Garofalo and G. V. Smith, "The Effect of Time and Temperature on Various Mechanical Properties During Strain Aging of Normalized Low Carbon Steels," Trans ASM, 47, 957-983, (1955).
20. J. R. Low and M. Gensamer, "Aging and the Yield Point in Steel," Trans AIIME - Iron and Steel Division, 158, 207, (1944).
21. N. B. Pilling - Private communication to G. Sachs in reference 15
22. J. D. Fast, "Aging of Iron and Steel," Iron and Coal Trades Review, 837-844, (April, 1950).
23. H. C. Rogers, "The Influence of Hydrogen on the Yield Point in Iron," Acta Metallurgica, 4, 114-117, (1956).
24. H. C. Rogers, "A Yield Point in Steel Due to Hydrogen," Acta Metallurgica, 2, 167, (1954).
25. W. C. Leslie and R. L. Rickett, "Influence of Aluminum and Silicon Deoxidation on the Strain Aging of Low Carbon Steels," Journal of Metals Transactions, 102, (August, 1953).
26. A. H. Cottrell and A. T. Churchman, "Change of Electrical Resistance During the Strain Aging of Iron," Journal of Iron and Steel In-

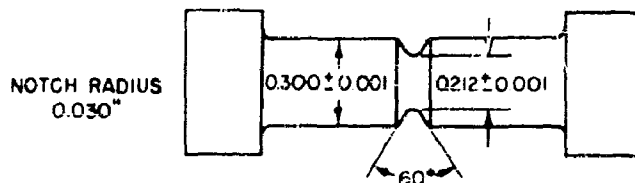
stitute, 271-276, (July, 1949).

27. A. H. Cottrell, "Creep and Aging Effects in Solid Solutions," Creep and Fracture of Metals at High Temperatures, Her Majesty's Stationery Office, 141-152, (1954).
28. F. D. Rossi and F. C. Perkins, "Mechanical Properties and Strain Aging Effects in Titanium," Trans ASM, 45, 972-992, (1953).
29. F. D. Cuff and N. J. Grant, "Stress Rupture Characteristics of Unalloyed Titanium Plotted," Iron Age, 170, 134-139, (November 20, 1952).
30. N. Makrides, "High Temperature Brittleness in Titanium Alloys," M. S. Thesis, Case Institute of Technology, (1958).
31. H. M. Burte, "Strain Aging Hydrogen Embrittlement in Alpha-Beta Titanium Alloys," Transactions of the Society of Rheology, 1, 119-151, (1957).
32. M. W. Toaz and E. J. Ripling, "Flow and Fracture Characteristics of Binary Wrought Magnesium-Lithium Alloys," The Journal of the Institute of Metals, 3, 137-144, (December, 1956)
33. W. R. Kiessl and M. S. Sinnott, "Creep Properties of Commercially Pure Titanium," Journal of Metals - Transactions Supplement, 5, 331-338, (February, 1953)
34. N. J. Grant and A. R. Chaudhuri, "Creep and Fracture," Creep and Recovery, ASM, 284-344, (1956)
35. G. Schoeck, "Theory of Creep," Creep and Recovery, ASM, 199 - 226, (1956)
36. J. V. Gluck and J. W. Freeman, "A Study of Creep of Titanium and Two of Its Alloys," WADC Report No. 54-54, (March, 1956).
37. W. J. Barnett and A. R. Troiano, "Crack Propagation in the Hydrogen-Induced Brittle Fracture of Steel," Trans. AIME, 486-494, (1957).
38. H. S. Gurev and W. M. Baldwin, Jr., "Research on Strain Aging Effects in Titanium," Quarterly Report No. 1, Air Force Contract No. AF 33(616)-5691, (August, 1958).
39. H. M. Burte, E. F. Erbin, G. T. Hahn, R. J. Kotfila, J. W. Seeger,

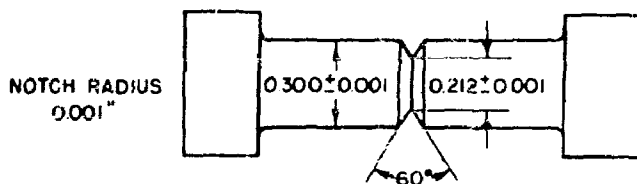
- and D. A. Wruck, "Hydrogen Embrittlement of Titanium Alloys," *Metal Progress*, 115-120, (May, 1955).
40. R. J. Wasilewski and C. L. Kehl, "Summary Report on Diffusion of Hydrogen, Nitrogen, and Oxygen in Titanium," Watertown Arsenal Laboratory Report 401/149-11A (July, 1953).
41. J. D. Lubahn, "Notch Tensile Testing," *Fracturing of Metals* ASM, 90-132, (1948).
42. M. B. Bever, "On the Thermodynamics and Kinetics of Recovery," *Creep and Recovery*, ASM, 14-51, (1956)
43. E. C. W. Perryman, "Recovery of Mechanical Properties," *Creep and Recovery*, ASM, 111-145, (1956).
44. J. E. Reynolds and R. I. Jaffee, "The Diffusion of Interstitial and Substitutional Elements in Titanium," Titanium Metallurgical Laboratory Report No. 21, (October, 1955)



UNNOTCHED TENSILE SPECIMEN



MILD NOTCH TENSILE SPECIMEN



SHARP NOTCH TENSILE SPECIMEN

FIG. I : SPECIMEN TYPES USED IN HYDROGEN EMBRITTLEMENT INVESTIGATION.

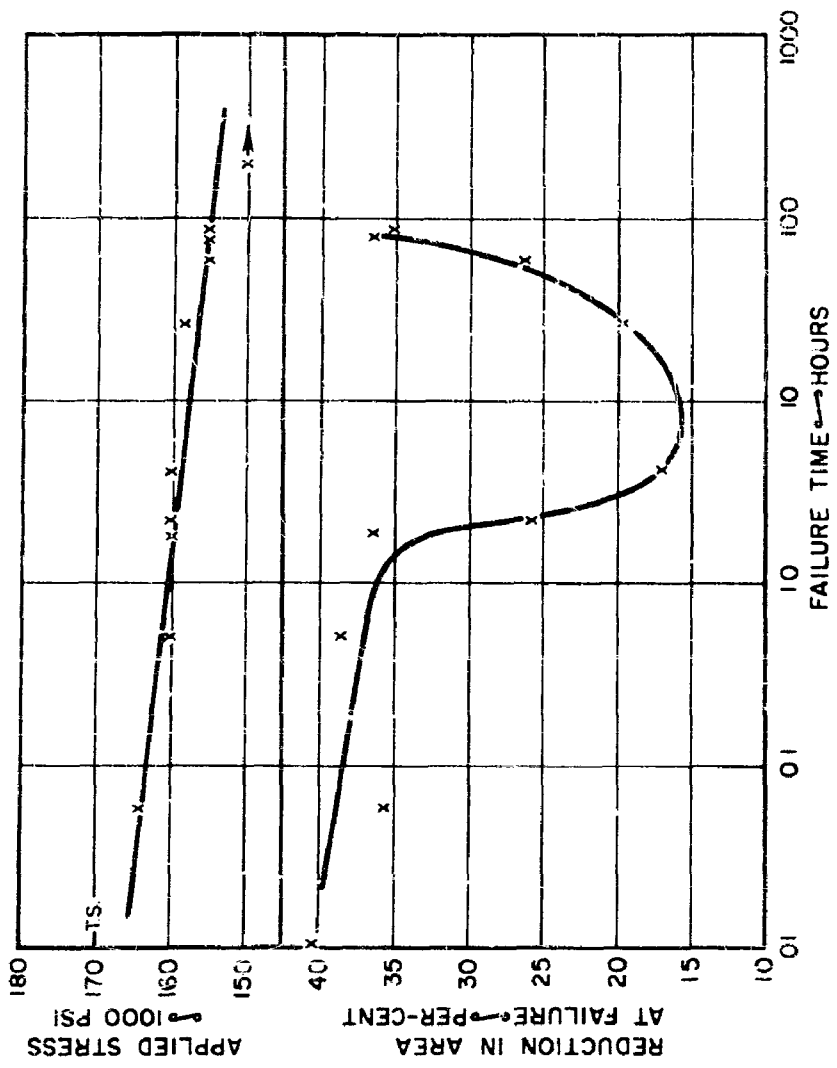


FIG. 2 : APPLIED STRESS FOR DELAYED FAILURE AND REDUCTION IN AREA AT FAILURE FOR C-130 AM ALLOY, 200 PPM HYDROGEN, 170,000 PSI STRENGTH LEVEL, UNNOTCHED SPECIMENS.

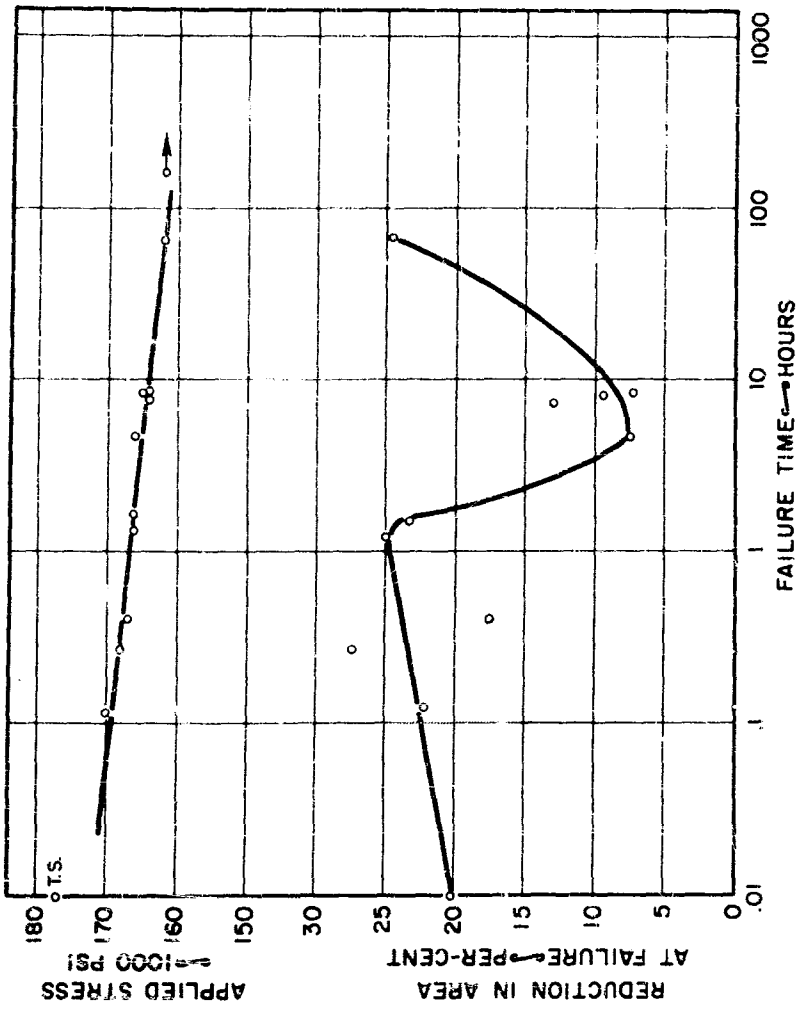


FIG. 3 :APPLIED STRESS FOR DELAYED FAILURE AND REDUCTION IN AREA
AT FAILURE FOR C-130 AM ALLOY, 260 PPM HYDROGEN, 170,000 PSI
STRENGTH LEVEL, UNNOTCHED SPECIMENS.

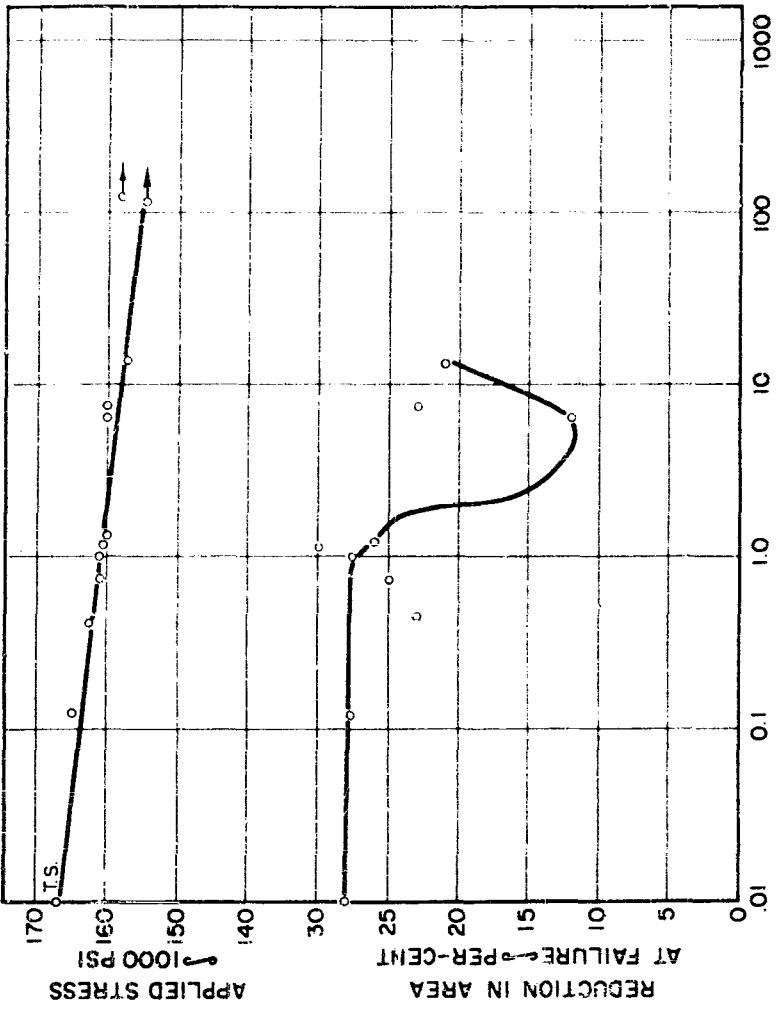


FIG. 4 :APPLIED STRESS FOR DELAYED FAILURE AND REDUCTION IN AREA AT FAILURE FOR C-130 AM ALLOY, 330 PPM HYDROGEN, 170,000 PSI STRENGTH LEVEL, UNNOTCHED SPECIMENS.

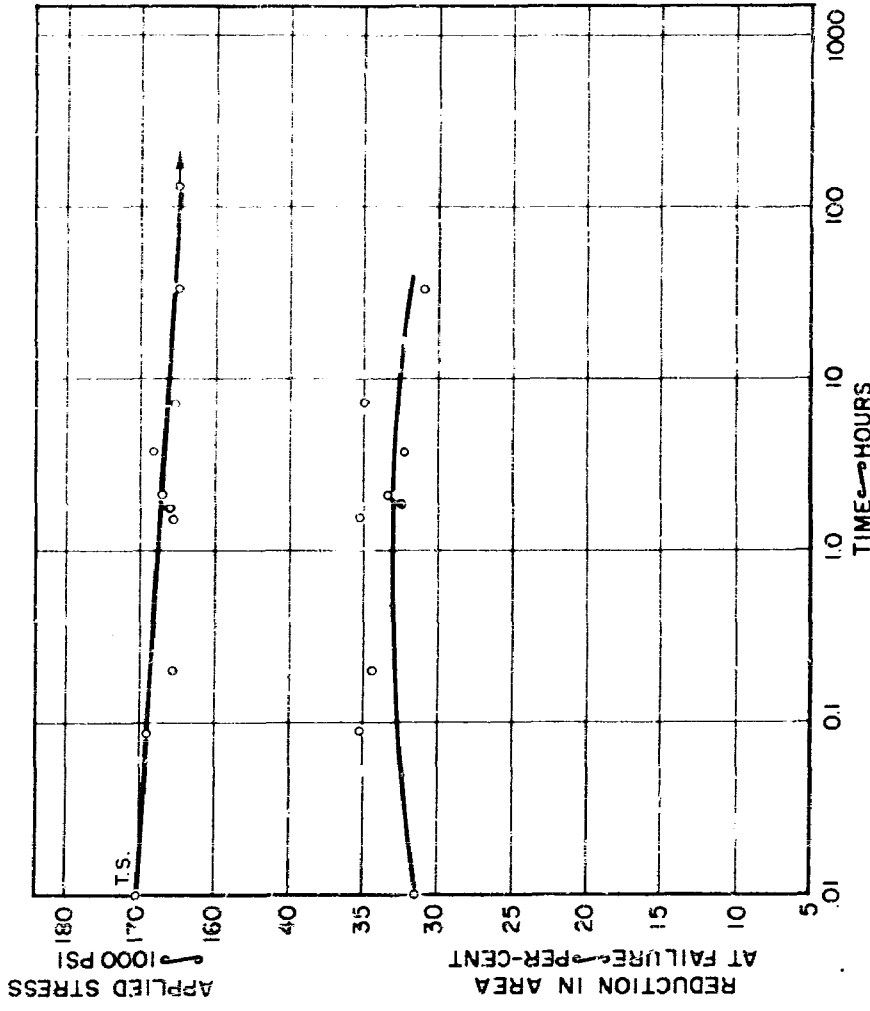


FIG. 5 APPLIED STRESS FOR DELAYED FAILURE AND REDUCTION IN AREA
AT FAILURE FOR C-130 AM ALLOY, 80 PPM HYDROGEN, 170,000 PSI
STRENGTH LEVEL, UNNOTCHED SPECIMENS.

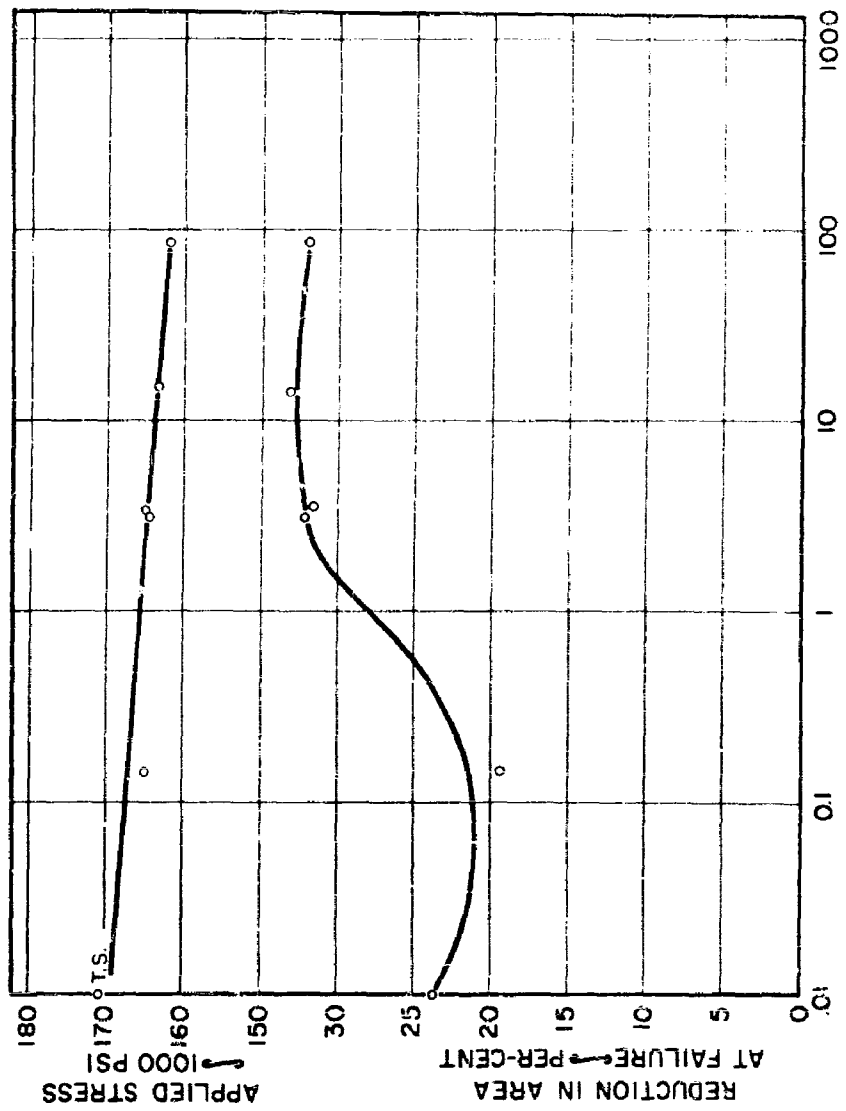


FIG. 6 : APPLIED STRESS FOR DELAYED FAILURE AND REDUCTION IN AREA AT FAILURE FOR C-130 AM ALLOY, 20 PPM HYDROGEN, 170,000 PSI STRENGTH LEVEL, UNNOTCHED SPECIMENS.

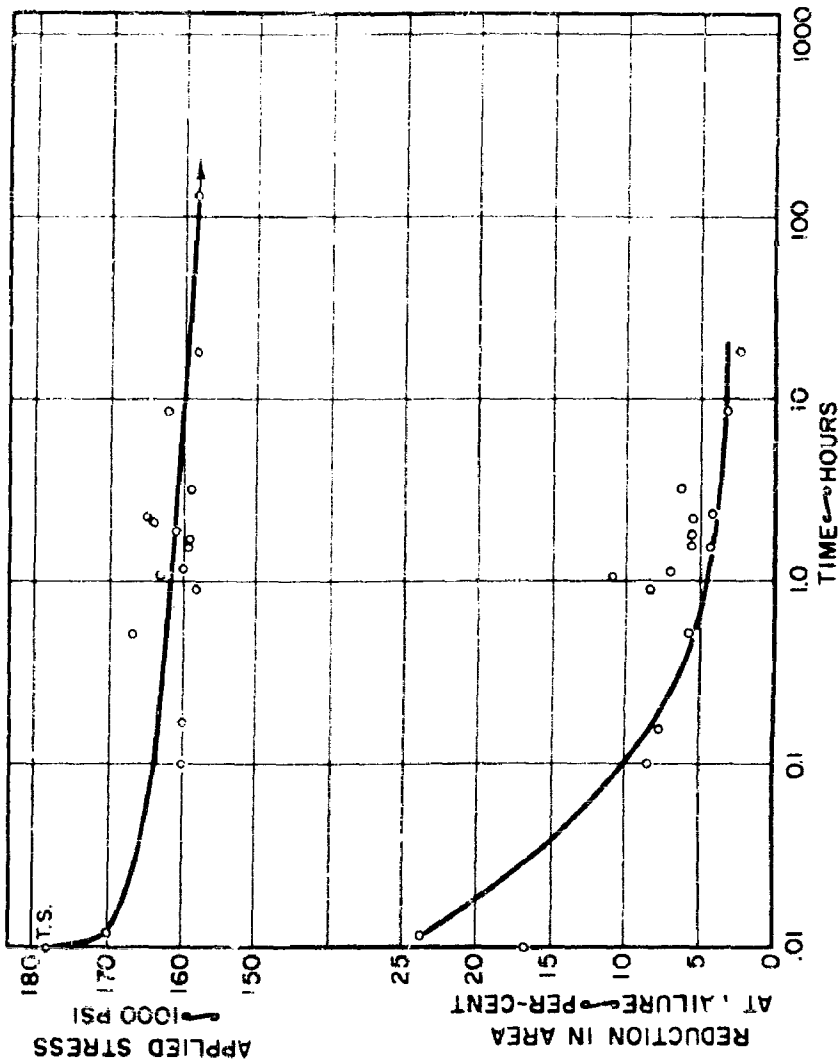


FIG. 7 .APPLIED STRESS FOR DELAYED FAILURE AND REDUCTION IN AREA AT FAILURE FOR C-130 AM ALLOY, 420 PPM HYDROGEN, 170,000 PSI STRENGTH LEVEL, UNNOTCHED SPECIMENS.

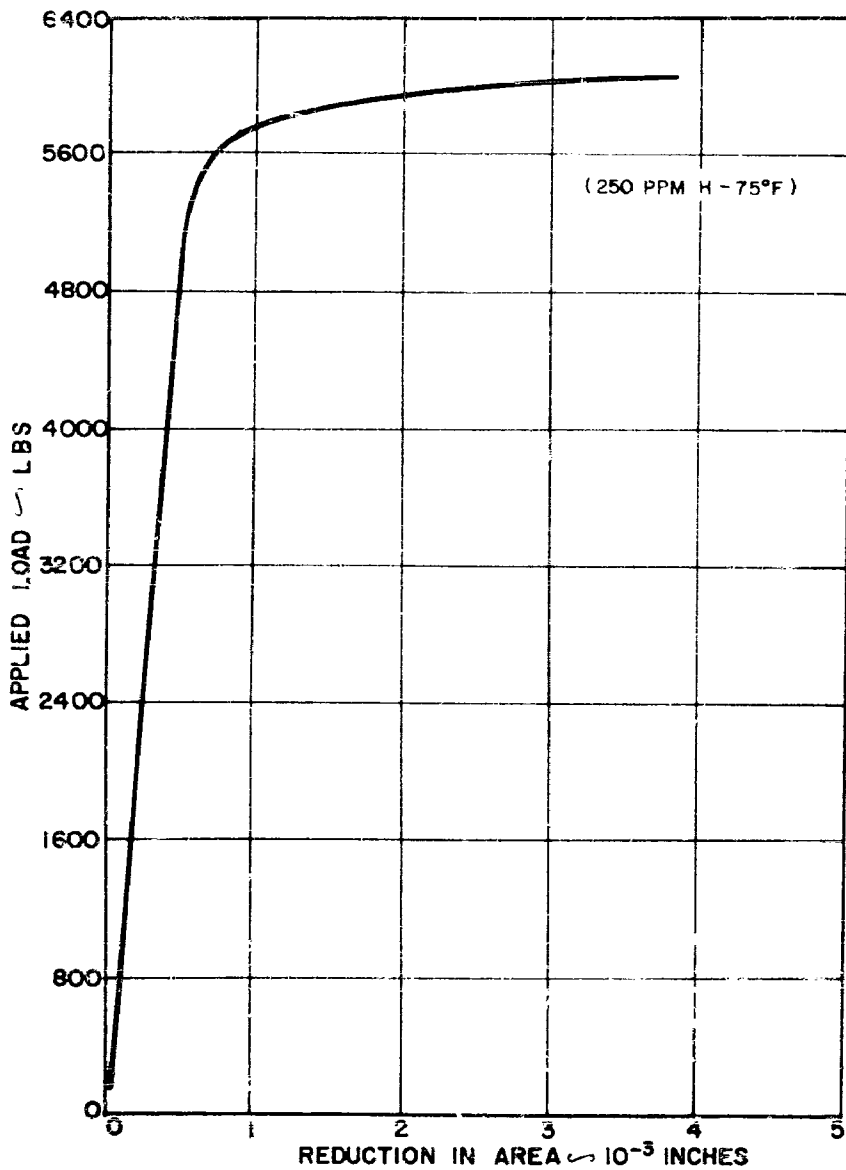


FIG. 8 :TYPICAL STRESS-STRAIN CURVE FOR C-130 AM ALLOY,
QUENCHED AND AGED, 170,000 PSI STRENGTH LEVEL.

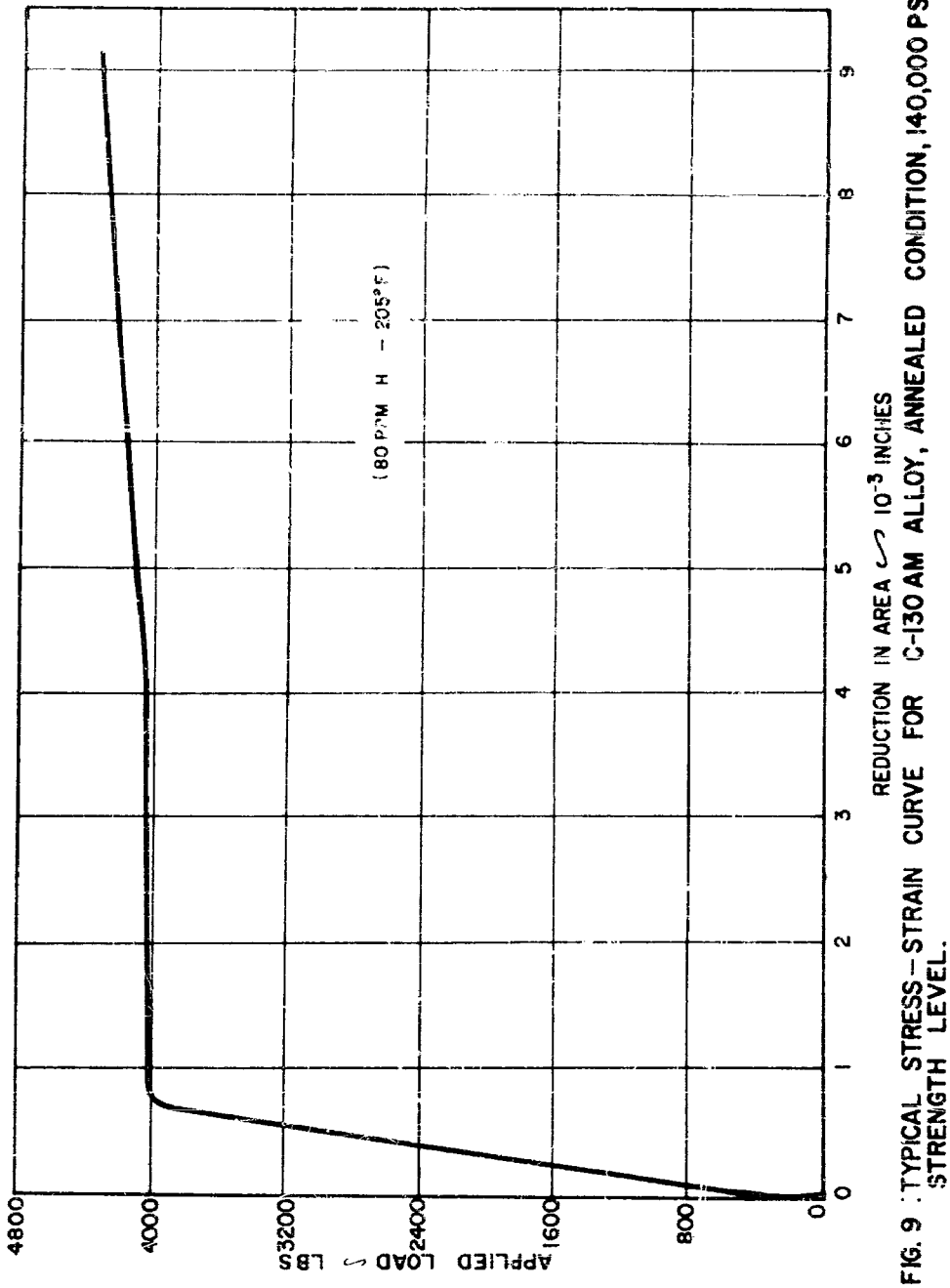


FIG. 9 TYPICAL STRESS-STRAIN CURVE FOR C-130 AM ALLOY, ANNEALED CONDITION, 140,000 PSI STRENGTH LEVEL.

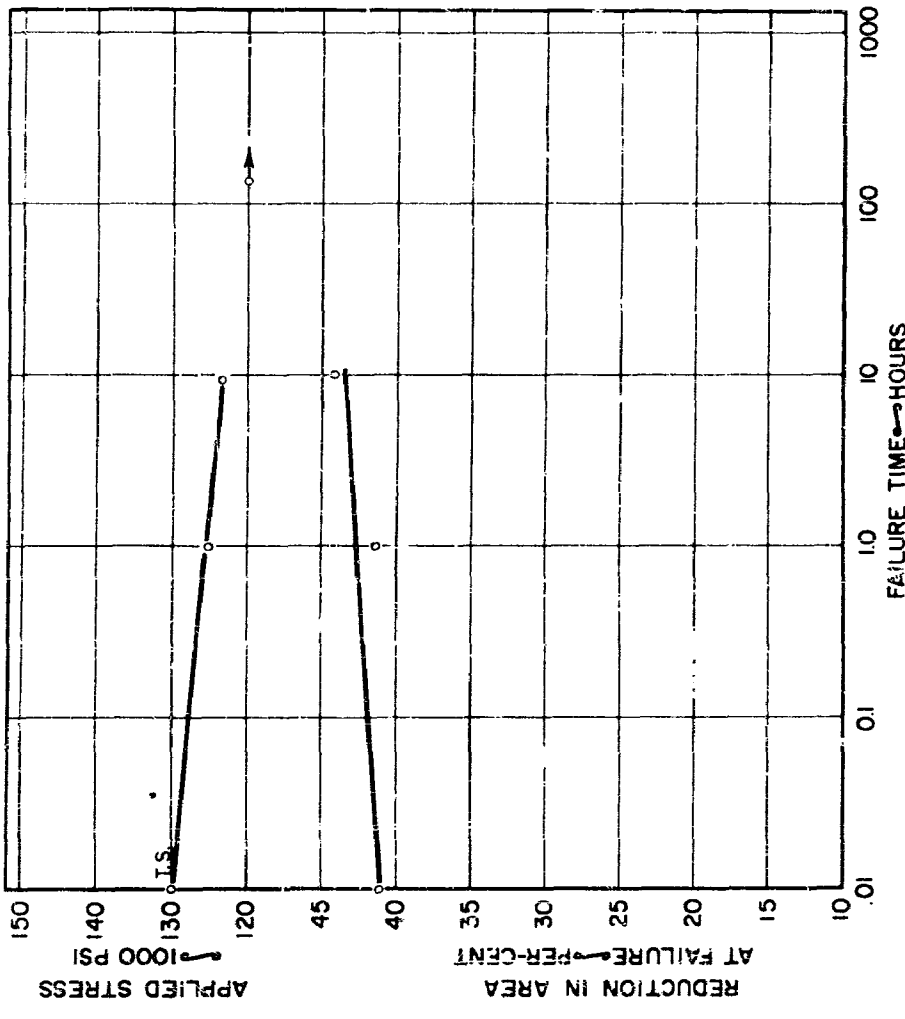


FIG. 10. APPLIED STRESS FOR DELAYED FAILURE AND REDUCTION IN AREA AT FAILURE FOR C-130 AM ALLOY, 15 PPM HYDROGEN, ANNEALED CONDITION, UNNOTCHED SPECIMENS.

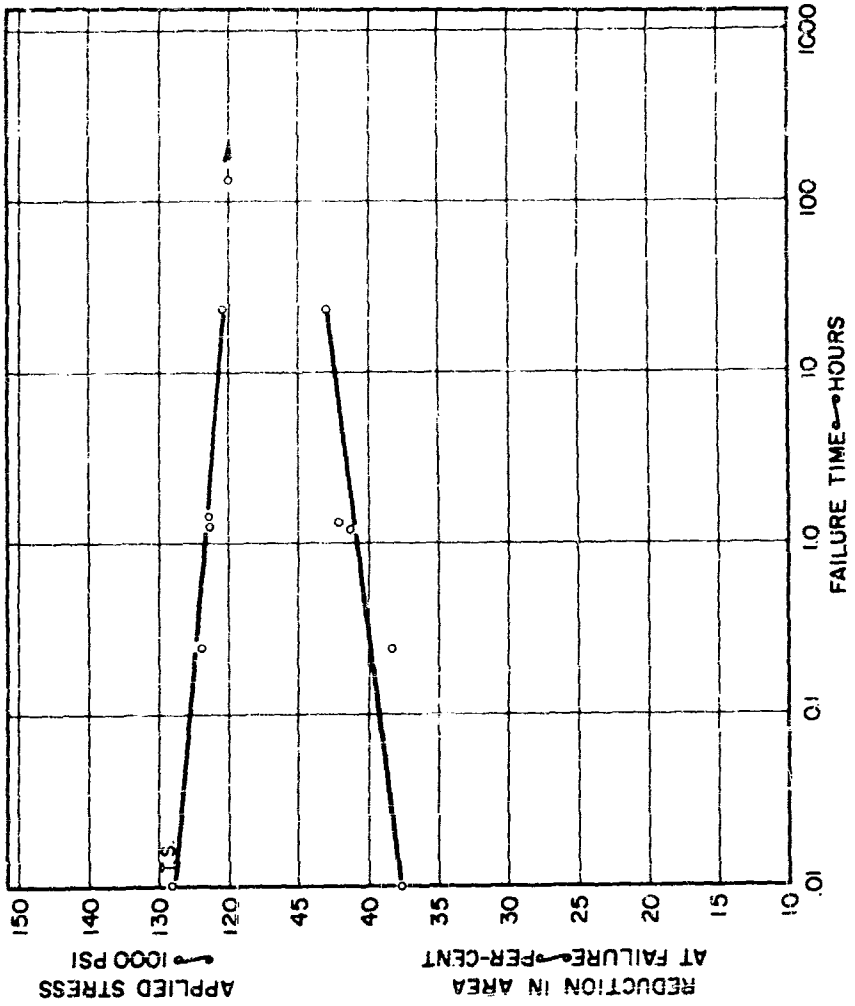


FIG. II : APPLIED STRESS FOR DELAYED FAILURE AND REDUCTION IN AREA AT FAILURE FOR C-130 AM ALLOY, 80 PPM HYDROGEN, ANNEALED CONDITION, UNNOTCHED SPECIMENS.

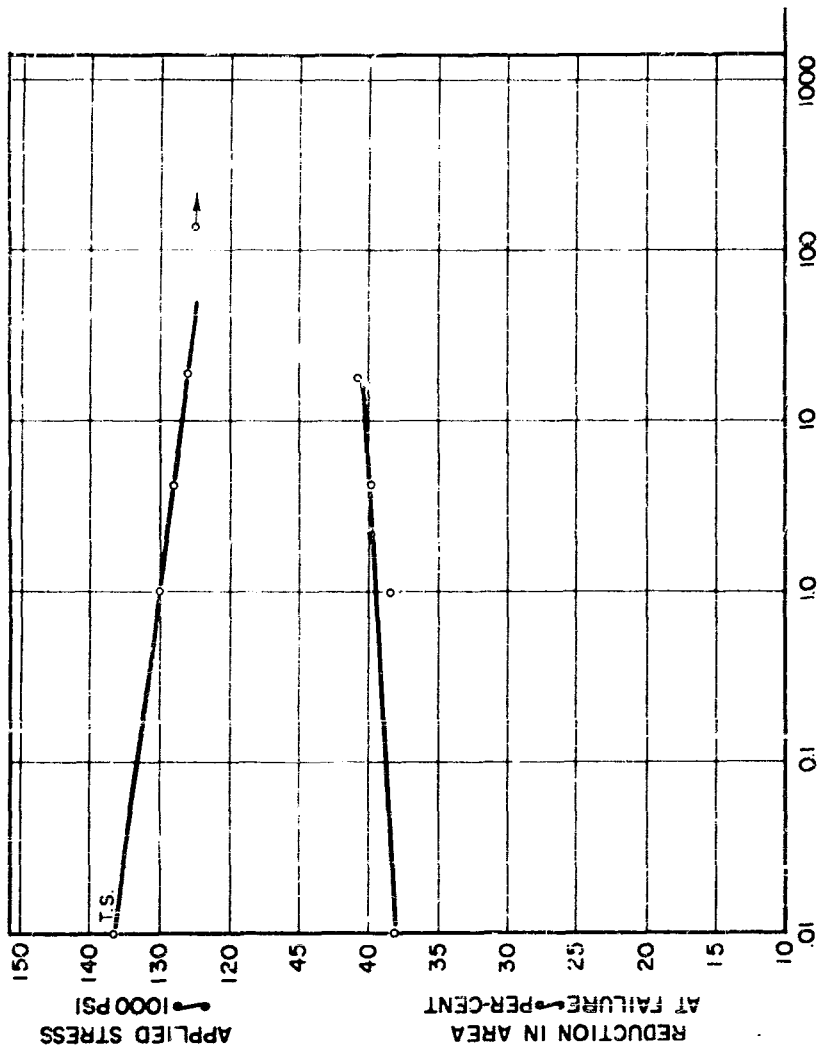


FIG.12 : APPLIED STRESS FOR DELAYED FAILURE AND REDUCTION IN AREA AT FAILURE
FOR C-130 AM ALLOY, 430 PPM HYDROGEN, ANNEALED CONDITION, UNNOTCHED
SPECIMENS.

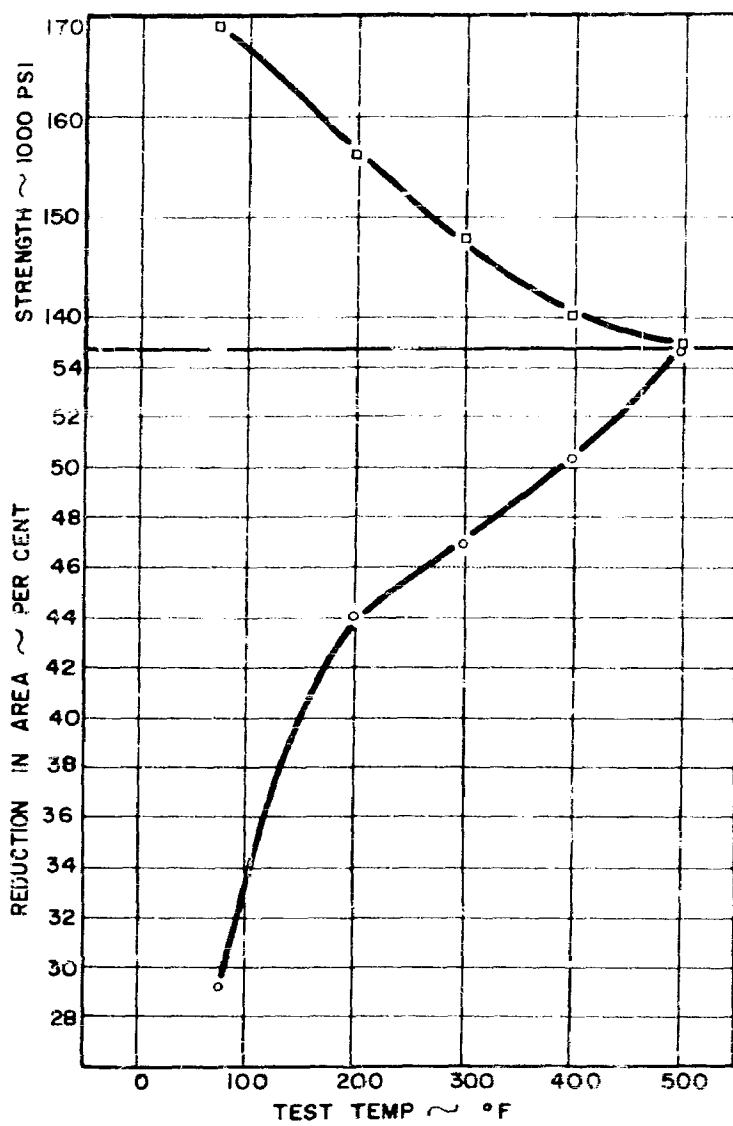
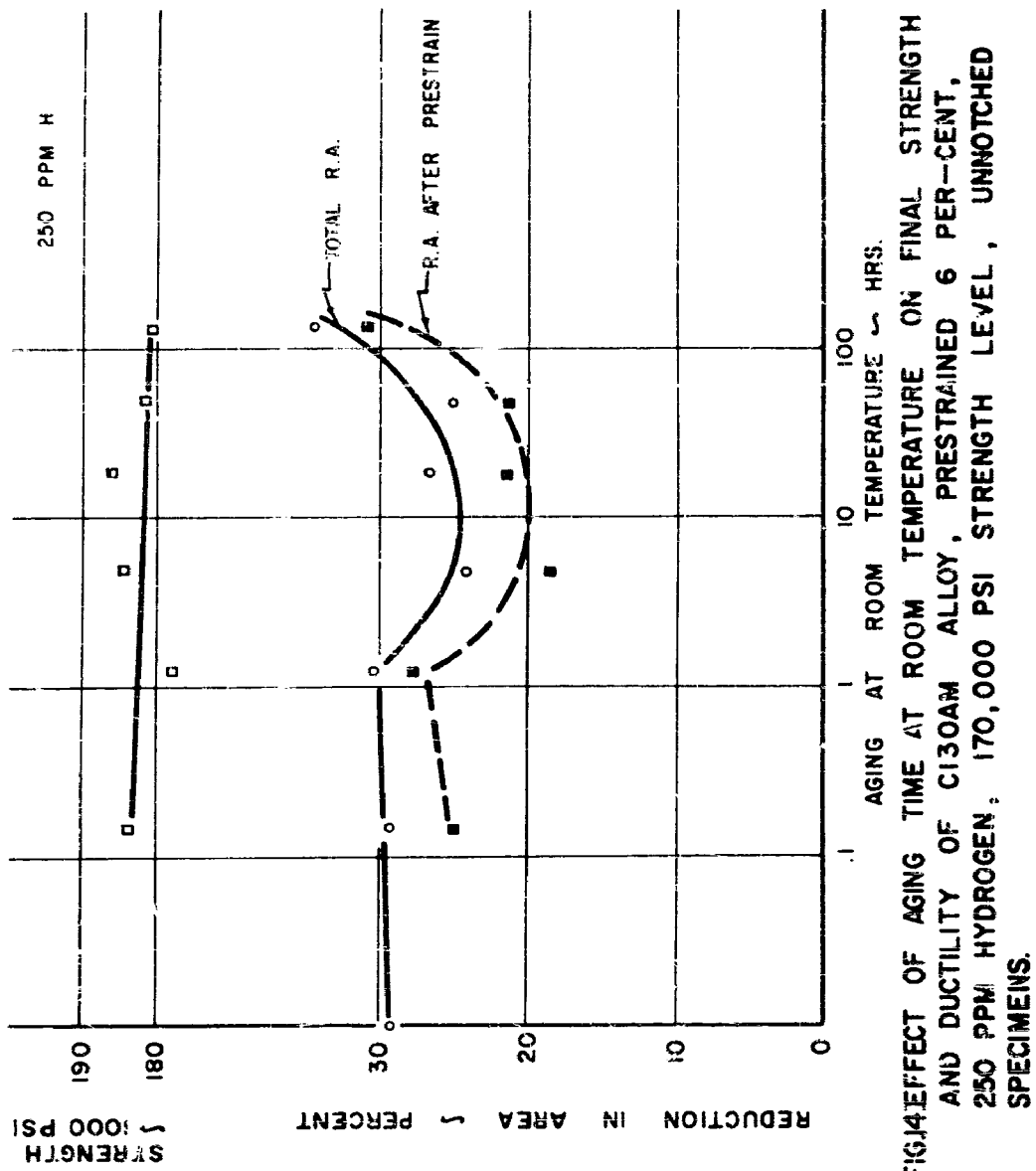


FIG. 13 : EFFECT OF TEST TEMPERATURE ON STRENGTH AND DUCTILITY OF C-130 AM ALLOY, 250 PPM HYDROGEN, 170,000 STRENGTH LEVEL, UN-NOTCHED SPECIMENS, .05 IN/IN/MIN STRAIN RATE.



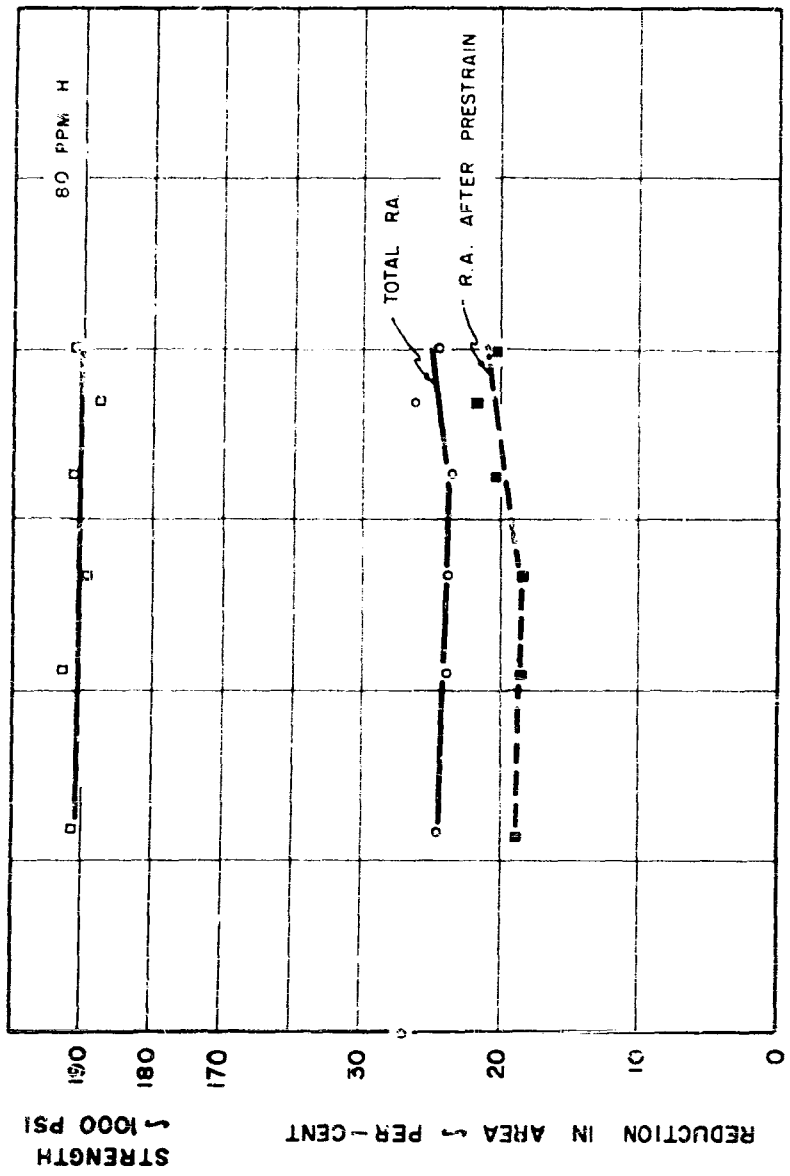


FIG. 15 : EFFECT OF AGING TIME AT ROOM TEMPERATURE ON FINAL STRENGTH AND DUCTILITY OF C130AM ALLOY, PRESTRAINED 6 PER-CENT, 80 PPM HYDROGEN, 170,000 STRENGTH LEVEL, UNNOTCHED SPECIMENS.

REDUCTION IN AREA → PER-CENT
1000 PSI

WADC TR 59-172

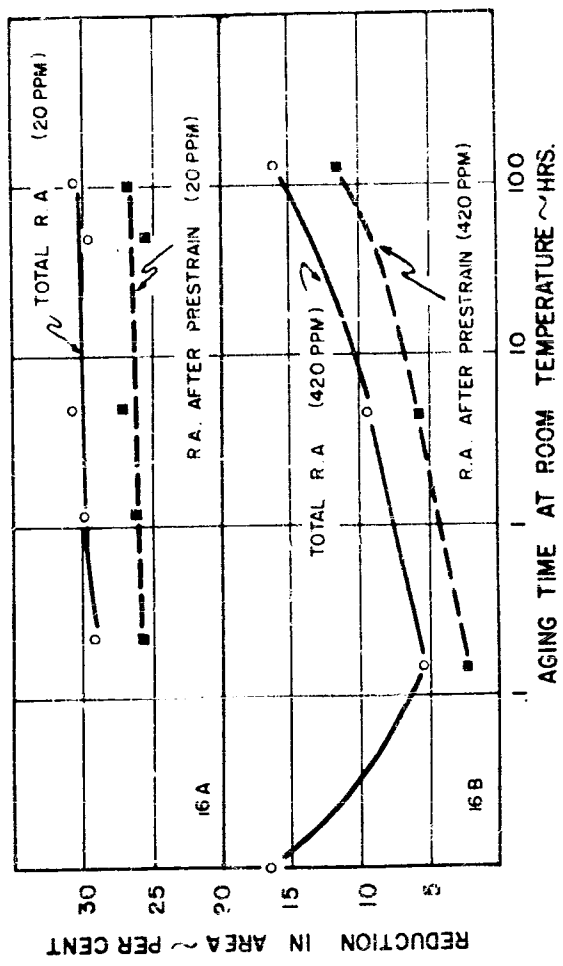


FIG. 16. EFFECT OF AGING TIME AT ROOM TEMPERATURE ON FINAL DUCTILITY OF C-130 AM ALLOY CONTAINING 20 OR 420 PPM HYDROGEN, PRESTRAIN 4-6%, 170,000 PSI STRENGTH, UNNOTCHED SPECIMENS.

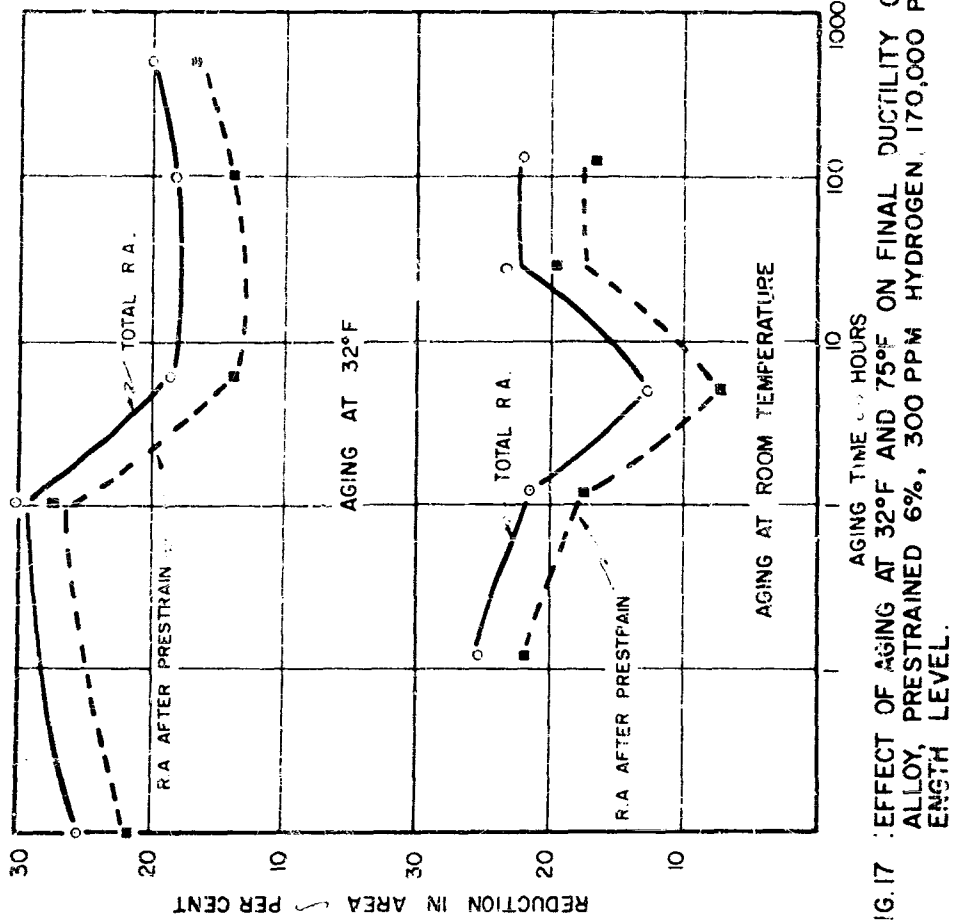


FIG. 17 EFFECT OF AGING AT 32°F AND 75°F ON FINAL DUCTILITY OF C-120 AM ALLOY, PRESTRAINED 6%, 300 PPM HYDROGEN, 170,000 PSI STRENGTH LEVEL.

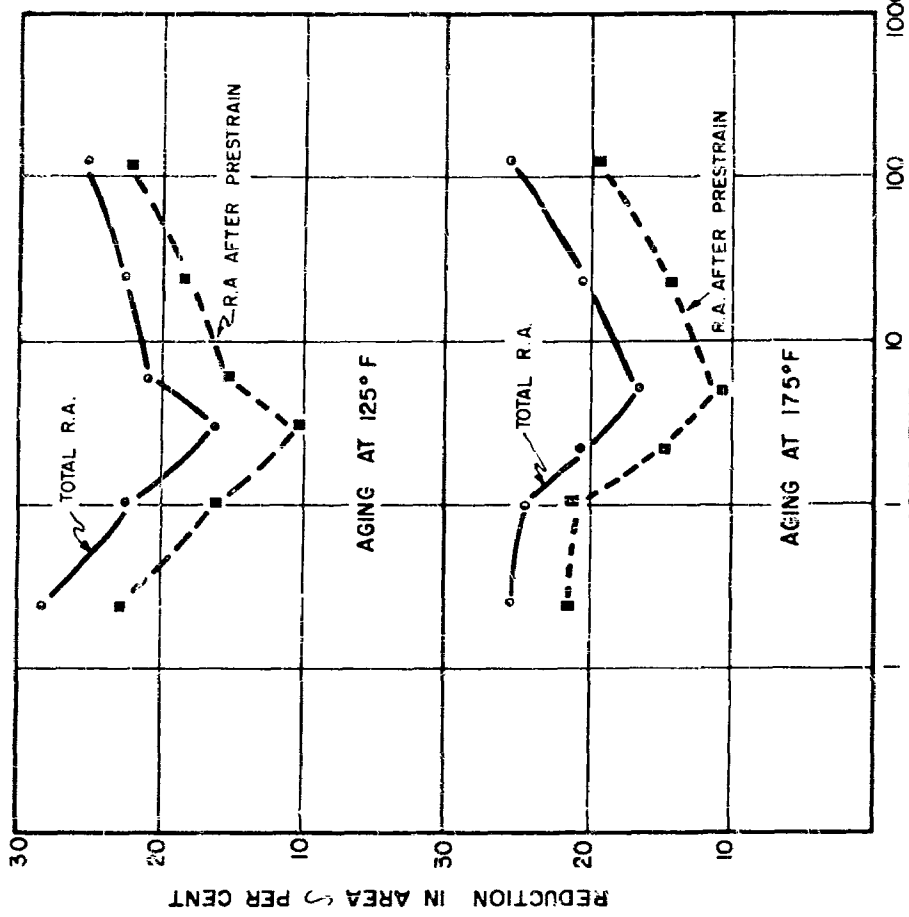


FIG. 18 : EFFECT OF AGING TIME AT 125°F & 175°F ON FINAL DUCTILITY OF C-350 AM ALLOY, PRESTRAINED 6%, 300 PPm HYDROGEN, 170,000PSI STRENGTH LEVEL.

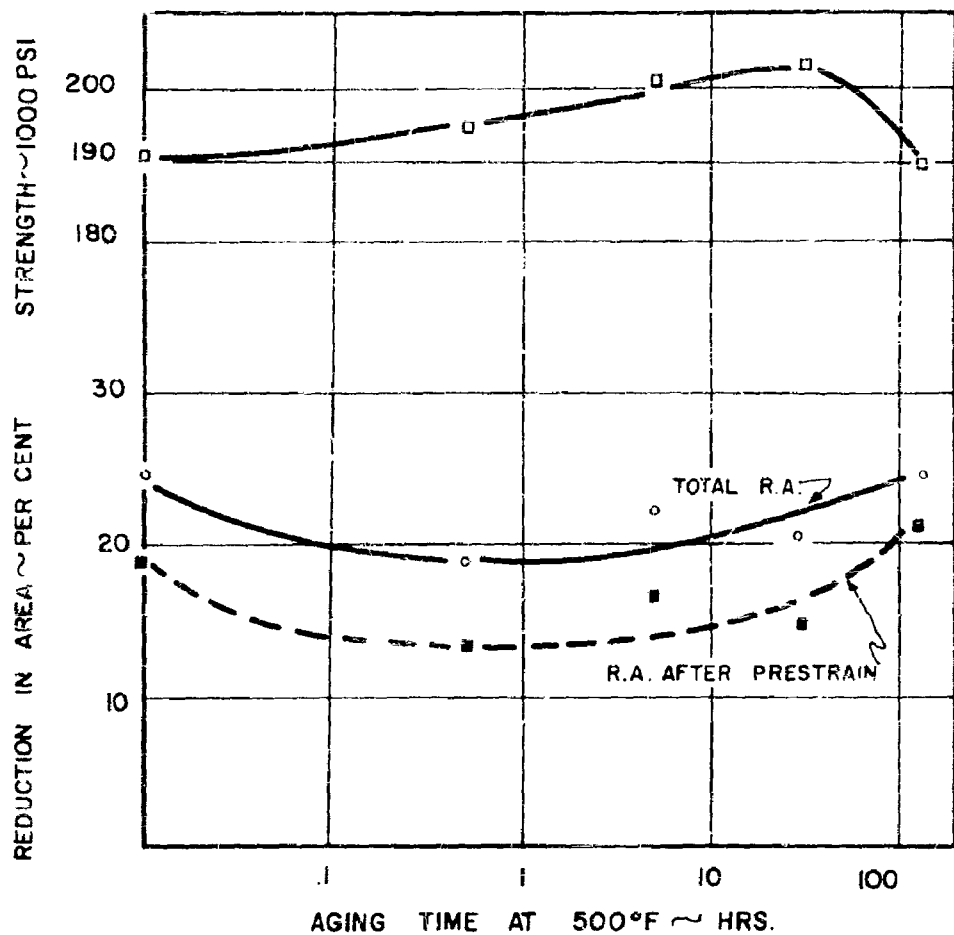


FIG. 19 EFFECT OF AGING TIME AT 500°F ON FINAL STRENGTH AND DUCTILITY OF C-130 AM ALLOY, PRESTRAINED 6%, 80 PPM HYDROGEN, 170,000 PSI STRENGTH LEVEL, UNNOTCHED SPECIMENS.

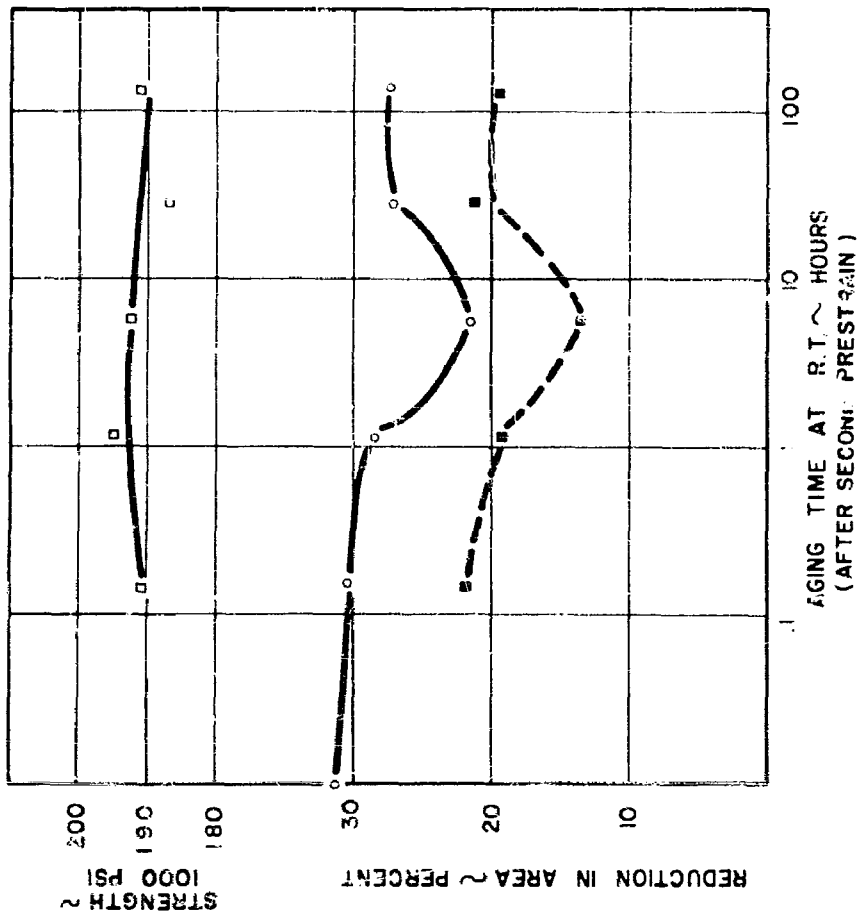


FIG. 20 : EFFECT OF AGING TIME AT ROOM TEMPERATURE ON FINAL STRENGTH AND DUCTILITY OF C-130 AM ALLOY PRESTRAINED 6%, AGED 120 HRS. AT ROOM TEMPERATURE, THEN PRESTRAINED AGAIN 3%; 250 PPM HYDROGEN, [70,000 PSI STRENGTH LEVEL], UNNOTCHED SPECIMENS.

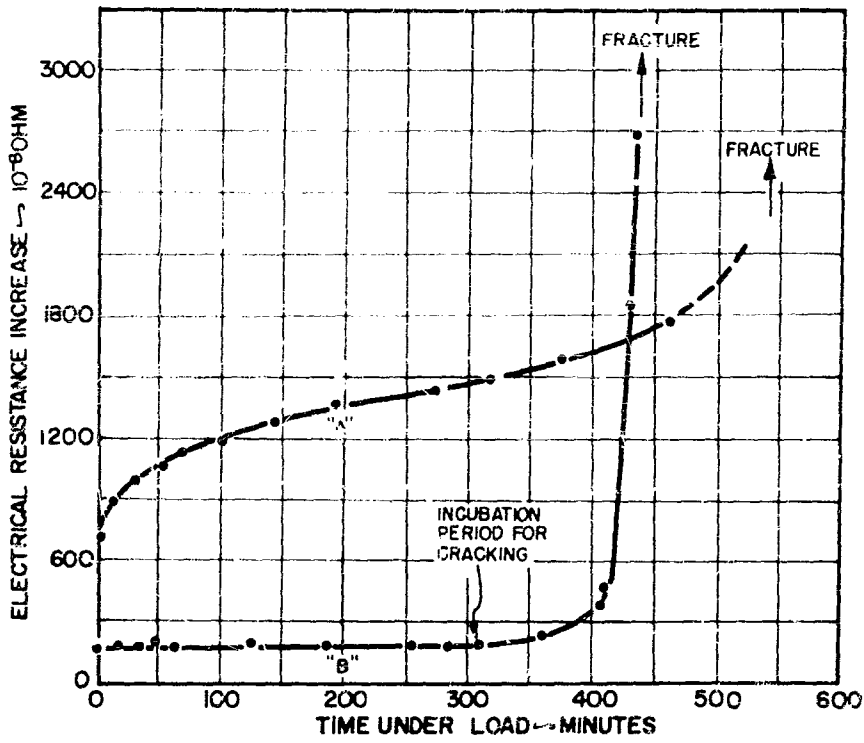


FIG.21 : ELECTRICAL RESISTANCE VERSUS TIME FOR SHARP NOTCHED SPECIMENS UNDER STATIC LOAD, AFTER DANIELS, QUIGG, AND TROIANO (7).

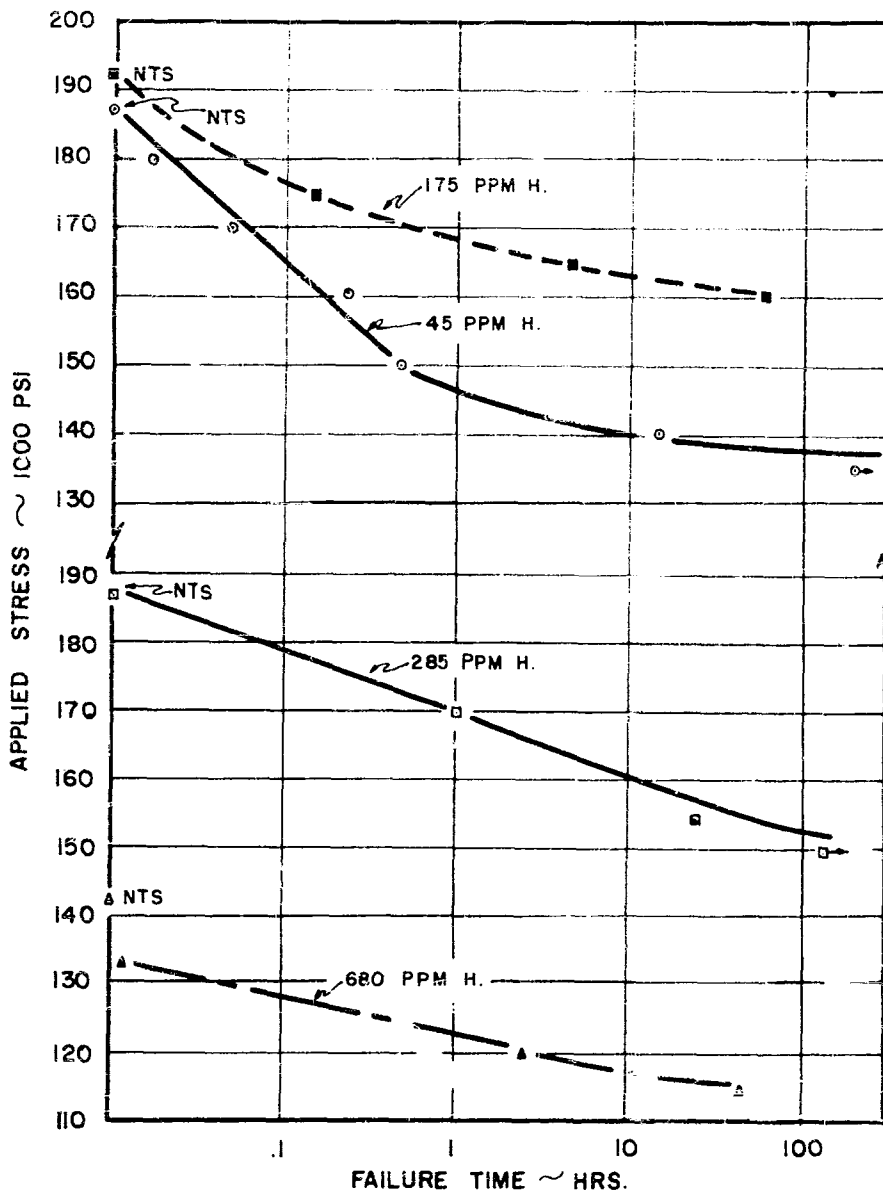


FIG. 22 NOTCHED STRESS RUPTURE CURVES FOR
A-110 AT ALLOY AT VARIOUS HYDROGEN LEVELS.

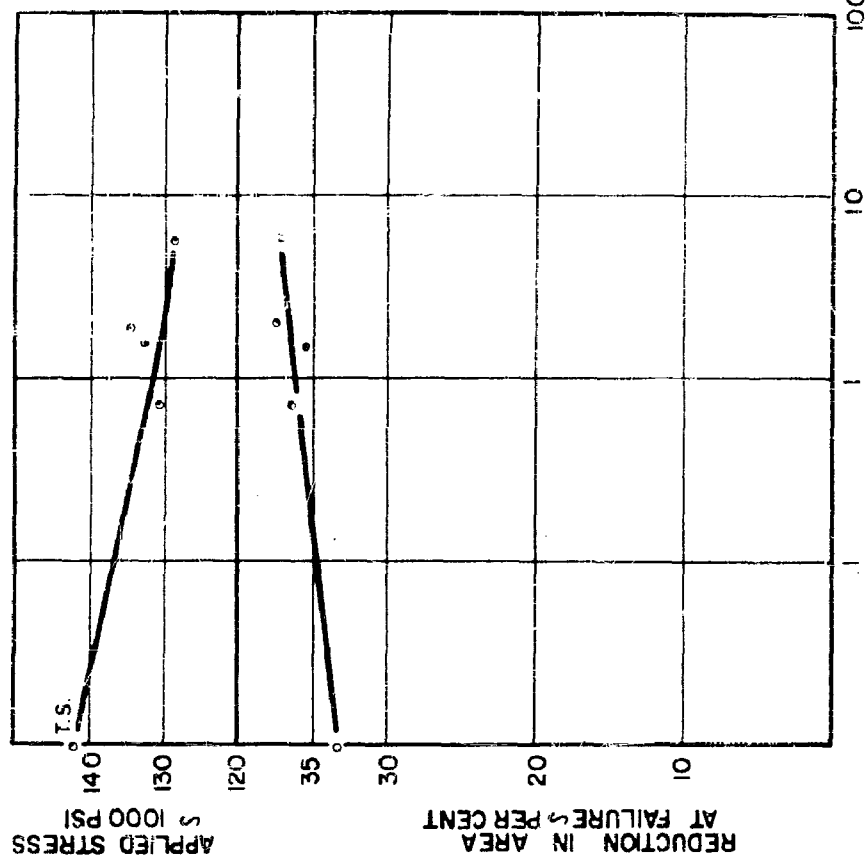


FIG. 24: APPLIED STRESS FOR DELAYED FAILURE AND REDUCTION IN AREA AT FAILURE FOR 5Al-2.5 Sn ALLOY, 160 PPM HYDROGEN, UNNOTCHED SPECIMENS.

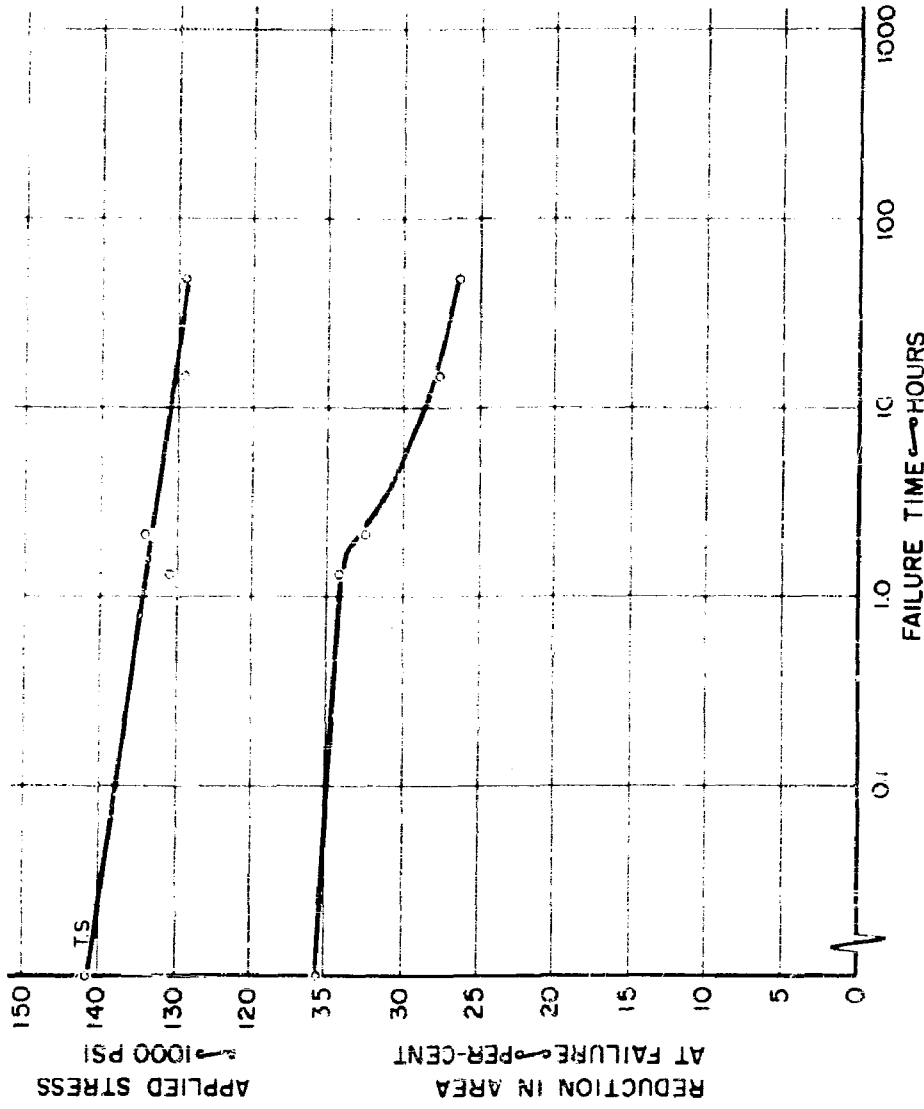


FIG. 25. APPLIED STRESS FOR DELAYED FAILURE AND REDUCTION IN AREA AT FAILURE FOR 5 Al-2.5 Sn ALLOY, 285 PPM HYDROGEN, 140,000 PSI STRENGTH LEVEL, UNNOTCHED SPECIMENS.

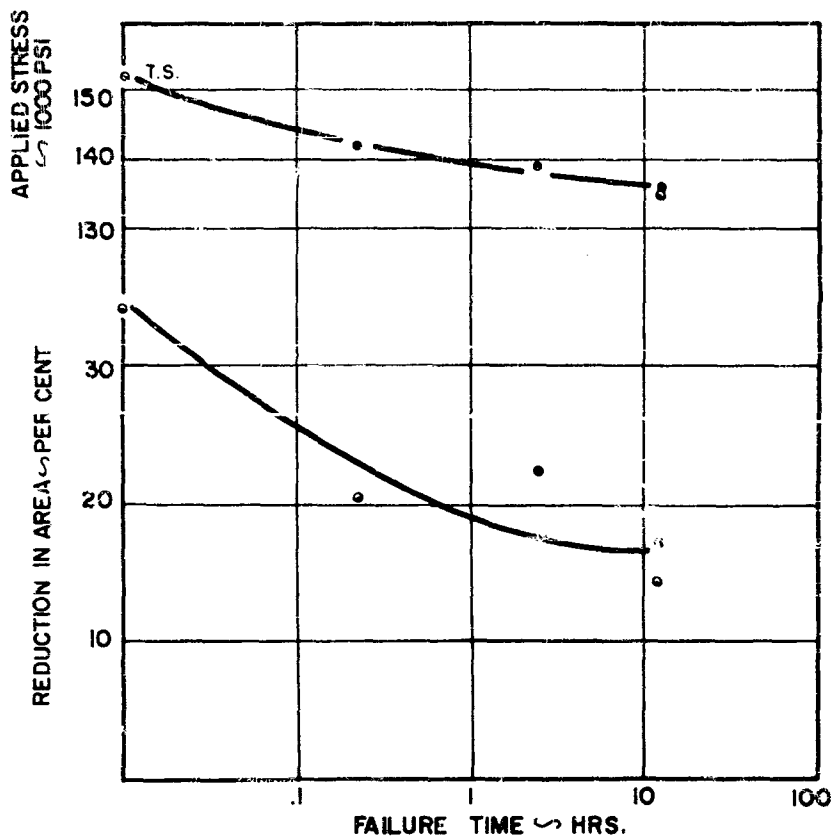


FIG.26: APPLIED STRESS FOR DELAYED FAILURE AND REDUCTION IN AREA AT FAILURE FOR 5AL-2.5SN ALLOY, 690 PPM HYDROGEN, UNNOTCHED SPECIMENS.

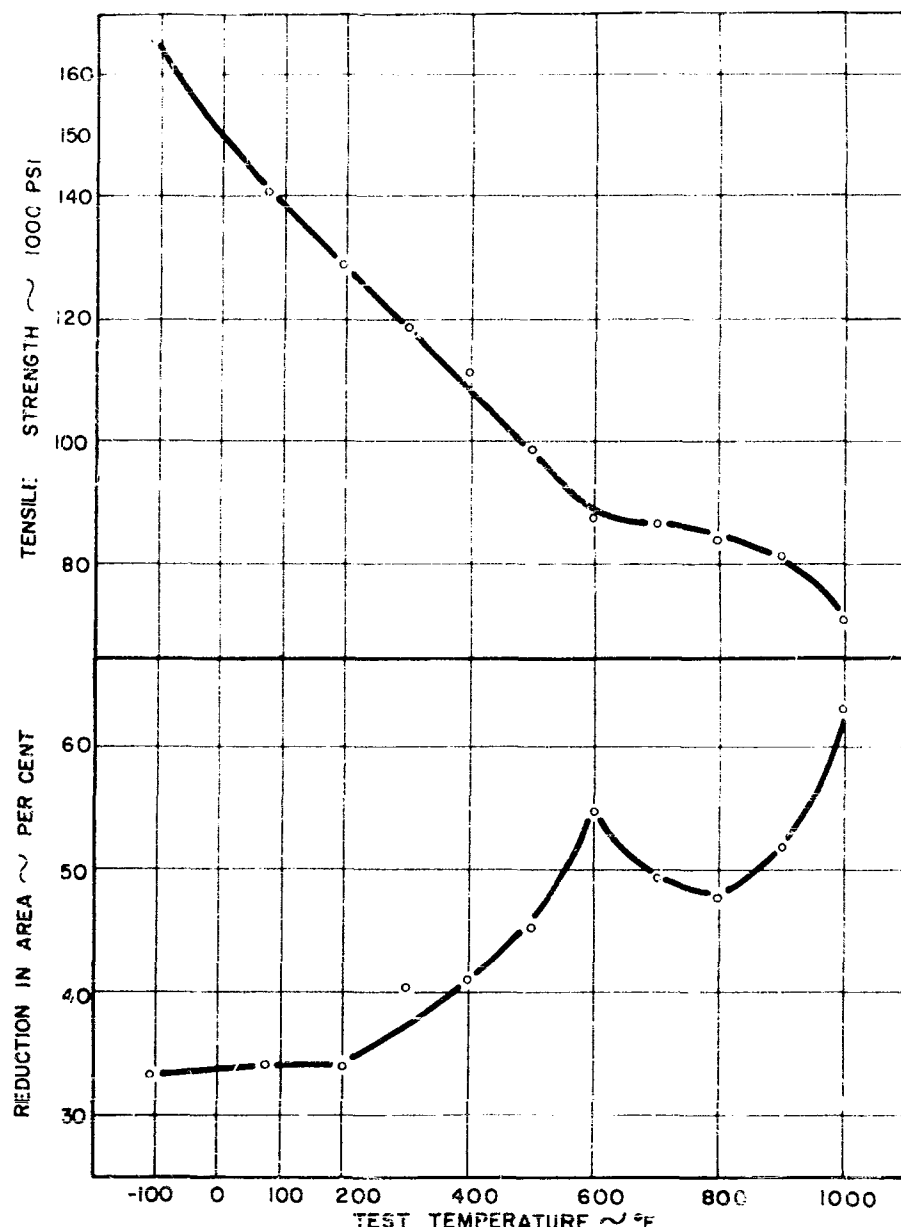


FIG. 27 EFFECT OF TEST TEMPERATURE ON STRENGTH AND DUCTILITY OF A-110AT ALLOY, 45 PPM HYDROGEN, UNNOTCHED SPECIMENS, .05 IN./IN./MIN STRAIN RATE.

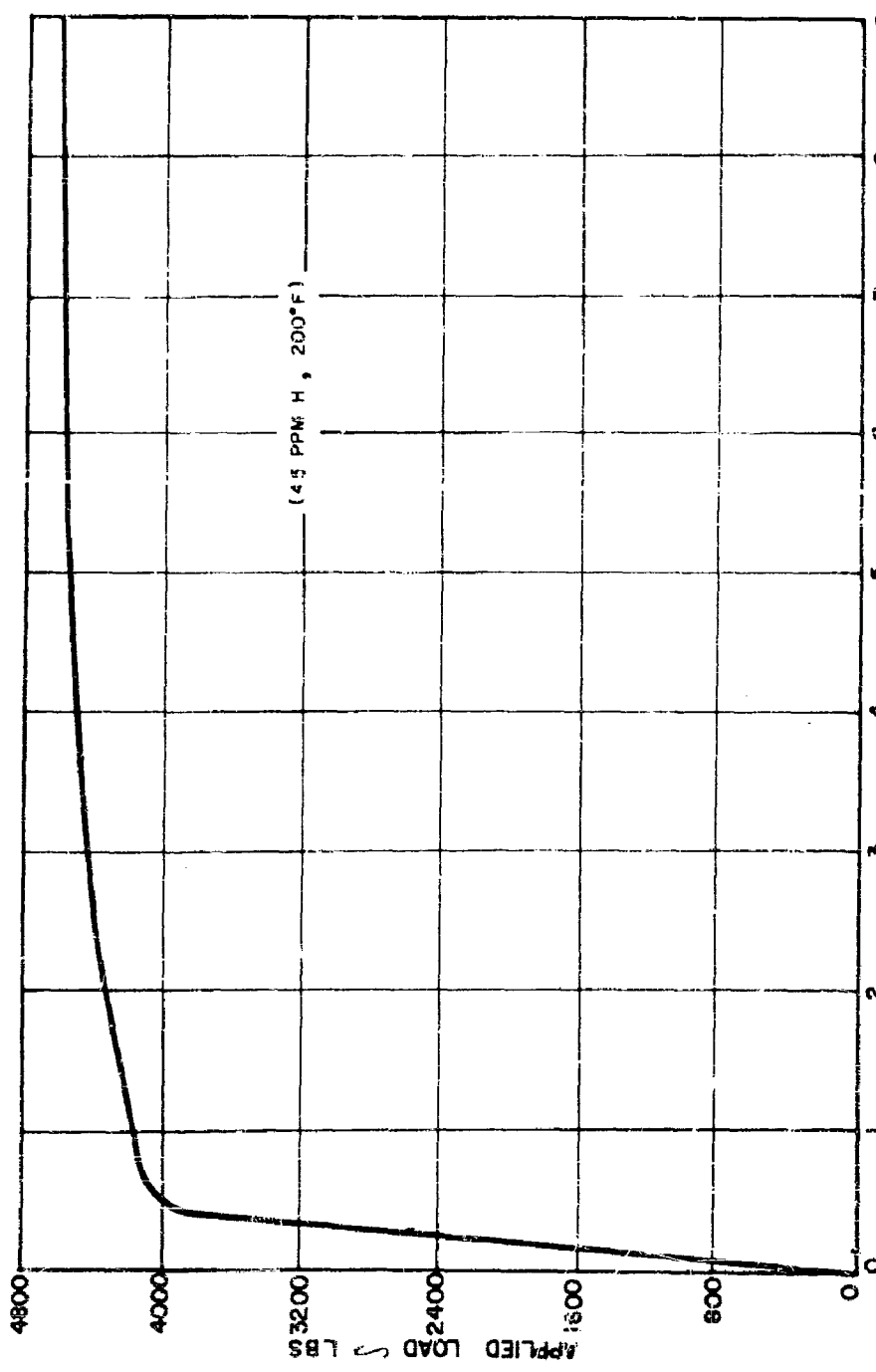


FIG.28: TYPICAL STRESS-STRAIN CURVE FOR A-110 AT ALLOY, 140,000 PSI STRENGTH LEVEL.

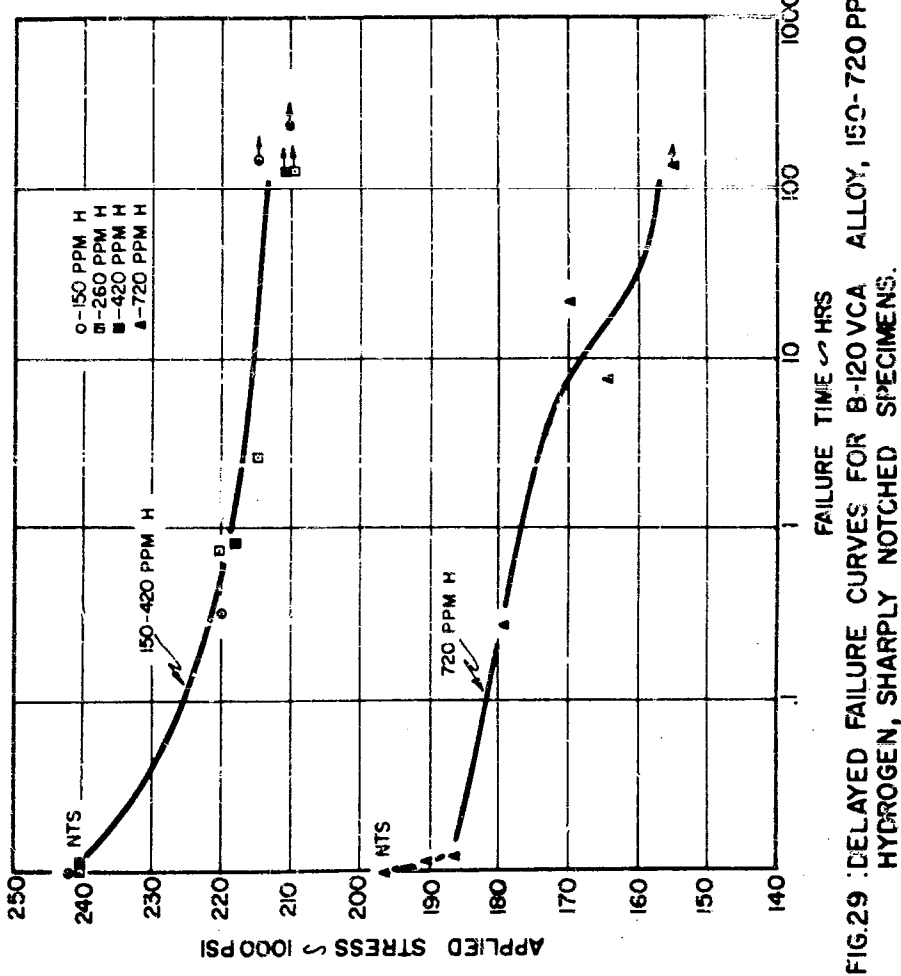


FIG.29 : DELAYED FAILURE CURVES FOR B-120 VCA ALLOY, 150-720 PPM HYDROGEN, SHARPLY NOTCHED SPECIMENS.

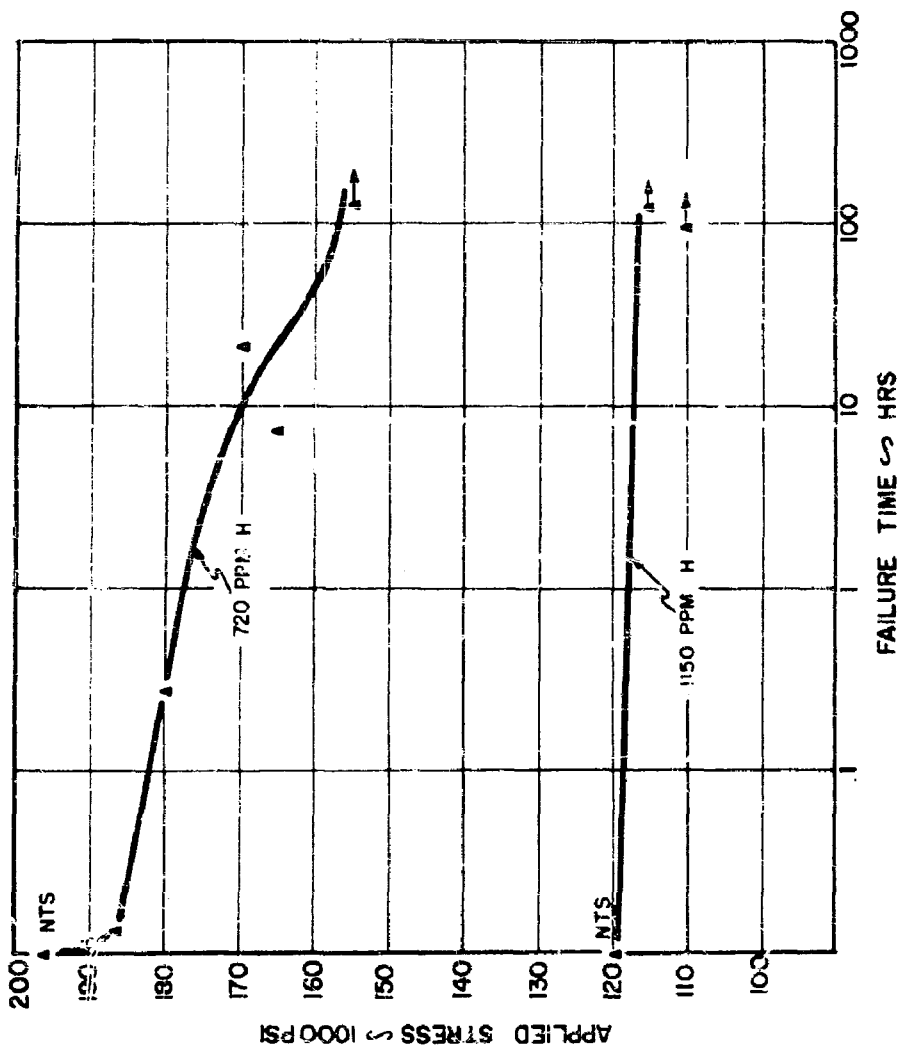


FIG. 30 : DELAYED FAILURE CURVES FOR B-120 VCA ALLOY, 720 AND 1150 PPM HYDROGEN, SHARPLY NOTCHED SPECIMENS.

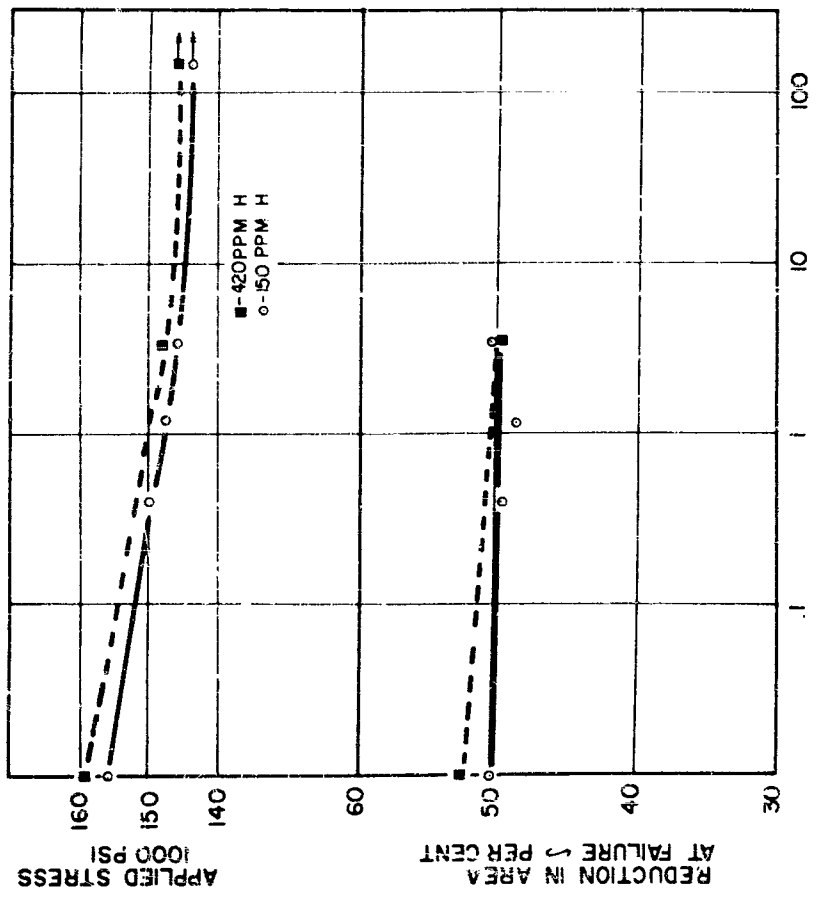


FIG. 3 | APPLIED STRESS FOR DELAYED FAILURE AND REDUCTION IN AREA AT FAILURE FOR B-120 VCA ALLOY, 150 AND 420 PPM HYDROGEN, UNNOTCHED SPECIMENS.

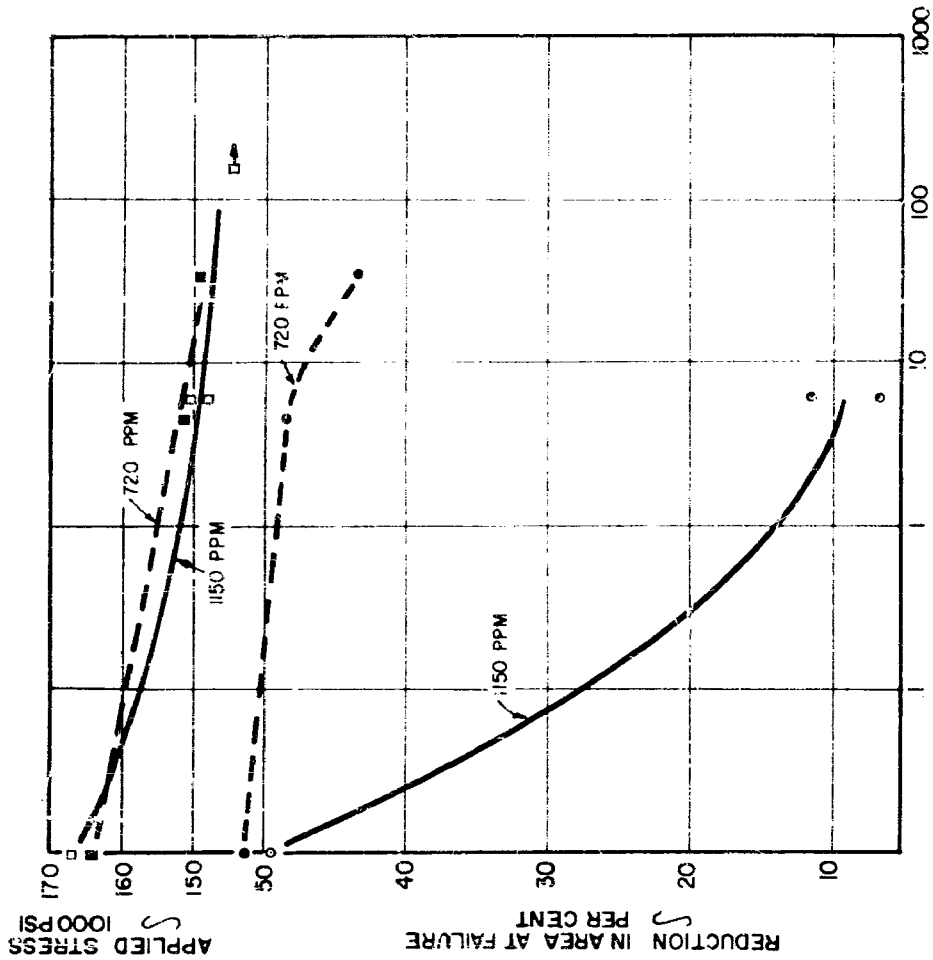


FIG. 32: APPLIED STRESS AND REDUCTION IN AREA AT FAILURE FOR B-120 VCA ALLOY, 720 AND 1150 PPM HYDROGEN, UNNOTCHED SPECIMENS.

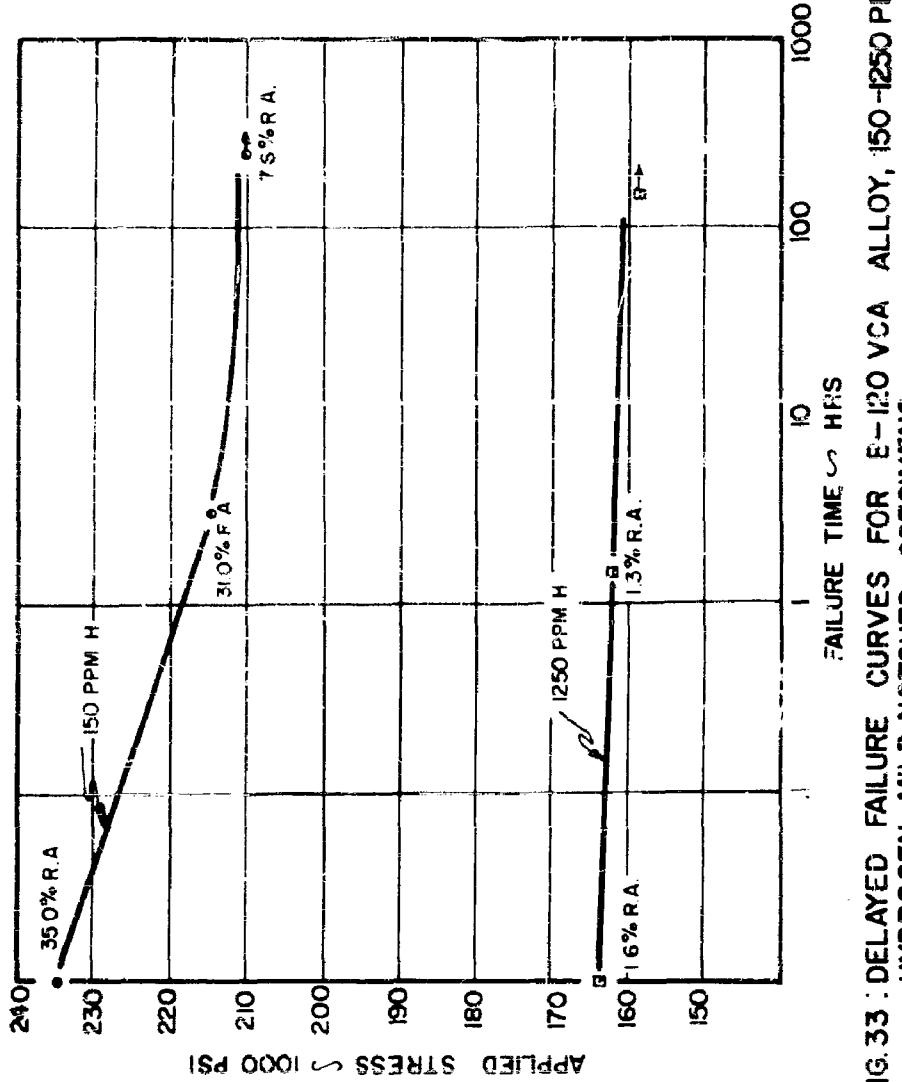


FIG. 33 : DELAYED FAILURE CURVES FOR E-120 VCA ALLOY, 150-1250 PPM HYDROGEN, MILD NOTCHED SPECIMENS.

SECTION II

HYDROGEN EMBRITTLEMENT OF
SEVERAL FACE-CENTERED CUBIC ALLOYS

P. A. Blanchard
A. R. Troiano

ABSTRACT

The hydrogen embrittlement of austenitic Ni-Cr-Fe alloys and OFHC copper has been investigated. Ni-Cr-Fe alloys were embrittled by hydrogen and their embrittlement was demonstrated to be of the same nature as that of steel.

A qualitative mechanism was presented which indicated that only the transition metals should be capable of conventional hydrogen embrittlement. This mechanism also accounted for the observed decrease of embrittlement in the austenitic Ni-Cr-Fe alloys with increasing (Fe + Cr) content.

LIST OF TABLES

	Page
I. Chemical Analysis of Material	100
II. Tensile Properties of the Alloys Used in This Investigation	101
III. Notch Tensile Strength of Nickel A in the Charged and Uncharged Condition	104
IV. Ductility of OFHC Copper in the Charged and Uncharged Condition	106

LIST OF FIGURES

Figure		Page
1.	Specimen Types Used in This Investigation	114
2.	Ductility at Fracture as a Function of Strain Rate in Charged and Uncharged Nickel	115
3.	Ductility at Fracture as a Function of Strain Rate in a Charged and Uncharged 72% Ni - 28% Fe Alloy	116
4.	Ductility at Fracture as a Function of Test Temperature in Charged and Uncharged Nickel	117
5.	Influence of Aging at 250°F on the Ductility of a Hydrogenated 80% Ni - 20% Cr Alloy	118
6.	Influence of the Composition of Ni - Cr - Fe Alloys on Their Hydrogen Embrittlement	119
7.	Variation of the Diffusion Rate of Hydrogen with Nickel Content in Binary Iron - Nickel Alloys at Various Temperatures	120
8.	Density of States of 3d and 4s Bands in Copper, Hydrogen Free and Hydrogen Charged Nickel and of Nickel Base - Chromium - Iron Alloys	121

I INTRODUCTION

The increased application of high strength materials, particularly steel and titanium, has stimulated an extensive study of hydrogen embrittlement which limits the use of these materials in severe service conditions (1)*. Thus far, most of the investigations have been concerned with titanium and body-centered cubic steel (1, 2, 3) although a few have dealt with austenitic steels (1 - 9). The latter materials, where virtually no embrittlement is found (4, 5), are used where feasible to circumvent failures due to hydrogen embrittlement (10, 11, 12). This difference in susceptibility to embrittlement between body-centered and face-centered cubic steels appears even when the two materials have the same composition, i.e. an austenitic steel which is not affected by hydrogen additions becomes susceptible to embrittlement when it undergoes the $\gamma \rightarrow \alpha$ transformation either by cooling to low temperatures or by cold working (4, 12, 13).

The influence of structure has been explained by the different characteristics of the two lattices with respect to two of the most important factors influencing hydrogen embrittlement, i.e. the equilibrium solubility and the diffusion rate of hydrogen (1, 4, 10, 14). The solubility of hydrogen is approximately three to four times greater in austenite than in ferrite. Therefore it may be expected that more hydrogen is necessary to embrittle austenite than ferrite. Furthermore, the rate of diffusion of hydrogen in austenite is much slower than in ferrite. Since the degree of embrittlement and the rate of crack propagation in embrittled specimens are controlled by the diffusion of hydrogen (15, 16), the lower diffusion rate may lead to a very different apparent effect of hydrogen in face-centered cubic alloys though the same mechanism may be operative. The hydrogen embrittlement of ferritic steels disappears at both low and high test temperatures and also at high strain rates (17). The slower rate of diffusion would make a tensile test of hydrogen-charged austenitic material equivalent to one at either high strain rates or low temperatures in ferritic materials.

Since a number of alloy systems had been examined it was inferred by many investigators that no face-centered cubic metal can be embrittled by hydrogen (4). An exception to this was the hydrogen embrittlement of nickel discovered by Eisenkoib and Ehrlich (13). Their results suggested that the above rule was not universal.

* Numbers in parentheses pertain to references in the Bibliography

The purpose of this work was twofold, first, to determine whether the hydrogen embrittlement of nickel is of the same nature as that of steel and secondly, to examine the effect of alloying on the magnitude of the embrittlement in nickel. For reasons which will be discussed later, the hydrogen embrittlement of pure copper was also investigated. The "optimum" conditions for hydrogen embrittlement which have been determined previously (17) were used.

II. MATERIALS AND PROCEDURE

I. SPECIMEN PREPARATION

Eight alloys were used in this investigation, commercially pure nickel (Nickel A), 72% Ni - 28% Fe, 51% Ni - 49% Fe, Nilvar, Nichrome I and Nichrome V, 25-20 stainless steel and OFHC copper. The compositions of the first seven alloys are listed in Table I. The specimen types used are shown in Fig. 1. The sharply-notched specimens were

TABLE I

Chemical Analysis of Material

	% Ni	% Cr	% Fe
Nickel A	99.4		0.15
72% Ni - 28% Fe	72.7		27.2
51% Ni - 49% Fe	51		49
Nilvar	36		64
Nichrome I	60	16	24
Nichrome V	80	20	
25-20 Stainless Steel	19.7	24.9	52.8

employed for the notch tensile strength determinations and delayed failure studies while the unnotched specimens were used for the tensile strength and ductility measurements.

All nickel base alloys were used in the as-received condition. The 25-20 stainless steel was studied immediately after annealing thirty minutes at 2050°F or after annealing and cold swaging 67%.

The OFHC copper was obtained from a wirebar and cold rolled 51% prior to machining. The thermal charging acted simultaneously as a recrystallization treatment.

The tensile properties of these alloys are presented in Table II for the uncharged condition.

TABLE II

Tensile Properties of the Alloys Used in This
Investigation for a 0.05 inch/minute Gross Head Speed
in the Tensile Test

	Strength Level (psi)	Reduction in Area at Fracture
Nickel A	118,000	73%
78% Ni - 28% Fe	95,500	74%
51% Ni - 49% Fe	108,000	64%
Nilvar	71,000	78%
Nichrome I	109,000	54.5%
Nichrome V	102,000	72.5%
25-20 Steel Annealed	83,000	79%
25-20 Cold Worked 7%	140,000	61%
OFHC copper	30,000	40%

2. HYDROGENATION AND CADMIUM PLATING

Both thermal and cathodic charging were used in this investigation. Thermal charging was used for 25-20 stainless steel in which the diffusion rate of hydrogen is slow and in copper which is permeable to hydrogen only at high temperatures. The procedure used was the following:

- a) heat the furnace up to 2050° F for 25-20 stainless steel and 1115° F for OFHC copper.
- b) flush the tube with argon.
- c) introduce the specimen into the furnace.
- d) flush the tube again with argon.
- e) substitute hydrogen for argon with a pressure slightly above atmospheric pressure.
- f) charge 10 hours.
- g) flush the furnace tube with argon.
- h) open the tube and quench the specimen in water.

The other alloys were cathodically charged. The charging bath was a 2N sulfuric acid solution poisoned with 250 mg of arsenic is sodium arsenite per liter. The specimens were degreased with carbon tetrachloride before charging. Current densities employed were 22 amperes per square inch for the unnotched specimens and 12.6 amperes per square inch for the notched specimens. The bath was heated by the current to a temperature varying between 170°F and 185°F. Because of the abundant loss of electrolyte during charging, fresh liquid was added to the bath every half hour.

Immediately after charging, the specimens were cadmium plated to avoid subsequent degassing. Cadmium plating was performed in a sodium cyanide bath with a current density of 20 amperes per square foot for 5 minutes when no subsequent heating of the specimen was to be performed, and for 20 minutes when baking was necessary to produce a homogeneous distribution of hydrogen.

3. TESTING

Tensile testing was carried out in a hydraulic testing machine at constant crosshead speeds. Various speeds in the range 0.01 to 10 inches per minute were used. Higher strain rate tensile tests were performed on a draw bench at crosshead speed of 100 inches per minute. A constant load, lever-arm stress-rupture machine was used for delayed failure tests.

III. RESULTS AND DISCUSSION

1. SIMILARITY OF THE HYDROGEN EMBRITTLEMENT OF NICKEL AND NICKEL BASE-CHROMIUM-IRON ALLOYS WITH THAT OF STEEL

The effect of cathodically introduced hydrogen on the ductility of nickel and nickel base-chromium-iron alloys was investigated. These alloys were embrittled by hydrogen. To determine whether this embrittlement was of the same type as that of steel its dependence on strain rate and temperature of testing was studied.

A. Strain Rate Dependence of the Embrittlement

The variations of the ductility of charged and uncharged nickel and 72% Ni-28% Fe are plotted in Fig. 2 and Fig. 3. The embrittlement of both alloys decreased as strain rate increased. The ductility of the charged specimens was lowest at the minimum strain rate employed and equal to that of the uncharged specimens at high strain rates.

B. Temperature Dependence of the Embrittlement

The variation of the embrittlement of nickel with temperature is presented in Fig. 4. For a particular charging condition, it disappeared at low and high test temperatures and was maximum in an intermediate range of temperature.

The hydrogen embrittlement of nickel and high nickel-chromium-iron alloys has, therefore, the same dependence on strain rate and test temperature as that of steel and hence is also a diffusion controlled phenomenon since it disappears when diffusion is inhibited either by a high strain rate or a low testing temperature. This behavior is opposite to that of other kinds of embrittlement, e.g. the embrittlement produced by the presence of hydrides, which increases with increasing strain rate and decreasing test temperature (18).

C. Recovery

Aging produced a recovery of the ductility of the charged alloys indicating that the embrittlement was reversible. One of these alloys, 80% Ni - 20% Fe, was used for detailed study of recovery. The ductility of the charged alloy increased with increasing baking times at 250°F, and the embrittlement disappeared completely with sufficient baking (Fig. 5).

2. NOTCH TENSILE AND DELAYED FAILURE TESTS

The effect of hydrogen on the notch tensile strength of nickel was studied at various temperatures. The results shown in Table III indicate that the notch tensile strength of nickel was not reduced by hydrogen.

TABLE III

Notch Tensile Strength of Nickel A in the Charged and Uncharged Condition

Test Temperature	Uncharged Specimens	Specimens Charged 7 hrs with a 12.6 amp/sq. current density	
		144,300 psi	144,000 psi
70° F	144,000 psi	144,300 psi	
200° F	122,500 psi	144,000 psi	
350° F	142,000 psi	138,600 psi	

No delayed failure was observed on notched specimens of nickel charged 7 hours with a current density of 12.6 amperes per square inch. These results are explainable by the fact that with the charging conditions used, the fracture of embrittled nickel was still a ductile one. The reduction in area at fracture was only reduced to 50% and necking still occurred in the unnotched specimens. Furthermore, the stress-strain curves of notched specimens also reached a maximum. It is known (15) that tensile and notched tensile strength are not modified by hydrogen embrittlement unless the ductility at fracture is reduced below the value necessary for necking. This accounts for the insensitivity of notched tensile strength to the embrittling of these alloys.

3. VARIATION OF THE EMBRITTLEMENT OF Ni-CR-FE ALLOYS WITH COMPOSITION

The variation of the hydrogen embrittlement of Ni-Cr-Fe alloys is presented in Fig. 6. In this figure, the circled figures represent the reduction in ductility due to a cathodic charging treatment of 4 hours as a function of the composition of the alloys. The reduction in ductility of the nickel base alloys decreases with increasing (iron + chromium) contents. The embrittlement was maximum for pure nickel and nil for 51% Ni - 49% Fe alloy, Nilvar and 25-20 stainless steel. It seemed to vary continuously for intermediate compositions.

Since the diffusion rate of hydrogen is very low in 25-20 steel at

room temperature thermal charging was used to produce a greater hydrogen content throughout the specimen. This treatment did not produce any embrittlement. Since the susceptibility of a given metal to hydrogen embrittlement increases when its strength level is increased or its ductility decreased, (15) some 25-20 stainless steel was cold swaged 67% - a treatment which reduces its ductility from 75% to 61% and raises its strength level from 83,000 psi to 146,000 psi. In addition, in an effort to embrittle the 25-20 steel more severe charging conditions were used according to the following sequence:

- a) Charge 5 hours, plate 20 minutes, bake 1 hour at 350°F.
- b) Deplate, charge 4 hours, plate 20 minutes, bake 1 hour at 350°F.
- c) Deplate, charge 4 hours, plate 20 minutes, bake 1 hour at 356°F
- d) Deplate, charge 5 hours

The intermediate baking treatment was performed to make the superficial skin of hydrogen produced by cathodic charging diffuse into the specimen. By this process a slight embrittlement was produced. The ductility of the charged alloy was reduced from 61% to 53%

This result indicates that the well known non-susceptibility of stainless steel to hydrogen embrittlement is due to its inherent ductility and to relatively low hydrogen contents.

4. THE HYDROGEN EMBRITTLEMENT OF OFHC COPPER

Oxygen-bearing copper is known to be embrittled by an annealing treatment in hydrogen (19). This embrittlement is due to the reduction of copper oxides by hydrogen, and the resulting high pressures produced in the metals by the water vapor. Oxygen free copper was used to determine whether copper is susceptible to hydrogen embrittlement without the masking effect of the water vapor reaction. A thermal charging of 16 hours at 1115°F was used. The results shown in Table IV show that there was no embrittlement.

TABLE IV

Ductility of OFHC Copper in the
Charged and Uncharged Conditions

<u>Test Temperature</u>	<u>Uncharged Specimens</u>	<u>Charged Specimens</u>
70° F	89.5%	89%
200° F	86.5%	88%
280° F	84.5%	85%
405° F	76.5%	75.5%

IV GENERAL DISCUSSION

The results presented above prove that, although an important factor, the structure of an alloy does not provide an absolute criterion for predicting an alloy's susceptibility to hydrogen embrittlement. Though austenitic iron-chromium-nickel alloys are in general less capable of being embrittled than ferritic and martensitic steels, they are definitely susceptible to hydrogen embrittlement and this susceptibility is a function of composition among other things. This result is not at variance with previous studies on austenitic steels (2, 3, 4, 5, 6, 7) which showed that these alloys were not embrittled by hydrogen. Previous work was generally performed with less severe charging conditions than those employed in this investigation and, for a given charging condition, the hydrogen embrittlement of Ni-Cr-Fe alloys appears only for high nickel alloys.

At this point two anomalies are apparent. First, the fact that the hydrogen embrittlement of a nickel-iron alloy decreases with increasing iron content is puzzling, especially when one considers that iron is the easiest metal to embrittle with hydrogen. Secondly, why copper, which is the neighbor of nickel in the periodic table, is not embrittled by hydrogen and more generally, why only transition metals have been thus far embrittled by hydrogen?

Several possible reasons which might account for the first of these questions and a tentative explanation for both these questions as a whole will be presented.

It is known that the strength level and the ductility of an alloy are important factors governing its susceptibility to hydrogen embrittlement (15). An alloy is more amenable to embrittlement when its strength level is increased or its ductility decreased. The mechanical properties of the alloys (Table II) indicate that, except possibly for copper, this factor cannot account for their differences in behavior since, for example, the 51% Ni - 49% Fe alloy has a higher strength level and a lower ductility than the 72% Ni - 28% Fe alloy and yet is less embrittled by hydrogen.

A second possible reason for the behavior is the variation of lattice parameter with composition. The lattice parameter of nickel-iron alloys increases by 1% with increasing iron content from zero to 60% (20). This corresponds to an increase of 6% of the volume of the interstitial sites for hydrogen and may account for a decrease of its action. The importance of this factor is hard to estimate, but it is not believed to vary enough to provide a conclusive explanation.

Thirdly, the variations of the diffusion rate of hydrogen with composition do not provide an explanation for the variation of embrittlement with composition. The variation of the diffusion rate of hydrogen with the composition of Ni-Fe alloys is presented in Fig. 7 (21). The speed of diffusion of hydrogen is higher in the 51% Ni - 49% Fe alloy which is not embrittled than in the 72% Ni - 28% Fe alloy which is embrittled.

Finally, though the charging conditions of the seven Ni-Cr-Fe alloys were identical, it is not certain that their hydrogen contents were equal. The analyses performed do not give a conclusive answer to this question. The 51% Ni - 49% Fe alloy contained 4 ppm of hydrogen and the pure nickel, 5 ppm. This difference is small and may be due to experimental scatter. Furthermore the hydrogen distribution of the specimens is known to be inhomogeneous and this factor decreases the significance of any hydrogen analysis.

Another aspect of the problem will be now considered. It will be shown that the consideration of the electronic structure of the alloys studied may provide an explanation for the fact that only transition metals, i.e., iron, titanium, vanadium and nickel, have been shown to be susceptible to hydrogen embrittlement and that the embrittlement of nickel is decreased if its alloying with iron and chromium increases.

It is known that hydrogen ionizes when it goes into solution in a metal. The bare protons diffuse in the metal (22) and are preferentially located in dislocations (23).

Cottrell has described a mechanism of the fracture of a metal which implies the cracking of an array of coalesced dislocations (24). In this theory, the energy of such an array of dislocations and the stress necessary to make it grow indefinitely are calculated.

The presence of hydrogen in these arrays of dislocations increases their energy and hence lowers the applied stress necessary for fracture (25). A possible reason for this increase of the energy of an array of dislocations due to the presence of hydrogen can be obtained by an analysis of the effect of hydrogen on electronic structure.

The electrons of the hydrogen atoms in solution in a transition metal have been shown to join the d bands of the metallic cores (22) as schematically shown in Fig. 8 (b) and (c). On the other hand it is known (26) that the repulsive forces determining the interatomic distance of transition metals such as Ni and its neighbor in the periodic table, Cu, are due to the overlapping of their d bands. It may, therefore, be expected that any increase of the electronic concentration of these bands produces an increase

of the repulsive forces between the metallic cores, i.e. an increase of the energy of the region in which this effect occurs. This effect can occur only with a transition metal whose 3 d band is not full. It cannot happen in copper or any non-transition metal which has a completed 3 d band.

Furthermore, this effect should be lessened when either iron or chromium is added to nickel. The electronic concentration of iron and chromium are lower than that of nickel and therefore a Ni-Cr-Fe alloy also has a 3 d band which is less full than nickel, as appears in Fig. 8 (d). The increase of energy due to the addition of extra electrons to a band is higher when the band is nearly filled than when it is not. Therefore when a transition metal on the left of nickel in the periodic table is alloyed with it, the increase of energy due to the addition of hydrogen to the alloy decreases and the embrittlement may also be expected to decrease. When enough iron and chromium are added to nickel for the $\gamma \rightarrow \alpha$ transformation to occur, the change of structure is believed to account for the reversion of this trend, i.e. ferritic Ni-Cr-Fe is strongly embrittled by hydrogen. This assumption is supported by the fact that an austenitic steel which is not embrittled by hydrogen becomes susceptible to embrittlement if it undergoes the $\delta \rightarrow \alpha$ transformation.

V SUMMARY AND CONCLUSIONS

The susceptibility to hydrogen embrittlement of austenitic Ni-Cr-Fe alloys of various compositions and of OFHC copper has been investigated.

Nickel and nickel base-chromium-iron alloys were embrittled by cathodically introduced hydrogen. Their embrittlement was of the same type as that of steel, i.e., it decreased as strain rate increased, disappeared at low and high temperatures and was eliminated by an adequate baking treatment.

With a particular charging condition, the embrittlement of austenitic Ni-Cr-Fe decreased with increasing (chromium + iron) content. This trend was not explained by the consideration of the mechanical properties nor by the lattice parameter of the alloys.

A tentative explanation based on the consideration of the electronic configuration of the alloys studied was presented to explain that only transition metals are capable of conventional hydrogen embrittlement and that the hydrogen embrittlement of Ni-Cr-Fe alloys decreases with their (Fe + Cr) content.

This explanation was supported by the result that OFHC copper was not embrittled by thermally introduced hydrogen.

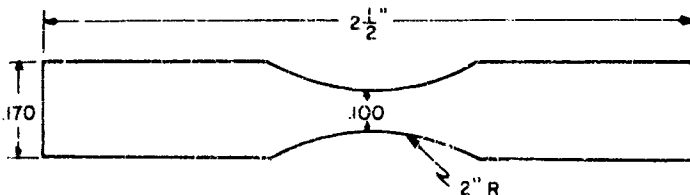
VI BIBLIOGRAPHY

1. R. W. Buzzard and H. E. Cleaves, "Hydrogen Embrittlement of Steel: Review of the Literature," National Bureau of Standards, Circular 511, (1951), 29 pp.
2. J. G. Morlet, H. H. Johnson and A. R. Troiano, "A New Concept of Hydrogen Embrittlement in Steel," Journal of the Iron and Steel Institute, 189, p. 37-44. (May, 1958)
3. R. D. Daniels, R. J. Quigg, and A. R. Troiano, "Delayed Failure and Hydrogen Embrittlement in Titanium," Trans. ASM, 51, (1959).
4. J. D. Hobson and J. Hewitt, "The Effect of Hydrogen on the Tensile Properties of Steel," Journal of the Iron and Steel Institute, 173, p. 131-140, (1953).
5. H. H. Burton, C. Sykes and C. C. Gegg, "Hydrogen in Steel Manufacture," Journal of the Iron and Steel Institute, 156, p. 155-180, (1947).
6. H. C. Van Ness "What Hydrogen Does to Metals," Petroleum Refiner, 35, p. 160-163, (1956)
7. H. C. Van Ness and B. F. Dodge, "Effects of Hydrogen at High Pressures on the Mechanical Properties of Metals," Chemical Engineering Progress, 51, p. 266-271, (1955).
8. E. R. Slaughter, "Review of the Effects of Hydrogen in Steel," Journal of Metals, 8, p. 430-431, (1956)
9. C. A. Zapffe and M. E. Haslem, "A Test for Hydrogen Embrittlement and Its Application to 17% Chromium, 1% Carbon Stainless Steel Wire," Trans. AIME, 167, p. 281-308, (1946)
10. C. E. Sims, "The Behavior of Gases in Solid Iron and Steel," Gases in Metals, (1953), American Society for Metals: Cleveland, p. 176-178.
11. B. B. Morton, "M-O-C for Hydrogen," Petroleum Refiner, 35, p. 164-166, (1956).
12. Anonymous, "Steel Lining Eliminates Failure of Pressure Vessels," Chemical Engineering News, 30, p. 2942, (1952)

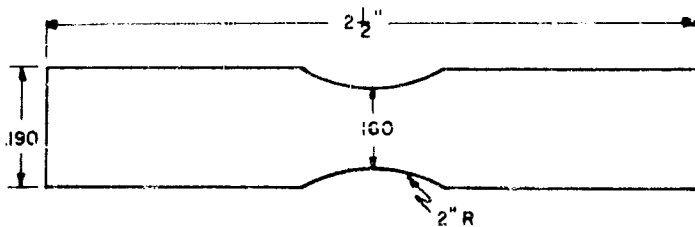
13. F. Eisenkolb and G. Ehrlich, "Hydrogen Pick-Up of Austenitic Steels in a Cathodic Charge," *Archiv für das Eisenhüttenwesen*, 25, p. 187-194, (1954).
14. H. H. Uhlig, "Action of Corrosion and Stress on 13% Cr Stainless Steel," *Metal Progress*, 57, p. 486-487, (1950).
15. R. P. Frohemberg, W. J. Barnett and A. R. Troiano, "Delayed Failure and Hydrogen Embrittlement in Steel," *Trans. ASM* 47, I, 892-925, (1955).
16. H. H. Johnson, J. G. Morlet and A. R. Troiano, "Hydrogen, Crack Initiation and Delayed Failure in Steel," *WADC Technical Report* TR-57-262 (May, 1957).
17. J. T. Brown and W. M. Baldwin, Jr., "Hydrogen Embrittlement of Steel," *Trans. AIME*, 200, p. 298-304, (1954).
18. D. N. Williams, "Report on Hydrogen in Titanium and Titanium Alloys," *Titanium Metallurgical Laboratory Report No. 199*, (May 16, 1958).
19. D. P. Smith, "Hydrogen in Metals," *The University Press of Chicago* (1947).
20. A. J. Bradley, A. H. Jay and A. Taylor, "The Lattice Spacing of Iron-Nickel Alloys," *Philosophical Magazine*, 23, p. 545, (1937).
21. A. A. Shcherbakova, "Diffusion of Hydrogen Through Iron and Binary Iron-Chromium and Iron-Nickel Alloys at High Pressures and Temperatures," *Journal of Applied Chemistry of the USSR*, 29, p. 952-960, (June, 1956).
22. R. E. Norberg, "Nuclear Magnetic Resonance of Hydrogen into Palladium Wires," *Physical Review*, 86, p. 745, (1952).
23. J. Plusquellec, P. Azou and P. Bastien, "Localization de l'Hydrogène dans le Réseau du Fer α ," *Comptes Rendus*, 244, p. 1195-1197, (February, 1957).
24. A. H. Cottrell, "Theory of Brittle Fracture in Steel and Similar Metals," *Transactions of the Metallurgical Society of AIME*, 212, p. 192-203, (April, 1958).
25. P. A. Blanchard, Master's Thesis, Case Institute of Technology.

Cleveland, Ohio, (1959).

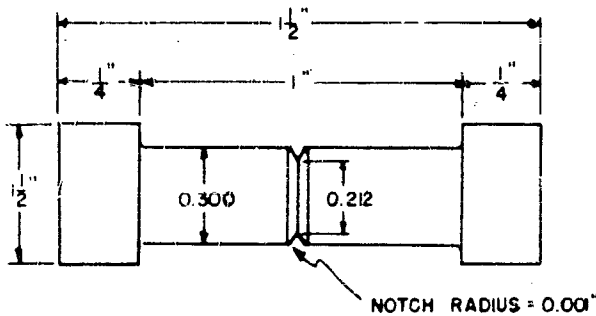
26. N. F. Mott and H. Jones, "The Theory of the Properties of Metals and Alloys," Dover Publications, New York, N.Y.



UNNOTCHED TENSILE SPECIMEN FOR Ni-Cr-Fe ALLOYS



UNNOTCHED TENSILE SPECIMEN FOR OFHC COPPER



SHARP NOTCH SPECIMEN

FIG. I: SPECIMEN TYPES USED IN THIS INVESTIGATION.

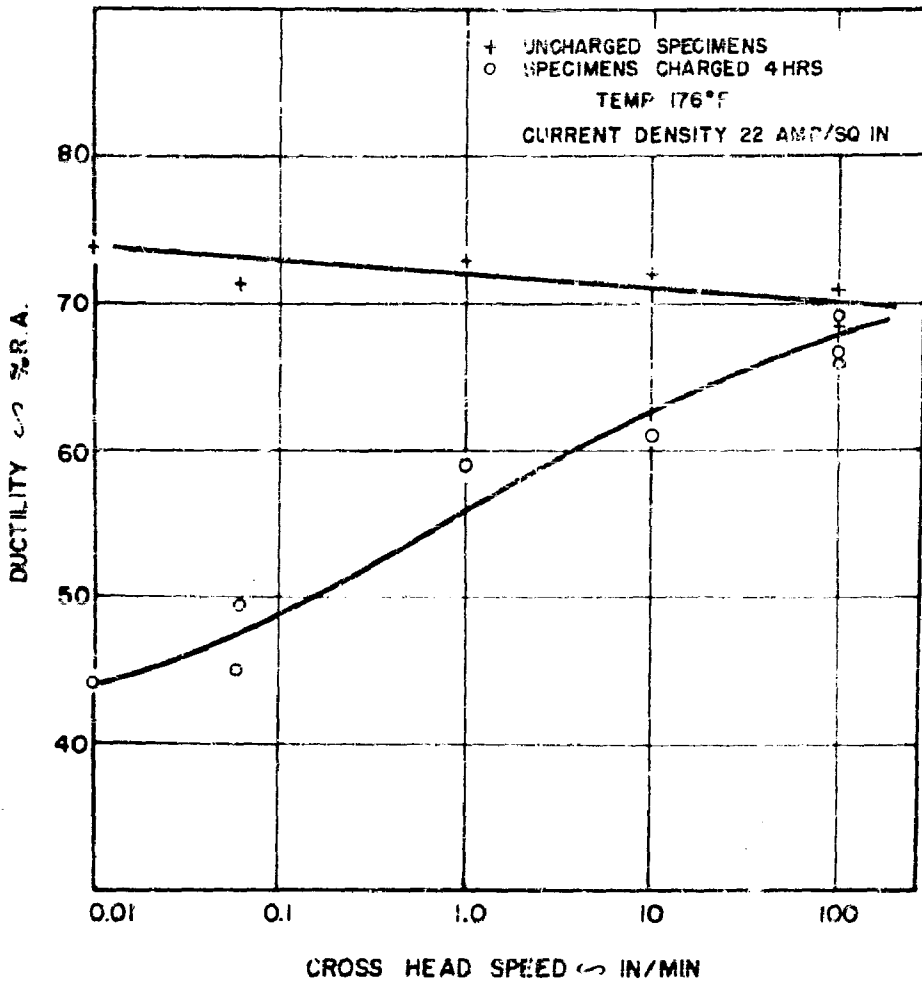


FIG.2: DUCTILITY AT FRACTURE AS A FUNCTION OF STRAIN RATE IN CHARGED AND UNCHARGED NICKEL.

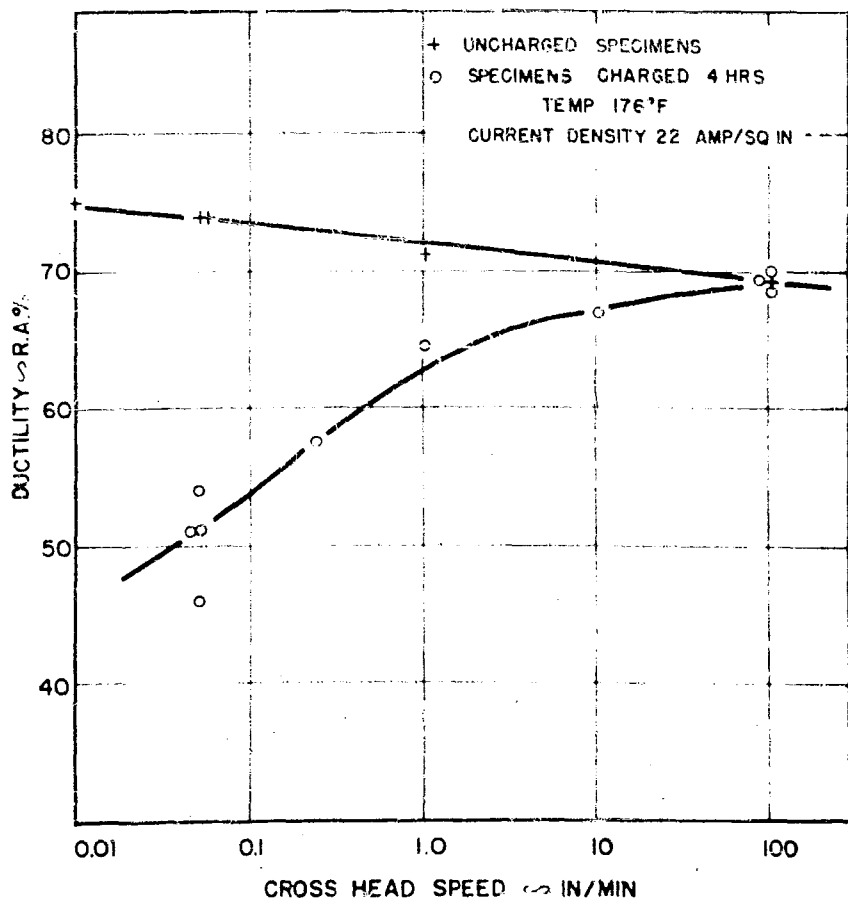


FIG.3: DUCTILITY AT FRACTURE AS A FUNCTION OF STRAIN RATE IN A CHARGED AND UNCHARGED 72% NI-28% Fe ALLOY.

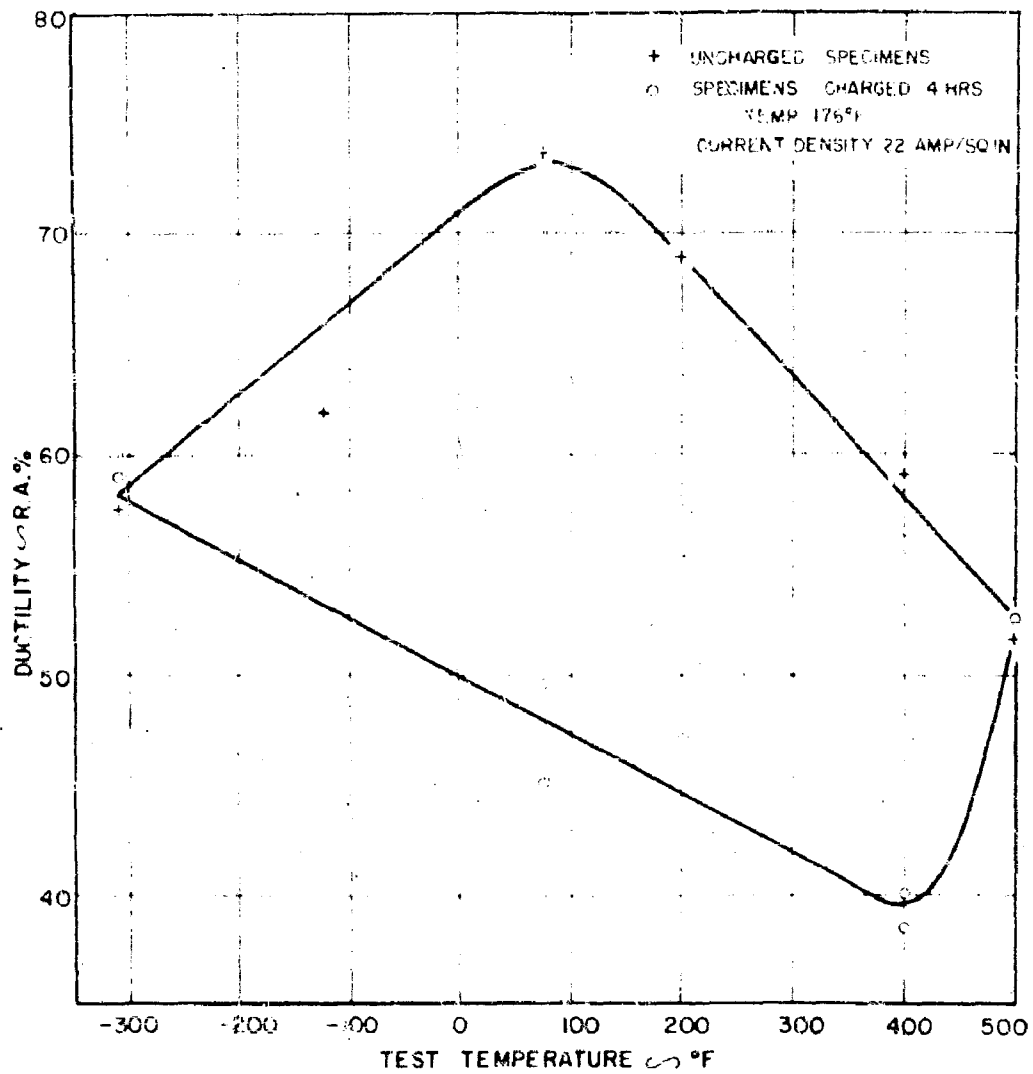


FIG. 4 DUCTILITY AT FRACTURE AS A FUNCTION OF TEST TEMPERATURE IN CHARGED AND UNCHARGED NICKEL. STRAIN RATE 0.05 IN./IN./MIN.

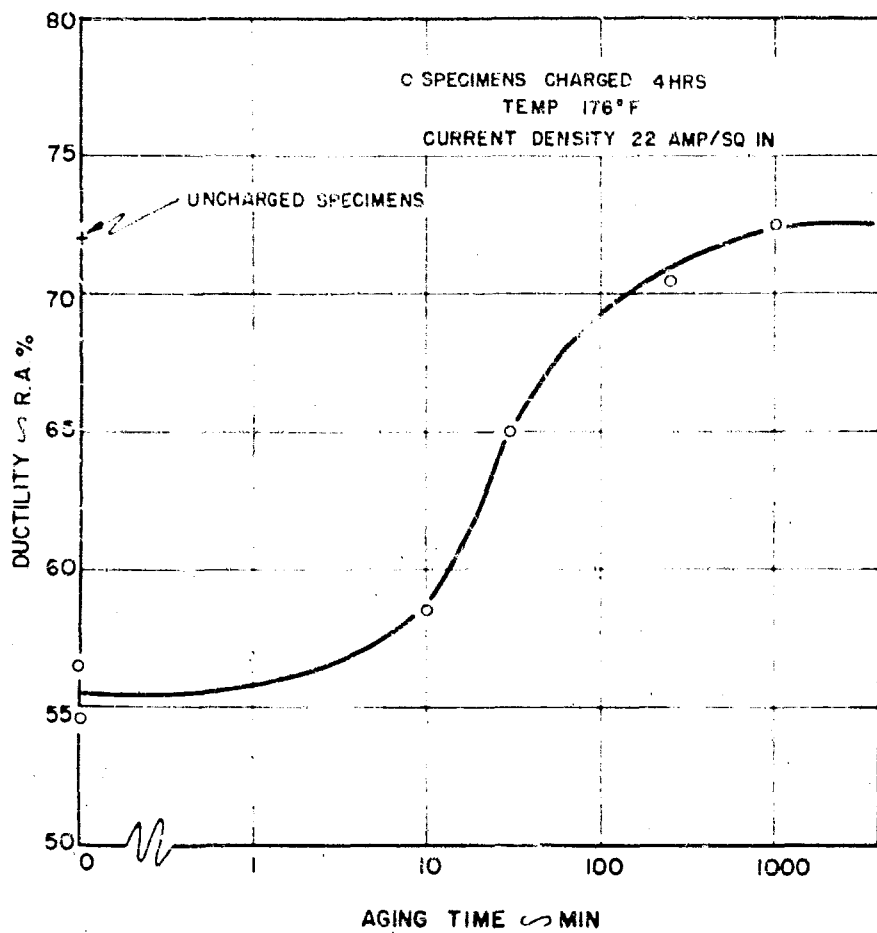


FIG.5: INFLUENCE OF AGING AT 250°F ON THE DUCTILITY OF A HYDROGENATED 80% NI - 20% CR ALLOY.

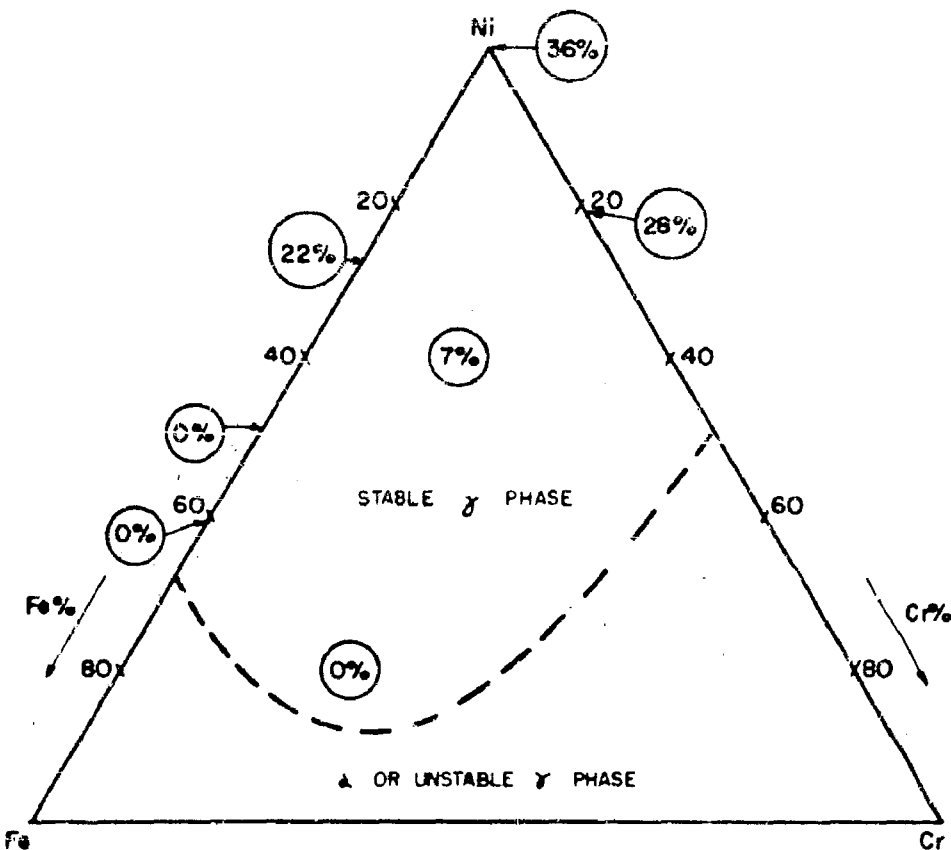


FIG. 6. INFLUENCE OF THE COMPOSITION OF Ni-Cr-Fe ALLOYS ON THEIR HYDROGEN EMBRITTLEMENT. ALL SPECIMENS WERE CHARGED 4 HRS AT 176°F WITH A CURRENT DENSITY OF 22 AMP/SQ IN. CIRCLED FIGURES REPRESENT THE REDUCTION OF DUCTILITY BROUGHT ON BY HYDROGEN CHARGING.

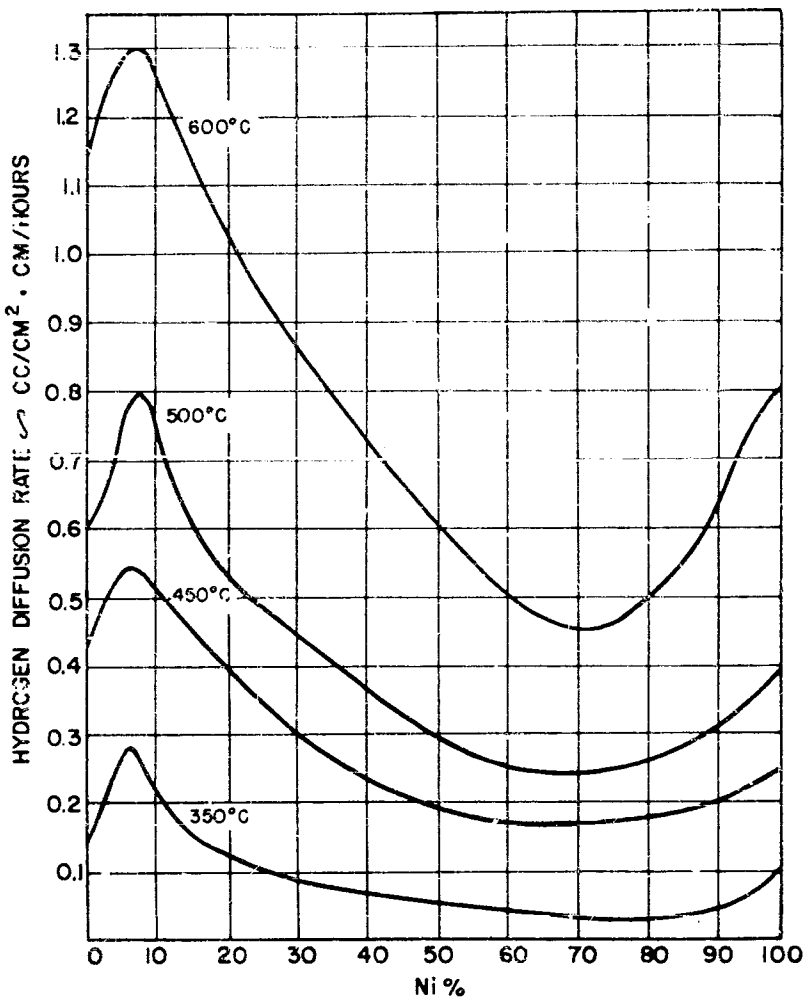
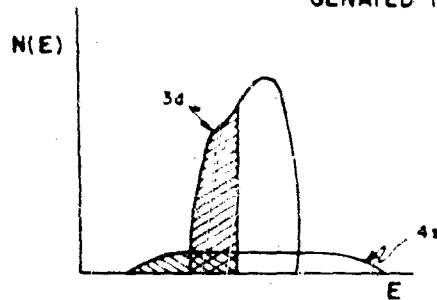
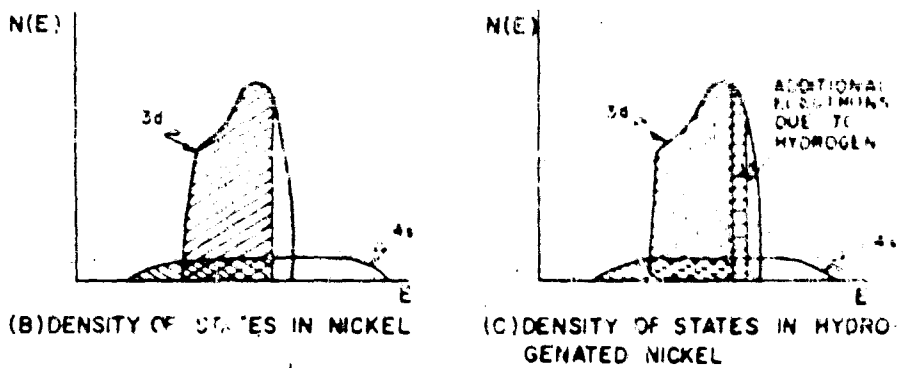
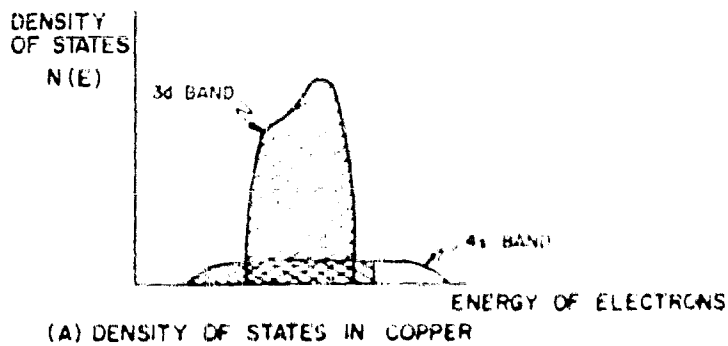


FIG. 7: VARIATION OF THE DIFFUSION RATE OF HYDROGEN WITH NICKEL CONTENT IN BINARY IRON-NICKEL ALLOYS AT VARIOUS TEMPERATURES (19).



(D) DENSITY OF STATES IN A NI BASE-Fe-Cr ALLOY

FIG.8:DENSITY OF STATES OF THE 3d AND 4s BANDS OF COPPER.
HYDROGEN FREE AND HYDROGEN CHARGED NICKEL AND
OF NICKEL BASE - CHROMIUM - IRON ALLOYS.